Prepared in cooperation with the U.S. Army Corps of Engineers

Evaluation of the Biological and Hydraulic Performance of the Portable Floating Fish Collector at Cougar Reservoir and Dam, Oregon, 2014

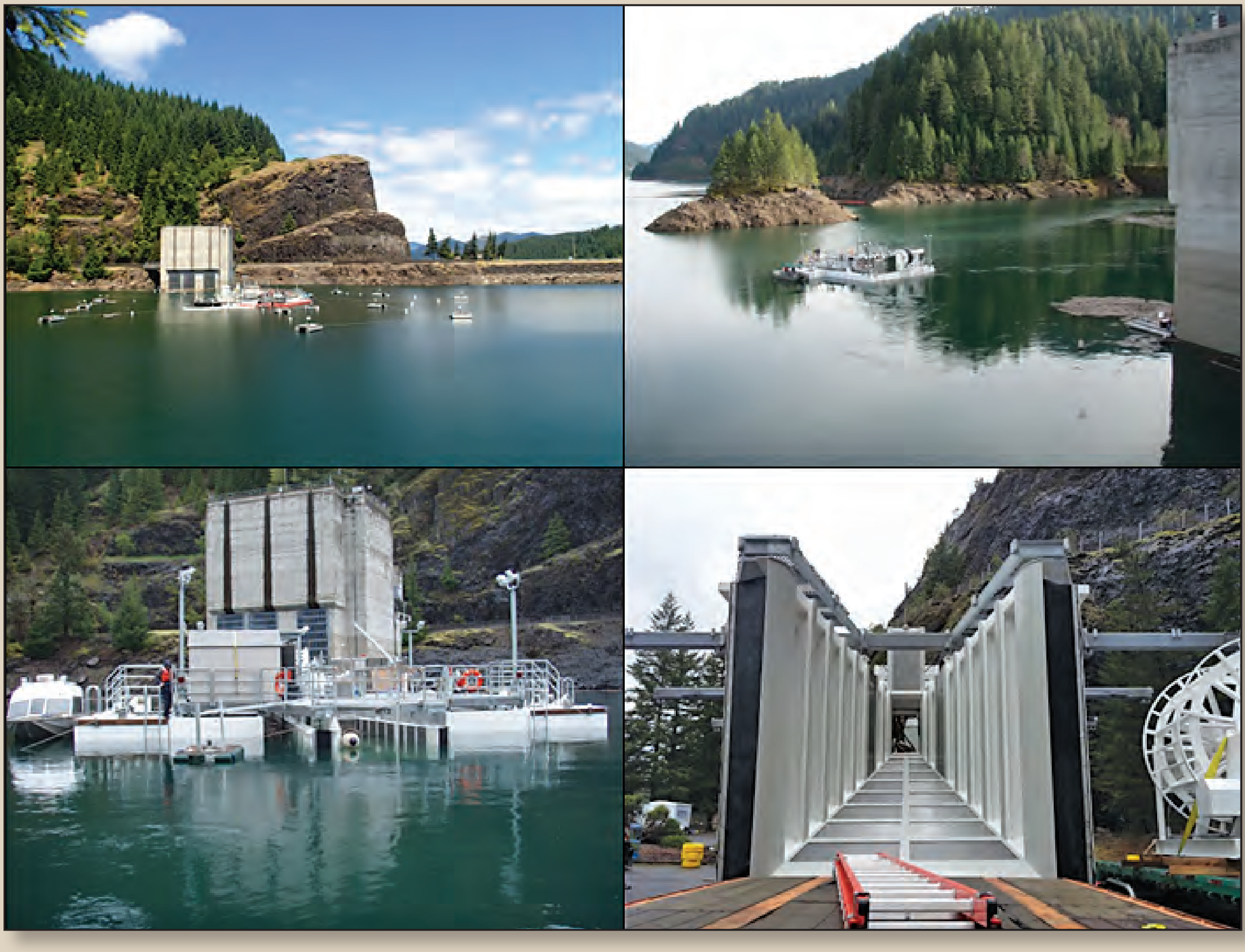

Open-File Report 2016–1003

U.S. Department of the Interior
U.S. Geological Survey

Cover: Photographs of the portable floating fish collector (PFFC) at Cougar Reservoir and Dam, Oregon, 2014.

Clockwise from the top left:
Temperature control tower, platforms suspending hydrophones, and the bow of the PFFC.
Stern of the PFFC relative to the temperature control tower.
Close up of the bow of the PFFC in front of the temperature control tower.
Entrance to the PFFC during assembly.

Photographs by Todd Pierce, U.S. Army Corps of Engineers, and Gabriel Hansen and Philip Haner of the U.S. Geological Survey.

Evaluation of the Biological and Hydraulic Performance of the Portable Floating Fish Collector at Cougar Reservoir and Dam, Oregon, 2014

By John W. Beeman, Scott D. Evans, Philip V. Haner, Hal C. Hansel, Amy C. Hansen, Gabriel S. Hansen, Tyson W. Hatton, Jamie M. Sprando, Collin D. Smith, and Noah S. Adams

Prepared in cooperation with the U.S. Army Corps of Engineers

Open-File Report 2016-1003

U.S. Department of the Interior
U.S. Geological Survey

U.S. Department of the Interior
SALLY JEWELL, Secretary

U.S. Geological Survey
Suzette M. Kimball, Director

U.S. Geological Survey, Reston, Virginia: 2016

Suggested citation:
Beeman, J.W., Evans, S.D., Haner, P.V., Hansel, H.C., Hansen, A.C., Hansen, G.S., Hatton, T.W., Sprando, J.M., Smith, C.D., and Adams, N.S., 2016, Evaluation of the biological and hydraulic performance of the portable floating fish collector at Cougar Reservoir and Dam, Oregon, 2014: U.S. Geological Survey Open-File Report 2016-1003, 127 p., http://dx.doi.org/ 10.3133/ofr20161003.

ISSN 2331-1258 (online)

Acknowledgments

This study was completed with assistance from many people and organizations. The staff at Oregon State University and cooperators on the Wild Fish Surrogate Study provided the hatchery-origin study fish, and the staff at Leaburg Hatchery provided space and facilities for us to hold them. U.S. Army Corps of Engineers staff at Cougar Dam and Todd Pierce and Andrew Janos of the Willamette Valley Project were instrumental in coordinating our activities to install equipment and monitor the tagged fish near the dams, as were David Griffith, Bob Wertheimer, and Mary Karen Scullion at the Portland District office. The Oregon Department of Transportation, City of Salem, Multnomah County, and Union Pacific Railroad provided access to the Willamette River bridges. Our administrative and science colleagues at the Columbia River Research Laboratory (particularly Theresa Liedtke, Kyle Martens, Matthew Sholtis, and Nick Swyers) contributed greatly to this study. The report was improved by reviews of Gary Johnson and Toby Kock through the U.S. Geological Survey peer review program and Todd Pierce and Stephanie Burchfield through the U.S. Army Corps of Engineers peer review program. This study was funded by the U.S. Army Corps of Engineers under contract W66QKZ33384747.

This page left intentionally blank

Contents

Figures

Tables

Conversion Factors

Inch/Pound to International System of Units

Multiply	By	To obtain
foot (ft)	0.3048	meter (m)
foot per second (ft/s)	0.3048	meter per second (m/s)
foot per square second (ft/s^2)	0.3048	meter per square second (m/s^2)
cubic foot per second (ft^3/s)	0.02832	cubic meter per second (m^3/s)

International System of Units to Inch/Pound

Multiply	By	To obtain
millimeter (mm)	0.03937	inch (in.)
centimeter (cm)	0.3937	inch (in.)
meter (m)	3.281	foot (ft)
kilometer (km)	0.6214	mile (mi)
kilometer (km)	0.5400	mile, nautical (nmi)
meter per second (m/s)	3.281	foot per second (ft/s)
liter (L)	0.2642	gallon (gal)
gram (g)	0.03527	ounce, avoirdupois (oz)

Temperature in degrees Celsius (°C) may be converted to degrees Fahrenheit (°F) as °F = (1.8 × °C) + 32.

Datum

Vertical coordinate information is referenced to the National Geodetic Vertical Datum of 1929 (NGVD 29).

Elevation, as used in this report, refers to distance above the vertical datum.

Supplemental Information

Concentrations of chemical constituents in water are given in milligrams per liter (mg/L).

Abbreviations

ADV	acoustic Doppler velocimeter
ANOVA	analysis of variance
CPUE	catch per unit effort
CSV	comma-separated values
dBBMM	dynamic Brownian Bridge Movement Model
DPE	dam passage efficiency
EE	entrance efficiency
FBE	forebay passage efficiency
FF	fish flux
FCE	fish collection efficiency
FCF	fish collection effectiveness
FPGL	Fish Performance and Genetics Laboratory
GNSS	Global Navigation Satellite System
GPS	Global Positioning System
HSD	honestly significant difference
IQR	interquartile range
JSATS	juvenile salmon acoustic telemetry system
PFFC	portable floating fish collector
PIT	passive integrated transponder
PRI	pulse rate interval
rkm	river kilometer
PVC	polyvinyl chloride
RO	regulating outlet
RPE	reservoir passage efficiency
UD	utilization distribution
USACE	U.S. Army Corps of Engineers
USGS	U.S. Geological Survey

Evaluation of the Biological and Hydraulic Performance of the Portable Floating Fish Collector at Cougar Reservoir and Dam, Oregon, 2014

By John W. Beeman, Scott D. Evans, Philip V. Haner, Hal C. Hansel, Amy C. Hansen, Gabriel S. Hansen, Tyson W. Hatton, Jamie M. Sprando, Collin D. Smith, and Noah S. Adams

Abstract

The biological and hydraulic performance of a new portable floating fish collector (PFFC) located in a cul-de-sac within the forebay of Cougar Dam, Oregon, was evaluated during 2014. The purpose of the PFFC was to explore surface collection as a means to capture juvenile salmonids at one or more sites using a small, cost-effective, pilot-scale device. The PFFC used internal pumps to draw attraction flow over an inclined plane about 3 meters (m) deep, through a flume at a design velocity of as much as 6 feet per second (ft/s), and to empty a small amount of water and any entrained fish into a collection box. Performance of the PFFC was evaluated at 64 cubic feet per second (ft^3/s) (Low) and 109 ft^3/s (High) inflow rates alternated using a randomized-block schedule from May 27 to December 16, 2014. The evaluation of the biological performance was based on trap catch; behaviors, locations, and collection of juvenile Chinook salmon (*Oncorhynchus tshawytscha*) tagged with acoustic transmitters plus passive integrated transponder (PIT) tags; collection of juvenile Chinook salmon implanted with only PIT tags; and untagged fish monitored near and within the PFFC using acoustic cameras. The evaluation of hydraulic performance was based on measurements of water velocity and direction of flow in the PFFC.

The PFFC collected 156 juvenile Chinook salmon and 280 individuals of other species, primarily dace (Cyprinidae) and largemouth bass (*Micropterus salmoides*). The collection included one of the 212 acoustic+PIT-tagged fish detected near the PFFC and two of the 1,505 PIT-tagged fish released near the head of the reservoir. No juvenile salmonids were collected between early July and early September when water temperatures near the water surface were greater than about 16 degrees Celsius (°C). Depths of acoustic+PIT-tagged fish indicated a preferential selection of water temperature of 13–15 °C, which was often deeper than the entrance to the PFFC, and those fish rarely were at depths with water temperatures greater than 16 °C. Dam passage of acoustic+PIT-tagged fish was similar to previous years, but much of the passage occurred prior to the date the PFFC began operation. Discovery Efficiency, the proportion of acoustic+PIT-tagged fish detected in the cul-de-sac that were within 10 m of the PFFC entrance and 0–6 m deep (the Discovery Zone), was 0.736 during the Low treatment and 0.639 during the High treatment. Entrance Efficiency, the proportion of fish in the Discovery Zone that were collected by the PFFC, was 0.007 during the Low treatment and 0.000 during the High treatment. Fish Collection Efficiency, the proportion of acoustic+PIT-tagged fish collected of those detected in the cul-de-sac, was 0.005 and 0.000 during the Low and High treatments, respectively. The areas of highest use by acoustic+PIT-tagged fish were between the stern of the PFFC and the outlet of the reservoir (a water temperature control tower), with the greatest use being near the tower.

Results from untagged fish detected with acoustic cameras indicated that most fish near and within the PFFC were in the 90–250-millimeter length bin and few were less than 60 millimeters long; most fish were present during crepuscular periods; trajectories of fish outside the PFFC were rarely directed toward the entrance; and many fish entering the PFFC swam back out before they could be collected.

The hydraulic performance of the PFFC did not achieve the design goals of smooth acceleration of inflow culminating in a peak water velocity of 6 ft/s and, as a result, the hydraulic performance likely contributed to the low biological performance. The greatest water velocity measured in the PFFC (1.87 ft/s) was lower than designed due at least in part to the PFFC being lower in the water column than expected. Additionally, difficulties during anchor deployment prevented placement of the PFFC as near to the reservoir outlet as planned, resulting in a PFFC position outside the prevailing flow field and known areas of high fish densities. Overall, the results indicate that location, hydraulic conditions, water temperature, and shallow depth of the entrance were among the factors contributing to the low biological performance of the PFFC in 2014.

Introduction

The U.S. Army Corps of Engineers (USACE) operates the Willamette Valley Project (Project) in western Oregon, including a series of dams, revetments, and hatcheries. The primary purpose of the Project is flood risk management, but it is also operated to provide water for hydroelectricity, irrigation, navigation, instream flows for wildlife, and recreation. The hatcheries provide mitigation for lost salmon habitat. Cougar Dam and several other dams are located on tributaries of the Willamette River (fig. 1). In 2008, the National Oceanic and Atmospheric Administration determined that the Project was jeopardizing the sustainability of anadromous fish stocks in the Willamette River Basin and mandated a series of Project improvements (National Oceanic and Atmospheric Administration, 2008).

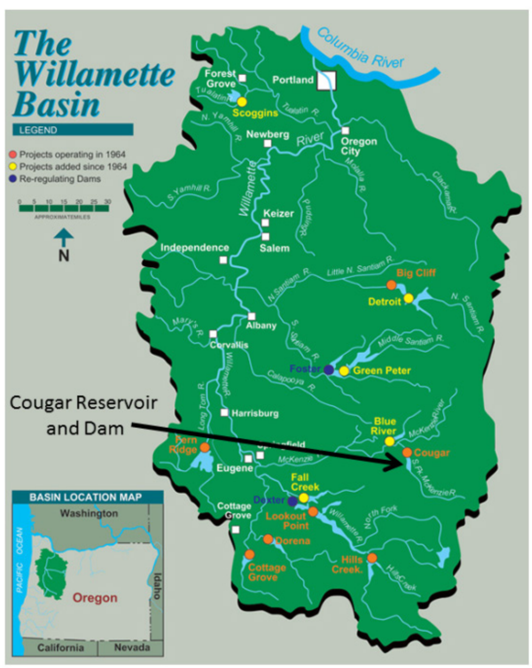

Figure 1. Graphic of Willamette River Basin Project showing Cougar Reservoir and Dam, Oregon. Graphic from U.S. Army Corps of Engineers.

Cougar Dam is a 158-m-high rock-fill dam on the South Fork of the McKenzie River about 63 km east of Springfield, Oregon. The dam, completed in 1964, is owned and operated by the USACE. It has a hydraulic capacity of 1,050 ft^3/s and two Francis turbine units capable of generating a total of 25 megawatts. During normal operations, all water passing through the dam goes through a water temperature control tower on the western end of the dam (fig. 2). The tower allows waters from various depths to be selectively passed through the dam to control downstream water temperatures using a series of moveable gates. Discharge from the tower is routed through penstocks to the powerhouse, through a regulating outlet (RO), or both. A spillway with a pair of Tainter gates is located on the eastern side of the dam, but is not used during normal dam operations. As part of the flood-control purpose of the dam, the forebay elevation is maintained at high levels during summer and low levels during winter. A maximum conservation pool elevation of 1,690 ft typically is reached in May, and a minimum flood-control pool elevation of 1,532 ft usually is reached in December and maintained until the end of January.

Figure 2. Photograph of water temperature control tower (background) and the portable floating fish collector (foreground) in the forebay of Cougar Dam, Oregon, 2014. Small floating platforms suspend hydrophones of an acoustic telemetry system. Photograph by Todd Pierce, U.S. Army Corps of Engineers, June 19, 2014.

The jeopardy finding by the National Oceanic and Atmospheric Administration spurred a series of studies including those focused on improving downstream passage of juvenile salmonids at Cougar Dam. These studies described the timing of juvenile Chinook salmon (*Oncorhynchus tshawytscha*) entering the reservoir, their growth and movements within the reservoir, the timing of their dam passage, their locations near the tower, factors affecting their dam passage, and their dam passage survival (Normandeau and Associates, Inc., 2010; Monzyk and others, 2011a, 2011b, 2012, 2013; Monzyk, 2012; Beeman and others, 2012, 2013, 2014a, 2014b; Khan and others, 2012; Romer and others, 2012, 2013; Adams and others, 2015). In response to the information provided by the studies, the USACE determined that it may be feasible to improve downstream fish passage by collecting fish near the reservoir outlet and moving them downstream, and they determined to do so with a floating surface collector. Surface collection has been shown to be a viable method of attracting juvenile salmonids (Sweeney and others, 2007), and floating surface collectors have been used at several high-head dams in the Pacific Northwest, including Upper Baker Lake (see http://www.westcoast.fisheries.noaa.gov/stories/2012/2013_01_14_floating_surface_collector.html). As a result of successes at Upper Baker Lake and elsewhere, a portable floating fish collector (PFFC) was installed in Cougar Reservoir during spring 2014 and evaluated throughout much of that year.

The PFFC was designed as a portable means to test the efficacy of surface collection at Cougar Dam including the use of multiple inflow rates with a single series of dewatering screens. To meet these goals, a modular design was used to enable the PFFC to be moved among reservoirs as needed, and the scale of the device was smaller and less expensive than a larger collector (HDR, 2012). The PFFC is about 20 × 20 m in size and uses pumps to draw water from the reservoir into a small flume, past dewatering screens, and into a collection box (fig. 3). The PFFC was designed for a maximum inflow of 100 ft^3/s and a minimum capture velocity of 6 ft/s (HDR, 2012). The PFFC was to be placed near the existing entrance to the tower to take advantage of the prevalent water currents there. The evaluation included two inflow conditions (hereinafter referred to as “treatments”) described further in section, “Operation and Hydraulic Indicators of PFFC Performance.”

The USACE installed a temporary ramp and weir in the PFFC flume prior to the study period to improve fish holding conditions by controlling bypass flow into the collection box. This was deemed necessary to reduce the volume of water entering the collection box and to improve fish holding conditions. The weir, operated at a height of about 38 cm during the Low treatment and 44 cm during the High treatment, was installed about 0.6 m downstream of the knife gate (fig. 4).

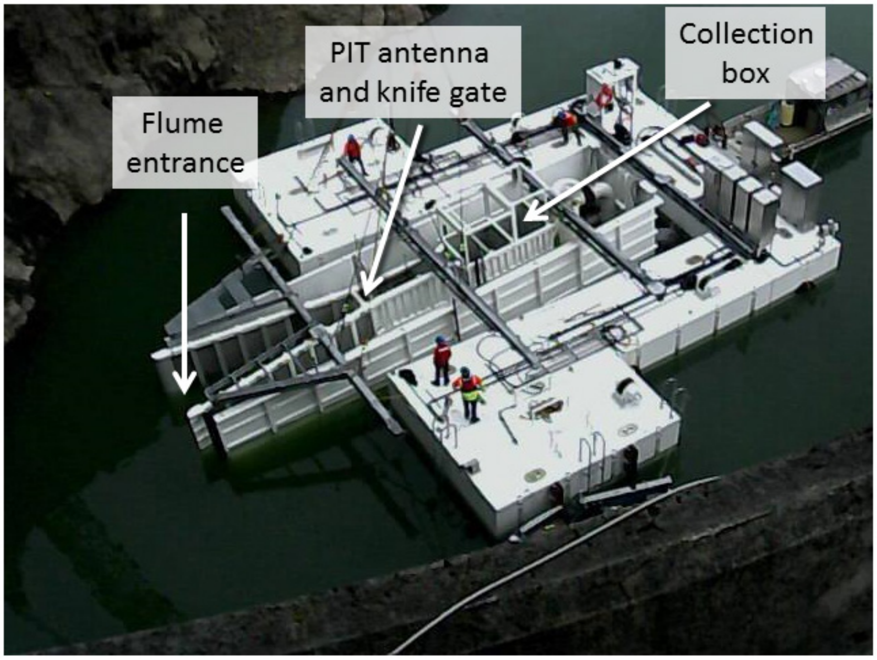

Figure 3. Photograph of portable floating fish collector during construction showing pertinent features. Photograph by Collin Smith, U.S. Geological Survey, March 26, 2014.

Figure 4. Photographs of temporary ramp and weir installed in the portable floating fish collector flume at Cougar Dam, Oregon, 2014. Photographs by Todd Pierce, U.S. Army Corps of Engineers, 2014.

The study summarized in this report was designed to provide empirical information about the movement, behaviors, collection, and passage of juvenile Chinook salmon at the tower and the PFFC to help inform decisions about future downstream passage solutions. The hydraulic performance of the PFFC was assessed by measuring water velocities near and within the flume. Measures of the biological performance were based on general fish collection by the PFFC, collection of tagged fish released near the head of the reservoir, and behaviors of fish near and within the PFFC identified using acoustic cameras. The study was designed to provide information for the following objectives:

- Estimate the seasonal and diel fish distributions within the cul-de-sac area relative to dam operations and the PFFC.
- Estimate the seasonal and diel fish behavior and movements into and within the cul-de-sac area relative to dam operations and the PFFC.
- Estimate the seasonal and diel metrics of fish passage at the temperature control tower.
- Estimate the seasonal and diel metrics of fish collection of the PFFC.

In addition to these objectives, the U.S. Geological Survey (USGS) also was contracted to measure water velocities in the PFFC, and to summarize PFFC and Cougar Dam operations and PFFC \fish collection data provided by the USACE.

Methods

Dam Operations and Environmental Conditions

Powerhouse discharge, RO discharge, reservoir elevation, depth (head) over the water temperature control tower weir gates, and water temperature data were summarized to document the environmental conditions that juvenile Chinook salmon experienced from April 9 to December 16, 2014. Hourly powerhouse discharge, RO discharge, reservoir elevation data, weir elevation, RO gate opening, and PFFC operation data were provided by the USACE. Hourly water temperature data were obtained from the USACE Web site: http://www.nwd-wc.usace.army.mil/ftppub/water_quality/tempstrings/. Elevations of the temperature sensors on the Web site were corrected to NAVD 29 datum minus 2.831 ft in accordance with deployment. Diel periods were assigned using U.S. Naval civil twilight time for Springfield, Oregon, and were obtained at http://aa.usno.navy.mil/data/docs/RS_OneYear.php. Data were summarized using the hourly observations, but mean daily values were plotted to increase clarity in the plots. Water elevation data are presented in feet and discharge is presented in cubic feet per second according to the local convention.

Operation and Hydraulic Indicators of PFFC Performance

Operating Conditions and Treatment Schedule

A randomized block design based on two inflow treatments was used in 2014. The treatments consisted of 85–90 percent of maximum speed of the attraction pumps, resulting in about 109 ft^3/s inflow at the mouth of the PFFC (High) and 50–60 percent maximum speed of the attraction pumps, resulting in about 64 ft^3/s inflow (Low; table 1). The treatment schedule prescribed 7-day treatments within 14-day blocks, except when the pumps were turned off for trap catch evaluation or other intermittent outages. A 7-day treatment length was determined to provide sufficient data for analysis and a reasonable change interval for PFFC operators.

Operating condition data for the PFFC were provided by Todd Pierce of the USACE through December 18, 2014, when the PFFC was turned off for upcoming modifications (see section, “Discussion”). The PFFC operation data include treatment blocks 1 to midway through block 15 (May 27–December 16, 2014). The PFFC operation data were independently entered by USGS and USACE employees, compared, and reconciled. The planned operating condition was assumed when pump attraction data or weir height data were missing.

Table 1. Planned portable floating fish collector operations during the acoustic telemetry and acoustic camera studies, Cougar Reservoir and Dam, Oregon, 2014.

[The Low treatment was an inflow of about 64 cubic feet per second (ft^3/s) and the High treatment was an inflow of about 109 ft^3/s]

Block	Treatment	Start	End
1	Low	05/27/2014	06/03/2014
	High	06/03/2014	06/10/2014
2	High	06/10/2014	06/17/2014
	Low	06/17/2014	06/24/2014
3	High	06/24/2014	07/01/2014
	Low	07/01/2014	07/08/2014
4	High	07/08/2014	07/15/2014
	Low	07/15/2014	07/22/2014
5	Low	07/22/2014	07/29/2014
	High	07/29/2014	08/05/2014
6	Low	08/05/2014	08/12/2014
	High	08/12/2014	08/19/2014
7	High	08/19/2014	08/26/2014
	Low	08/26/2014	09/02/2014
8	High	09/02/2014	09/09/2014
	Low	09/09/2014	09/16/2014
9	High	09/16/2014	09/23/2014
	Low	09/23/2014	09/30/2014
10	High	09/30/2014	10/07/2014
	Low	10/07/2014	10/14/2014
11	High	10/14/2014	10/21/2014
	Low	10/21/2014	10/28/2014
12	High	10/28/2014	11/04/2014
	Low	11/04/2014	11/11/2014
13	High	11/11/2014	11/18/2014
	Low	11/18/2014	11/25/2014
14	High	11/25/2014	12/02/2014
	Low	12/02/2014	12/09/2014
15	Low	12/09/2014	12/16/2014
	High	12/16/2014	12/23/2014

Water Velocities

A SonTek® acoustic Doppler velocimeter (ADV; San Diego, California) was used to measure hydraulic conditions under two operating conditions within and at the opening of the flume at the PFFC. Interpolation between point samples was used to create three-dimensional-flooded representations of velocity magnitude and point vector direction of flow for the volume sampled using Tecplot 360™software (Bellevue, Washington). Hydraulic profiles of velocity, gradient, and acceleration were calculated using methods consistent with Sweeney and others (2007).

PIT Interrogator

A single passive integrated transponder (PIT) antenna was installed during PFFC construction. The antenna was near the knife gate approximately 6 m inside the opening of the PFFC and was controlled with an IS1001 MTS controller (Biomark®, Boise, Idaho). The MTS controller was configured to produce hourly noise and status reports and transmit virtual test signals (an electronic tag signal sent from the controller to the antenna). Information from the PIT-tag interrogator was manually downloaded and detection data were uploaded into the PTAGIS database (www.ptagis.org) using the site code CGJ. Evaluation of the detection probability of the interrogator is summarized in appendix A.

Fish Collection by the PFFC

The collection of fish by the PFFC was monitored by USACE Monday through Thursday at the beginning of the season, and then 1–3 days per week later in the season because catch was lower than expected. The collection data were provided through December 18, 2014, when the PFFC was shut off for upcoming modifications. The data included collection from May 28 to December 16, 2014. The data provided were electronically entered by USGS and USACE staff and used for analysis after any differences were reconciled.

Species in the PFFC trap catch were identified by USACE staff. Juvenile Chinook salmon were assigned to year classes based on the relative growth characteristics for Cougar Reservoir identified in Monzyk and others (2012). speckled dace (*Rhinichthys osculus*),longnose dace (*R. cataractae*), and unidentified dace were pooled into "dace." Adult and juvenile bluegill (*Lepomis macrochirus*) were pooled into "bluegill." The "other" group is comprised of sculpin (Cottidae, *N*=1), northern red-legged frog (*Rana aurora*, *N*=1), rough-skinned newt (*Taricha granulosa*, *N*=2), and unidentified species (*N*=2). Fish collected live that subsequently died prior to release were considered as trap mortality. The collected fish were attributed to the PFFC treatment in operation at the time of handling. Some fish were found in holding cells during trap maintenance and may have been collected in a different PFFC treatment. Data from four dead juvenile Chinook salmon were without size measurements, but were identified by the USACE staff as subyearlings and were included in the mortality summary as such.

We calculated the catch per unit effort (CPUE) as the number of juvenile Chinook salmon collected over the total hours of trap operation in each treatment within each block, and standardized the CPUE to fish per 24 hours of trap operation. We used two-way analysis of variance (ANOVA) to test for treatment and block effects on CPUE (version 9.3 of the SAS System for Microsoft Windows© 2002–2010, SAS Institute Inc., Cary, North Carolina). When an effect was significant, the Tukey-Kramer multiple-comparison test was applied to determine the source of differences between treatments and among blocks. An $\alpha = 0.05$ was used for the tests.

Acoustic- and PIT-Tag Telemetry

Transmitters

Fish implanted with acoustic tags also were implanted with a PIT tag. We used the juvenile salmon acoustic telemetry system (JSATS) for acoustic telemetry (McMichael and others, 2010). The model SS3300 JSATS tag was manufactured by Advanced Telemetry Systems (ATS; Isanti, Minnesota) and had a mean mass in air of 0.43 g (range 0.41–0.44 g). The dimensions were 11.74 mm long × 6.26 mm wide × 3.56 mm deep. Expected transmitter life at the nominal pulse rate interval (PRI) of 10 seconds was 150 days. A 12.5-mm long full-duplex PIT tag (model SST, Biomark®, Boise, Idaho) weighing 0.10 g was placed inside the body cavity along with the acoustic transmitter. In the spring and fall, we injected PIT tags into 1,505 fish without an accompanying acoustic transmitter to evaluate PFFC collection rates. The lives of a subset of acoustic transmitters were empirically determined to define the follow-up time for analysis (appendix B). A follow-up time equal to the 90th percentile of tag life, 144.0 days, was subsequently used for analysis of data from acoustic-tagged fish.

Handling, Tagging, and Release

Hatchery and wild origin spring Chinook salmon (hereinafter referred to as hatchery Chinook salmon and wild Chinook salmon, respectively) comprised the tagged study population. Yearling fish from each origin were released in the spring and summer with acoustic and PIT tags (acoustic+PIT), and subyearling fish of hatchery origin were released in the fall with only PIT tags. The hatchery Chinook salmon were reared at the Fish Performance and Genetics Laboratory (FPGL) in Corvallis, Oregon, as part of a Wild Fish Surrogate Program funded by the USACE. The wild Chinook salmon were collected from the reservoir or the PFFC.

In the spring, hatchery Chinook salmon were delivered and held at Leaburg Hatchery in Leaburg, Oregon, prior to acoustic tagging. All transported fish were delivered by FPGL employees prior to the tag date to allow time for acclimation and an extended recovery time after transport. There were two deliveries. The first group of 575 fish was delivered on March 13, 2014, and the second group of 370 fish was delivered on April 24, 2014. The fish were sorted by size prior to transportation to Leaburg Hatchery to meet a fork-length requirement of 95–180 mm. An outdoor circular pond (6.1 m wide × 0.7 m deep; 19,539 L in volume) supplied with continuously flowing McKenzie River water was used as a holding area. The first delivery group was held for 25–45 days prior to tagging and the second delivery group was held 11–24 days prior to tagging.

Water temperature and dissolved oxygen in the transport tank were monitored throughout transport to Leaburg Hatchery. Fish were tempered by FPGL personnel during transport because the water was warmer at FPGL than at Leaburg Hatchery. Tempering consisted of placing blocks of ice made from well water into the transport tank if the difference between temperatures was more than 6 °C. Personnel stopped periodically to monitor water temperature and dissolved oxygen throughout the 3 hours of transport time. Additional tempering was performed at the hatchery if the temperatures differed by more 2 °C at time of arrival.

Fish were moved from the hatchery into a 264-L transport tank on 1 or 2 days every other week and denied food from that time forward. Pre-tag holding times were within the 18–30 hours specification of the Surgical Protocols Steering Committee (2011) except for once, when a group of hatchery Chinook salmon were handled and tagged prior to the 18 hours minimum.

Lampara seining and PFFC catches were used to obtain wild Chinook salmon for surgical transmitter implantation in the spring. USGS personnel only used the Lampara seine during April 20–23, 2014, because of a low catch per unit effort. The seine was 91.4 m long and fished to a depth of approximately 7.6 m. The seine was deployed from a boat by encircling an area and hauling the net back onto the boat by hand. Seven wild Chinook salmon were netted from within Cougar Reservoir, placed in an aerated container with fresh river water, and transported to the Cougar Dam adult fish facility where they were treated in the same manner as the hatchery Chinook salmon. One wild Chinook salmon collected by the PFFC met the criteria for acoustic tagging. From the PFFC, wild fish were netted into a perforated bucket secured with a lid, loaded into a boat or kayak, and taken to the boat ramp where the bucket was placed inside an insulated cooler filled with river water and transported to the Cougar Dam adult fish facility where they were treated in the same manner as the hatchery Chinook salmon.

Acoustic transmitters and PIT tags were surgically implanted using the protocol specified by the Surgical Protocols Steering Committee (2011) and all tagging was performed by skilled USGS employees. Fish were considered suitable for tagging if they were free of major injuries; had no external signs of gas bubble trauma, major fin damage, or fungus; were less than 20 percent descaled; had no visible signs of deformities or disease; and were not previously tagged other than with a coded-wire tag. Fish were not tagged if more than five copepods (*Salmincola californiensis*) were observed during macroscopic examination of the branchial cavities. Fish were anesthetized using buffered tricane methane sulfonate (MS-222, Argent Chemical Laboratories, Redmond, Washington). The MS-222 concentration used varied between the hatchery and wild fish and with water temperature. The concentration range for hatchery Chinook salmon was 90–140 mg/L whereas the concentration range for the wild Chinook salmon was 80–90 mg/L. Weight and length of each anesthetized fish were recorded immediately prior to surgery. All weighing, measuring, and containment equipment were treated with a 0.25 mL/L concentration of Stress Coat Plus® (Aquarium Pharmaceuticals, Inc., Chalfont, Pennsylvania) to reduce handling-related stress to the fish through electrolyte loss. Fish were placed in a 19-L perforated bucket filled with 7 L of river water immediately after surgery. Dissolved oxygen concentrations were maintained between 80 and 110 percent saturation during recovery. The mean density in a recovery bucket was 25.3 g/L (range 7.3–32.4 g/L) for hatchery Chinook salmon and 4.3 g/L (range 1.7–6.7 g/L) for wild Chinook salmon, and we did not exceed more than four fish in a recovery bucket. Water quality (water temperature, dissolved oxygen, and total dissolved gas) was monitored in holding buckets, transport tanks, the recovery raceway, and at the release sites. Fish in the recovery buckets were observed periodically during the first 10 minutes after surgery to ensure they recovered from anesthesia. Recovery buckets, fitted with bicycle inner tubes near their tops for flotation, then were fitted with lids and floated in an outdoor raceway with flowing river water where fish were held prior to release with access to air to adjust their buoyancy.

To encompass smaller fish sizes to better represent the entire run during the spring, hatchery Chinook salmon with a minimum fork length of 65 mm were implanted with only a PIT tag to estimate the PFFC collection efficiency. Hatchery Chinook salmon between 65 and 180 mm fork length were PIT-tagged in May (N=503) and in October (N=1,027). Both the spring and fall PIT-tag sessions occurred in Corvallis, Oregon, at the FPGL. The PIT tags were the same model as those implanted with the acoustic transmitters. The fish tagged in the spring were held for 20 days after tagging and released on June 4, 2014, and the fish tagged in the fall were held for 6 days after tagging and released on October 22, 2014. The PIT-tagged fish were treated in the same manner as the fish tagged with acoustic tags in all aspects of handling, tagging, tempering, and releasing, following the Surgical Protocols Steering Committee (2011). All PIT tagging was performed by skilled USGS employees.

Fish handling and release procedures were designed to minimize fish stress and maintain water quality so that fish would flourish after release. Acoustic-tagged fish were released near the head of Cougar Reservoir after the 18–36-hour recovery period specified by the Surgical Protocols Steering Committee (2011). Recovery buckets were removed from the holding raceway, inspected for mortalities, and transferred to one of two insulated 1,556-L plastic tanks mounted on a flatbed trailer. The fish then were driven to the boat ramp, transferred into a boat, and transported upstream through Cougar Reservoir about 7 river kilometers (rkm) to the release site. The release site was about halfway between the two shorelines near the Slide Creek boat ramp (fig. 5). Fish were released by partially submerging their bucket in the reservoir and gently inverting them. In the spring, the fish tagged with only a PIT tag were netted and placed in an aerated transport tank filled with fresh river water and transported to the Slide Creek boat ramp where they were released through a pipe with a diameter of 10.2 cm. In the fall, the fish implanted with only a PIT tag were transported in the same manner as the spring PIT-tagged fish, but were released from the river bank approximately 2 rkm upstream of the Slide Creek boat ramp, because the Slide Creek boat ramp was inaccessible due to a low water elevation. Water-quality measurements were taken periodically and recorded throughout transport and then again at the release site to verify if tempering was needed. Tempering was done if the difference in water temperature between the recovery buckets or tank and the reservoir was greater than 2 °C, and this frequently occurred.

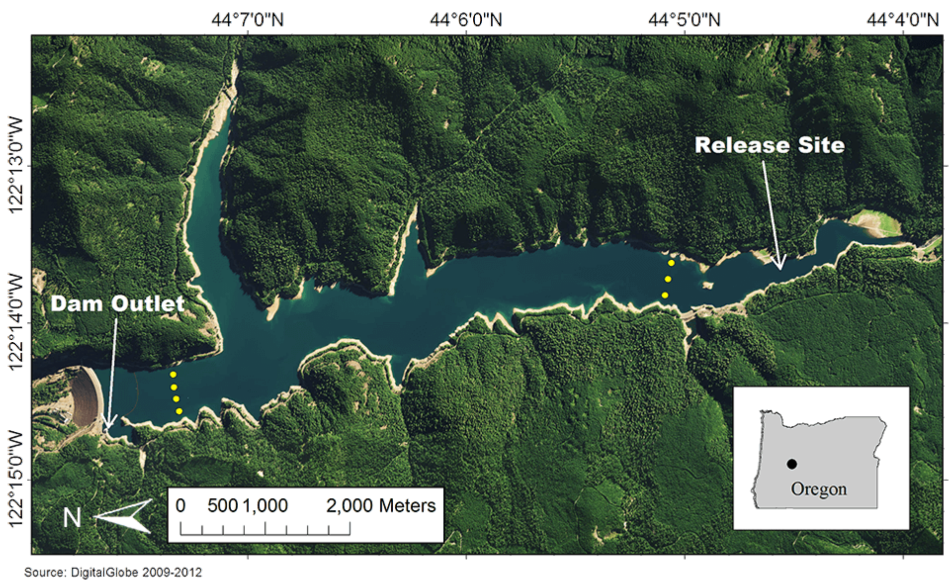

Figure 5. Orthoimage showing arrays of autonomous hydrophones (small circles) deployed in Cougar Reservoir, Oregon, 2014. The spring release location is indicated with an arrow and the fall release location is approximately 2 river kilometers upstream of that site on the right side of the image.

Acoustic Telemetry Detection Systems

Signals from acoustic transmitters were detected using two types of JSATS hydrophone systems provided by the USACE. Acoustic signals from tagged fish in the reservoir from approximately the log boom at the boat-restricted zone upstream to near the head of the reservoir were detected using autonomous hydrophones spaced across the reservoir width at two locations (fig. 5). In 2011, we empirically determined in the eastern arm of Cougar Reservoir that 82 percent of the expected number of transmissions were detected at a range of 105 m, and 10 percent were detected at a range of 180 m. Based on that data, the hydrophones were spaced about 100 m from shorelines and 200 m from each other at a depth of about 33 m from the water surface along lines across the reservoir (hereinafter referred to as “arrays”). Hydrophones were deployed using methods similar to those described by Titzler and others (2010), except that burlap bags filled with sand as anchors were used. The autonomous hydrophones were operational beginning on April 8, 2014, and were serviced at 2–3-week intervals.

Seven 4-hydrophone cabled systems linked to each other using a common clock were used to detect acoustic signals from tagged fish near the tower and PFFC. Each of these systems included four hydrophones connected with cables to a common computer. Each computer received its system time from a Global Positioning System (GPS) receiver (Meinberg GPS 170PCI, Meinberg Funkuhren GmbH & Co. KG, Bad Pyrmont, Germany). The use of a common time for all hydrophones allows the estimation of fish position based on time of signal arrival if hydrophone locations and the speed of sound in the study area are known. A GPS was used to determine locations of hydrophones deployed from floating platforms. Javad (San Jose, California) Global Navigation Satellite System (GNSS®) Sigma receivers were used to collect positional data on hydrophones anchored in the forebay. The receivers were programmed to provide real-time kinematic positions every 5 seconds. Dorne-Margolin choke ring antennas with Southern California Integrated GPS Network radomes were used to minimize multipath signals from surrounding concrete and rock structures to increase the quality of position solutions. This combination of equipment used GPS, GLONASS (Russian satellites), and Galileo satellites to compute positions within ±1 cm. The cabled hydrophone system is described by Weiland and others (2009, 2011).

The cabled hydrophone systems were installed along the upstream face of the temperature control tower at several elevations and from floating platforms (figs. 6 and 7). All hydrophones deployed from floating platforms were located 2.5 m below the water surface. Additional hydrophones were placed 17 m below the water surface at four locations near the entrance to the PFFC (fig. 7). All floating platforms around the PFFC were tied together and to the PFFC, and anchored such that the floating array moved with the PFFC as forebay elevation changed. The range of the cabled hydrophone systems was assumed to be similar to that of the autonomous hydrophones, so hydrophones were spaced with overlapping coverage. This assumption seemed reasonable because each transmitter signal typically was detected by most of the cabled hydrophones.

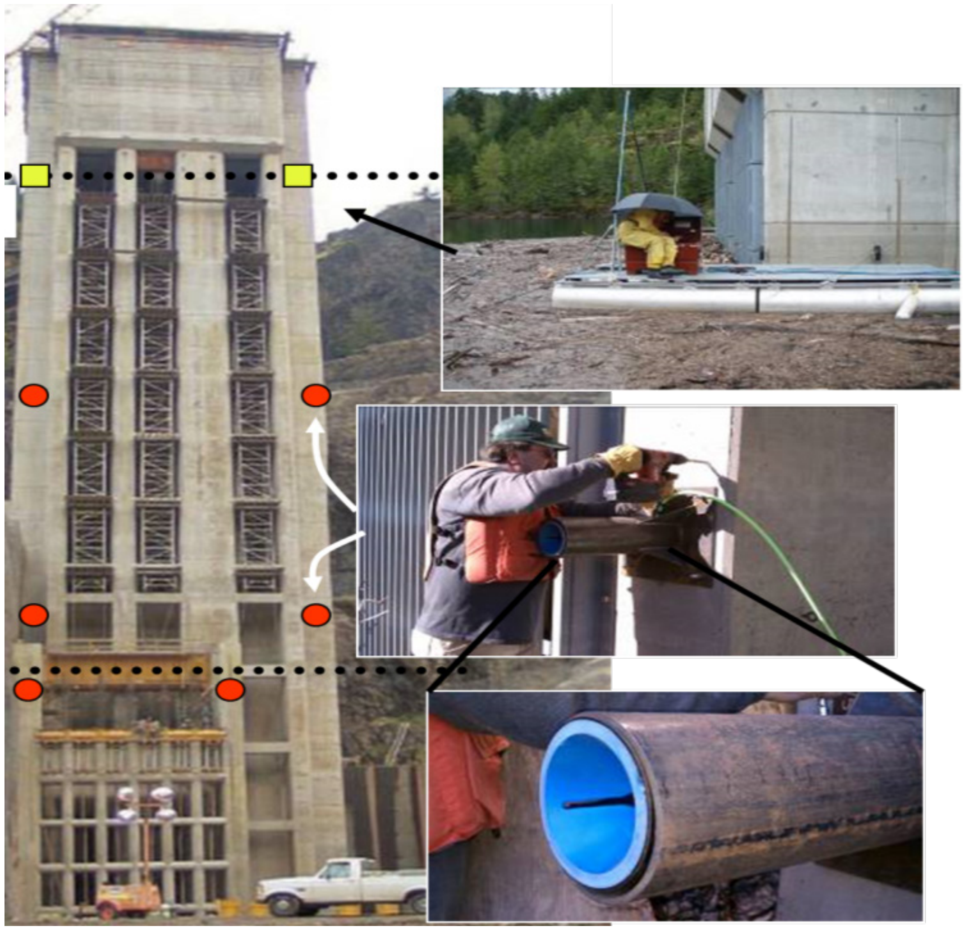

Figure 6. Photographs showing locations of cabled hydrophones nearest the water temperature control tower at Cougar Dam, Oregon, 2014. Round symbols represent hydrophones affixed to the water temperature control tower, and square symbols indicate hydrophones mounted from floating platforms. Dotted lines represent approximate locations of full and minimum conservation pool water elevations of 1,690 and 1,532 feet, respectively. Photograph taken during construction in 2005 provided by U.S. Army Corps of Engineers, and inset photographs taken by Amy Hansen (upper photo, May 17, 2011) and Scott Evans (February 2, 2011) of the U.S. Geological Survey.

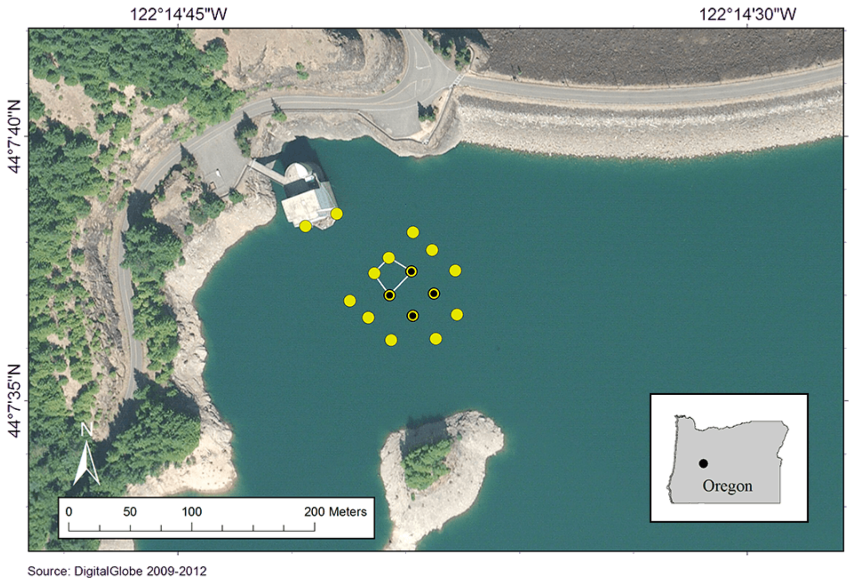

Figure 7. Orthoimage showing locations of hydrophones (circles) deployed 2.5 m below the water surface from floating platforms near the water temperature control tower at Cougar Dam, Oregon, 2014. Locations identified by darkened circles had an additional hydrophone 17 meters below the water surface. Hydrophone symbols at the corners of the portable floating fish collector are joined with a thin line.

Two cabled hydrophones were installed inside the temperature control tower to collect data for confirmation of tower entry and passage. These hydrophones temporarily were out of the water and not collecting data from August 9 (shallow hydrophone) and August 16 (deep hydrophone) through September 10 when the hydrophones were lowered back into the water. To detect acoustic-tagged fish as they migrated through the South Fork McKenzie, McKenzie, and Willamette Rivers, we deployed autonomous hydrophones at six locations downstream of Cougar Dam: (1) two hydrophones in the tailrace (one each in the powerhouse and RO tailraces); (2) one about 1.5 rkm downstream of the dam near USGS stream gage number 1415410; (3) two in the Leaburg Dam forebay (40.3 rkm downstream of Cougar Dam); and six each in (4) Salem, (5) Wilsonville, and (6) Portland (210, 283, and 323 rkm downstream of Cougar Dam, respectively).

Removing False-Positive Records

Data from the hydrophones were processed to remove false-positive records prior to analysis. False-positive records are those that indicate detection of a transmitter when the transmitter was not present, and are common in most active telemetry systems (Beeman and Perry, 2012). We used the procedures developed by Pacific Northwest National Laboratory (Mark Weiland, written commun., June 17, 2010) to remove false-positive records. The steps include removing records from tag codes not released, records suspected of being from reflections of valid tag signals (multipath), and records that are not close to a multiple of the tag pulse interval (McMichael and others, 2010). Records from the cabled hydrophone system also were required to be present on more than one hydrophone to be retained.

Estimating Fish Positions

Fish positions within the area monitored by the cabled-hydrophone system near the dam were estimated using software developed through a USGS subcontract with the University of Washington (Seattle, Washington). The software estimates fish positions using an iterative technique using the Gauss-Newton method to find the location that minimizes the root-mean squared misfit to all available arrival-time data by repeatedly solving a set of linearized equations relating adjustments in location to changes in the arrival time misfit (Klein, 1978; Lee and Stewart, 1981; Menke, 1989; Speisberger and Fristrup, 1990). The software uses all available hydrophones and can adjust the speed of sound in water for vertical changes in water temperature using the method of Moser (1991). Water temperatures from the temperature string near the temperature control tower were used for this purpose.

Fish position estimates were passed through a filter to identify and remove spurious results. The filter limited swim speeds to a burst speed of as much as 3 m/s for 20 seconds, or a sustained speed of as much as 1.0 m/s for more than 20 seconds based on values from the literature (Bainbridge, 1960; Webb, 1978; Taylor and McPhail, 1985; Mesa and others, 2008). The first observation of each trip into the monitored area was omitted because of the lack of data to estimate swim speed, and a new trip was assigned if the time elapsed between successive positions was greater than the 99th percentile (1,767 seconds). The filter identified 2.0 percent of the estimated positions.

Travel Times

Analyses of the timing of downstream movement in the reservoir and tower or PFFC passage were conducted using time-to-event methods (Hosmer and Lemeshow, 1999). The time elapsed from fish release to two event types was described using Kaplan-Meier survivorship functions. The event types were (1) detection by any autonomous hydrophone receiver near the log boom, and (2) detection within 10 m and at a depth of 0–6 m from the entrance to either the PFFC or tower. Analysis of travel times were restricted to after the PFFC operations began on May 27, 2014. Fish that passed the dam or had not experienced an event by the 90th percentile of the empirically determined transmitter life were right censored at that time.

Depths in the Cul-de-sac

Depths of fish were determined for acoustic+PIT-tagged fish from May 27, 2014, to the 90th percentile of each tag life, during all PFFC operations. To reduce outliers, we omitted positions outside the outermost barges in the cul-de-sac and the deepest 1 percent of fish depths by date. The mean hourly depths were calculated from the median hourly depths of each fish.

Temperature Selection

A standardized resource selection index was estimated to determine if water temperatures were preferentially selected by acoustic+PIT-tagged fish within 20 m of the PFFC entrance or within 20 m of the tower entrance. We used the method of Manly and others (1993) as described by Rettie and Messier (2000) with water temperature as the available habitat and the water temperature at the fish depths as the habitat selected. Water-temperature data from the string at the tower and fish depths from the acoustic telemetry system were used to estimate the index. A monthly index was estimated for each integer value of water temperature at depths within the 99th percentile of the daily maximum fish depth (the habitat available) based on the water temperatures at the mean of the median daily depths of each fish (the habitat selected). The sum of the monthly standardized resource selection index within an individual month is 1.

Spatial Intensity of Use

Fish distributions relative to the PFFC location and operating conditions were estimated spatially and temporally. Fish positions estimated using the acoustic telemetry array in the cul-de-sac were used to estimate utilization distributions (UDs) using the dynamic Brownian Bridge Movement Model (dBBMM) of Kranstauber and others (2012). The dBBMM uses both spatial and temporal information from a series of positions as well as the position-specific location estimation errors to estimate the UD as a probability of use among cells of a raster, where UD values in the raster sum to 1. Location estimation errors in the monitored area were empirically determined for this purpose and are described in appendix C. Data were prepared for use in the model by grouping positions from each tagged fish into quasi-independent trips (bursts) separated by gaps of at least 30 minutes using the adehabitatLT package for R software (R Core Team, 2014). The UDs were estimated using the Move package for R software with model parameters of a 5 × 5 m raster cell size, an extent of 0.7, a window size of 9, and a margin of 3. The window and margin sizes control the boundaries of a moving window used in estimating the UD. We used the smallest window and margin settings allowable due to the small spatial area of the cul-de-sac and high frequency of positions based on the 10-second PRI of the tags; this resulted in a minimum burst of 9 positions for inclusion in the analysis (an alternate method is described in the next paragraph). Location errors were based on data from stationary and moving test tags interpolated to the fish positions using the Kriging process (appendix C for estimates of positioning system accuracy). We estimated UDs for data divided into operational strata (Low and High treatments as well as before the PFFC treatments began and when the PFFC was off during the day), environmental strata (Day or Night defined using civil twilight times), and biological strata (five 3-m fish depth bins from the water surface to 15 m deep). The UD for each stratum was calculated by averaging UDs among bursts within each fish and then averaging UDs among fish. Differences between UDs during the Low and High treatments were estimated by raster subtraction ([Low treatment – High treatment] ÷ smaller of the two treatments) after projecting the data on the same raster and omitting values outside the 99th percentile of the largest UD within strata. The 99th percentile was determined after rounding UD probabilities to the nearest 0.001. This resulted in positive values when the UDs of the Low treatment were larger than UDs of the High treatment, and negative values for the opposite case. The total number of cells within each raster varied based on the extent of the data in each stratum, but was generally about 9,000. The spatial patterns in UDs were summarized in color-coded plots of UDs up to the 99th percentile of UD probabilities.

Fish use within 20 m of the PFFC entrance was not estimated using the dBBMM because of the limited sample size and the short burst lengths near the PFFC entrance. For that area, we estimated the spatial fish use by calculating the percentage of the positions from each burst within each of 60 4 × 4 m cells of a raster and averaging in the same manner as with the UDs for the cul-de-sac. This method has the advantage over the dBBMM of not restricting the data available by the number of positions within a burst, but does not include advantages of the dBBMM models such as incorporating position estimation errors; however, the estimation error varied little over this small area (appendix C). Differences between strata were estimated as for UD differences.

Behaviors near the PFFC Entrance

The bearings (directions) of individual fish trajectories within 10 m of the PFFC entrance were used to further characterize the movement behavior of tagged fish near the collector during each treatment. The sequential positions from each fish were divided into trips (bursts) as described for the spatial analysis (section , “Spatial Intensity of Use”), except a new trip was initiated whenever the gap between two consecutive positions was greater than 5 minutes instead of 30 minutes. Each position in a burst was assigned to 1 of 10 4 × 5 m cells in front of the PFFC and the bearing to the next location in the burst was calculated. Bearings were transformed so that a bearing of 0 degrees was oriented perpendicular to the collector. Mean bearings were estimated for each cell within a burst and then averaged among bursts using second-order circular analysis methods (Zar, 1999). The mean bearings for all fish positioned in a cell were displayed as a scatter of points on the circumference of a circle and then overlaid with a rose diagram with 24 sectors so they could be examined visually for trends. The nonparametric second-order Moore test was used to test whether the mean bearings in each plot came from a population of uniformly (randomly) distributed bearings, or alternatively, that the means were from a population in which the bearings were not randomly distributed (Zar, 1999). The Moore test was considered significant when $P < 0.05$.

Collection in the PFFC and Dam Passage

Passage of acoustic+PIT-tagged fish through the PFFC or water temperature control tower was determined using presence data from the cabled hydrophones nearest the outlets at Cougar Dam. The date and time of assumed dam passage were assigned if the first detection of the last transmitted message was at any of the hydrophones located closest to the water outlets. This method was selected to limit passage assignments to fish last detected in the area generally in the cul-de-sac, and was consistent with histories of tagged fish known to have passed the dam based on detections of PIT tags downstream. We estimated several general fish passage metrics (table 2). Ninety-five percent confidence intervals were calculated for these metrics using the Wald method.

Table 2. Passage and fish collection efficiency definitions.

["Number" refers to number of tagged fish. PFFC, portable floating fish collector. Reservoir passage efficiency and dam passage efficiency were measured from release through October 11, 2014. The DPE and FCE estimates are from data collected from May 27 through October 11, 2014. Routes include PFFC and tower. ft^3/s, cubic feet per second; m, meter]

Metric	Acronym	Definition
Reservoir passage efficiency	RPE	Number detected at log boom ÷ number released
Forebay passage efficiency	FBE	Number detected in cul-de-sac ÷ number detected at log boom
Dam passage efficiency	DPE	Number passing (Tower + PFFC) ÷ number detected at log boom
Discovery efficiency	DE	Number positioned within 10 m from route at 0–6 m deep ÷ number positioned in cul-de-sac
Entrance efficiency	EE	Number collected by route ÷ number positioned within 10 m from route at 0–6 m deep
Fish collection efficiency	FCE_{FB}	Number collected by route ÷ number detected at log boom
Fish collection efficiency	FCE_{CDS}	Number collected by route ÷ number detected in cul-de-sac
Fish collection effectiveness	FCF	Fish collection efficiency ÷ PFFC inflow normalized to 100 ft^3/s

Acoustic Cameras

Surveillance Systems

Two acoustic cameras were used to collect data on fish movements immediately upstream of and inside the PFFC. A DIDSON® 300 (1.8 MHz, 29° beam, 15 m range) and ARIS® 3000 (3.0 MHz, 30° beam, 5 m range) cameras were used at different times during the study period to monitor fish behavior inside the throat of the collector and perpendicular to the opening. These acoustic camera technologies were selected to optimize the likelihood of observing the greatest number of fish targets regardless of fish size. The ARIS® camera had a limited range compared to the DIDSON®, but was able to detect fish as small as 30 mm in length. The DIDSON® camera had a greater range but only detected fish greater than 40 mm. Regardless of the camera, it is important to remember that positively determining the species of each individual target, especially with small fish, is not possible with acoustic camera technology.

At the beginning of the study, the ARIS® acoustic camera was mounted in the center of the PFFC entrance flume at a depth of 0.5 m below the surface of the water, and aimed toward the center of the PFFC entrance (fig. 8). The DIDSON® acoustic camera was deployed from a floating platform positioned on the southwestern corner of the PFFC entrance (fig. 8). The platform was affixed by a rigid beam to the PFFC to provide stable positioning of the platform. The DIDSON® acoustic camera was attached to a pole mounted on the platform, lowered to a depth of 2 m below the surface of the water, and aimed perpendicular (west to east) to the entrance of the PFFC. Following the removal of the ARIS® acoustic camera on October 23, 2014, for servicing, the DIDSON® acoustic camera was removed from the floating platform and was positioned within the PFFC flume in a manner similar to the manner previously described for the ARIS® camera. Both cameras were deployed on rotators to enable aiming.

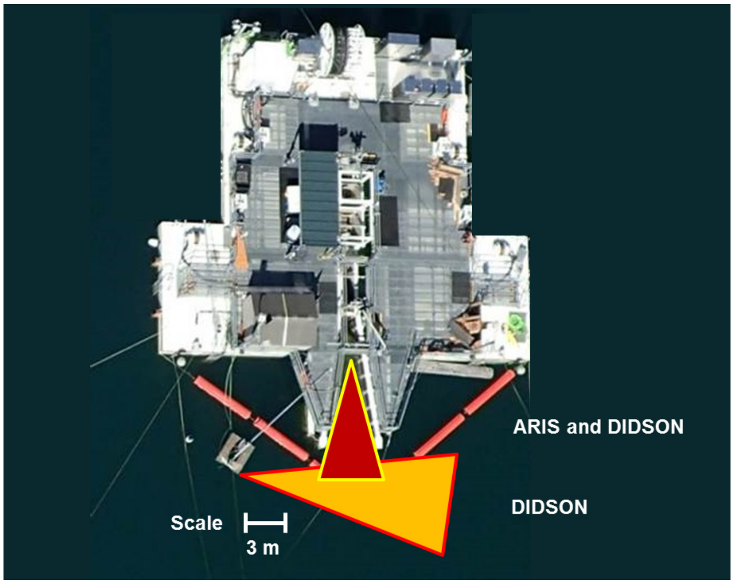

Figure 8. Schematic showing approximate coverage areas of the ARIS® and DIDSON® acoustic cameras at the entrance of the portable floating fish collector at Cougar Reservoir, Oregon, 2014.

Data Processing

Data were processed according to the area that was monitored by the acoustic cameras. All data collected with the DIDSON® camera when it was mounted outside of the PFFC to monitor fish behavior near the entrance were processed together. Similarly, all data collected by the ARIS® or DIDSON® cameras when they were positioned inside the flume viewing out through the entrance were processed together. The externally mounted DIDSON® view included dates from May 30 to October 22, 2014, and all data collected were processed and tracked without subsampling. Data were collected inside the PFFC with the ARIS® or DIDSON® cameras from June 20 to December 03, 2014. Because of the large volume of data collected with these cameras, we subsampled two 15-minute blocks of every hour for each 24-hour period. Additionally, between June 24 and July 07, 2014, there were fish with long residence times within the view of the acoustic camera, so we subsampled data at a rate of two randomly sampled 5-minute periods for each hour. For similar reasons, the data collected October 23–December 03, 2014, were subsampled for two 15-minute randomly sampled periods of each hour on approximately every fourth day. The duration of each subsampled date was from midnight to midnight. For subsampled hours, fish counts were extrapolated to 24-hour estimates for further analysis.

Signal processing of the raw acoustic signals was analyzed using Echoview® software (version 5.4, Myriax Pty. Ltd., Hobart, Tasmania, Australia). The software is a visualization and analysis program for hydroacoustic data that allows a greater proportion of data to be processed than could be done conventionally. The Echoview® platform allows the operator to use successive filters to manipulate data to enhance the acoustic signal and remove static objects and noise from acoustic returns (Kang, 2011). Non-stationary acoustic returns then are identified as targets within individual camera frames and converted into three-dimensional position and time data that can then be applied to target tracking. The conceptual layout of the virtual variable interface for the processing of acoustic camera data is depicted in figure 9. Each object in the layout represents operational steps applied to the original data, which allows each individual step to be optimized to maximize efficiency and improve consistency (Boswell and others, 2008).

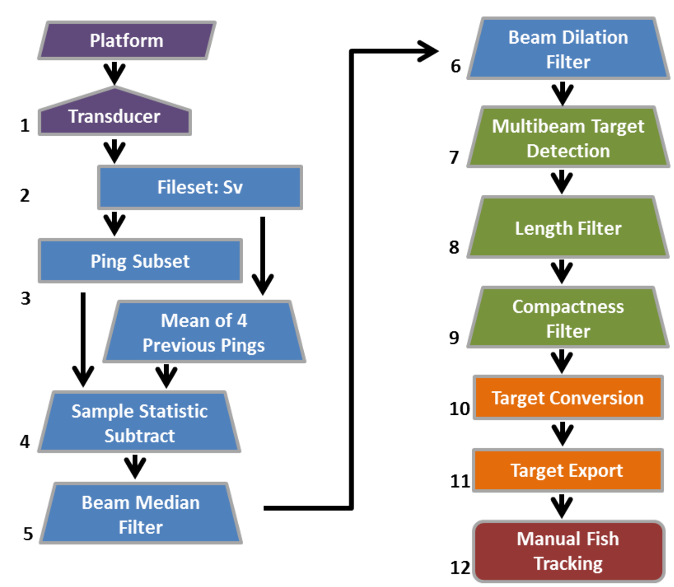

Figure 9. Data flow of the semi-automated Echoview® processing structure used to process acoustic camera targets at the portable floating fish collector at Cougar Reservoir, Oregon, 2014. Numbers represent steps in the process.

Analysis included a multi-step process. Initially, geospatial and positional data for each camera were associated with the geographic location of the platform to enable each target to be geospatially referenced (fig. 9, step 1). Next, acoustic camera data files were loaded into Echoview® and converted into volume back-scattering strength (Sv) from raw signal magnitudes (fig. 9, step 2). To remove stationary objects (such as the structure of the PFFC) from the data, targets were deemed immobile by calculating the mean results of the four previous pings, which also had targets that did not move. These targets then were removed from the dataset (fig. 9, step 3). Next, static noise was removed by implementing a sample statistic subtract operator (fig. 9, step 4). This process implements a synthetic ping into the background signal, and then subsequently subtracts the synthetic ping from each actual ping. This process leads to an increase in the signal-to-noise ratio by the removal of pings returned from inanimate objects and background noise. Following background noise subtraction, the image was enhanced by applying convolution (median and dilation) algorithm filters (fig. 9, steps 5 and 6). These filters used the median and maximum values of a data point and the eight direct neighboring cells to remove interference and smooth the image without significantly affecting the shape of the target. The next step was to use the multibeam target detection operator to generate multibeam targets from the multibeam data (fig. 9, step 7). These three-dimensional targets were created from groups of adjoining data points (clusters), which then were reduced to point data that include the geometric values of each fish target. Length and compactness filters then were applied (fig. 9, steps 8 and 9) to remove targets that were estimated to have physical properties outside the expected values for fish. The target conversion process was used next (fig. 9, step 10) to transform multibeam targets into single-point targets. Following the operational steps of filtering noise and smoothing the data, all single targets with all associated target properties were exported as comma-separated values (CSV; fig. 9, step 11). These CSV files then were reimported into Echoview® for further tracking and analysis (fig. 9, step 12). The purpose of fish tracking is to obtain counts and movements of individual fish, along with their associated behavioral and morphometric data (Simmonds and MacLennan, 2005).

Data Analysis

Summary statistics of fish targets derived from Echoview® (e.g., mean length, direction, speed, angle, orientation) were imported into SAS (version 9.3, of the SAS System for Windows© 2002–2010, SAS Institute Inc., Cary, North Carolina) for subsequent proofing and to combine datasets with PFFC operations and environmental conditions. Data were proofed to eliminate non-valid records or records that did not provide measurable morphometric or behavioral data. To consider a fish track as valid, we required that each fish track have at least five pings and a minimum duration of detection of 1 second. It is important to note that the acoustic camera technology cannot distinguish fish that have entered and exited the field of view multiple times; therefore, the detection duration for each individual fish track within a camera beam was determined by the time a fish was first detected by the camera, to the time that the fish exited the camera view. Datasets for each camera type then were exported as CSV files for statistical analysis.

A daily fish abundance index was calculated by summing the numbers of targets observed for each date. Where subsampling occurred, total fish number counts were adjusted to estimate the abundance for a 24-hour period.

Direction of Fish Travel

To summarize the directions of fish traveling in front of and within the entrance of the PFFC, we implemented circular statistics to calculate modes and measures of variability (Mardia and Jupp, 2000) using R software (R Core Team, 2014). Tests for randomness were performed to determine if the sample population presented either uniform (random) or directed travel paths. If the data were shown to conform to a Von Mises distribution (Zar, 1999; Pewsey and others, 2013), the Rayleigh z test was performed. Data that were multi-modal or did not follow a Von Mises distribution were subjected to the Rao's spacing test (Batschelet, 1981). In instances where travel paths had axially bimodal tendencies (modes are 180° apart from each other), angles were doubled (in accordance with Zar, 1999) to transform the bimodal sample into a unimodal sample for further analysis. If the *P*-value was significant (at the $\alpha = 0.05$ level), then it was assumed that the direction of fish travel was non-random.

Track Characteristics

Fish track characteristics were quantified using travel speed, duration in beam, and tortuosity variables exported from Echoview®. Travel speed was calculated as the average travel velocity of each individual target. Duration of observation is the time that a target was observed within the view of the acoustic camera. A tortuosity index (τ) was calculated as adapted from Johnson and Moursund (2000) where:

$$\tau = \left(\frac{\text{Sum of Length of a Track}}{\text{Straight Line Track Distance}}\right) \tag{1}$$

Applying this calculation of tortuosity, a fish traveling in a straight line will have a tortuosity index of 1.0, whereas a fish traveling in a non-linear path will have a tortuosity index of greater than 1.0.

For each of the fish track characteristics, ANOVA was used to test for significant differences between the PFFC treatments. If significant differences were found using ANOVA, an F-test by PFFC treatments and Tukey's honestly significant difference (HSD) test (Sokal and Rohlf, 1969) were used to locate the pairwise differences in concentrations between treatments. Statistical analyses were done using R software (R Core Team, 2014) with a significance level $\alpha = 0.05$.

Spatial Fish Distribution

Three-dimensional density plots were used to characterize the spatial distribution of fish upstream of the PFFC (Tecplot 360™, Bellevue, Washington). Because the spatial resolution within the view of each camera was relatively small (about 1 cm), we did not need to interpolate any of the data to create the density plots. The magnitude of the point count is defined as the count of unique observations of each individual fish location within each cell. Datasets for each camera type were used for plotting location data for each size category of fish by diel period.

Entrance and Rejection at the PFFC

Data collected with the cameras located inside the PFFC and directed outward were examined to determine if fish were approaching and then rejecting the entrance. To do this, we divided the entrance of the PFFC into four 2.5-ft-wide segments, and the direction a fish moved was characterized by observing fish moving from one segment into an adjacent segment. The proportion of fish moving in each direction was calculated by counting the number of fish traveling in either direction (e.g., toward or away from the PFFC) divided by the total number of fish observed within the segment. Only fish that could be observed moving into an adjacent segment were included in the analysis. The datasets for both acoustic cameras were used for plotting the direction data for each fish size category by PFFC treatment. The direction data also were overlaid on the flume water velocity data obtained by ADV sampling.

PFFC Collection Metrics

Fish collection metrics (table 3) at the entrance to the PFFC were estimated using the data collected with the acoustic cameras located inside the PFFC and directed outward between June 20 and December 3, 2014. This period offered daily acoustic camera data that could be compared to congruent trap operations and catch numbers from fish captured in the PFFC collection box. Fish numbers are based on the total fish observations for the entire study period. All size categories of fish were pooled because of the absence of length records for non-salmonids (primarily largemouth bass [*Micropterus salmoides*] and dace [*Rhinichthys* spp.]) collected in the trap.

Table 3. Fish collection metrics at entrance of the portable floating fish collector (PFFC) estimated using acoustic camera data collected in the forebay of Cougar Dam, Oregon, June 20–December 3, 2014.

Metric	Acronym	Definition
Entrance efficiency	EE	Number entering the PFFC ÷ number observed (0–2 meters outside)
Fish flux	FF	Number entering the PFFC- number leaving the PFFC
Fish collection efficiency	FCE	Number collected in PFFC ÷ number entering the PFFC
Fish collection effectiveness	FCF	Fish collection efficiency ÷ PFFC inflow (percent of 100 cubic feet per second)

Results

PFFC Operation and Data Collection Periods

Schedules for PFFC operation and installation of biological monitoring systems determined the periods available for analysis. The randomized-block treatment schedule of PFFC operations began on May 27, 2014, and ended on December 16, 2014 (table 4). Data from the four primary sources of biological data—the PFFC collection, the acoustic+PIT-tagged fish, the PIT-tagged fish, and the acoustic camera recordings—were available for different periods based on the installation dates; however, data from at least one of the systems was available from April 9, 2014, to March 30, 2015.

Table 4. Study periods based on operating conditions and data collection methods at the forebay of Cougar Dam, Oregon, 2014.

[PFFC, portable floating fish collector; JSATS, juvenile salmon acoustic telemetry system; PIT, passive integrated transponder]

Category	Dates
PFFC operations	May 27–December 16, 2014
JSATS releases	April 9–June 18, 2014
JSATS presence monitoring	April 9–October 28, 2014
JSATS positions in cul-de-sac	May 16–October 21, 2014
JSATS tag life for analysis	April 9–October 11, 2014
PIT releases and monitoring	June 4, 2014–March 30, 2015
Acoustic cameras	May 30–December 3, 2014

Dam Operations and Environmental Conditions

Dam operations and environmental conditions followed typical seasonal patterns, with the exception of reservoir elevation, which receded earlier than usual. Reservoir elevation increased until it reached full pool on May 8, 2014, and stayed at about 1,690 ft until it began to decline in early June 2014 (fig. 10). The reservoir elevation declined steadily until the end of the evaluation period on December 16, 2014. In most years, the reservoir elevation remains near full until September when the beginning of drawdown for flood risk management begins. In contrast, water temperature in the upper 13–19 ft of the water column increased steadily until it peaked at 21.3 °C on August 10, 2014, and the minimum water temperature of 5.6 °C occurred on April 1, 2014 (fig. 11). The top 13–19 ft of the water column near the tower were at least 17 °C in July, August, and September, and were predominantly less than 8 °C at depths greater than or equal to 33 ft (10 m) year round. Discharge peaked at 2,990 ft^3/s on May 10 at 11:00 a.m., and had smaller peaks in June, November, and December. Mean hourly discharge was 918.0 ft^3/s (range 380.0–2,990.0 ft^3/s) for the project, 652.0 ft^3/s (range 0.0–1,630.0 ft^3/s) for the powerhouse, and 266.7 ft^3/s (range 0.0–2,600.0 ft^3/s) for the RO (appendix E). The RO began operation on April 3, 2014, and operated intermittently during periods of high discharge through the spring and then operated nearly continuously from late October through December. Discharge was slightly higher during the night than during the day (appendix E). Temperature control regulated by the nine weir gates occurred until November 18, 2014, when the gates were returned to the top of the tower. The head over the weir gates commonly followed trends in discharge during the study period.

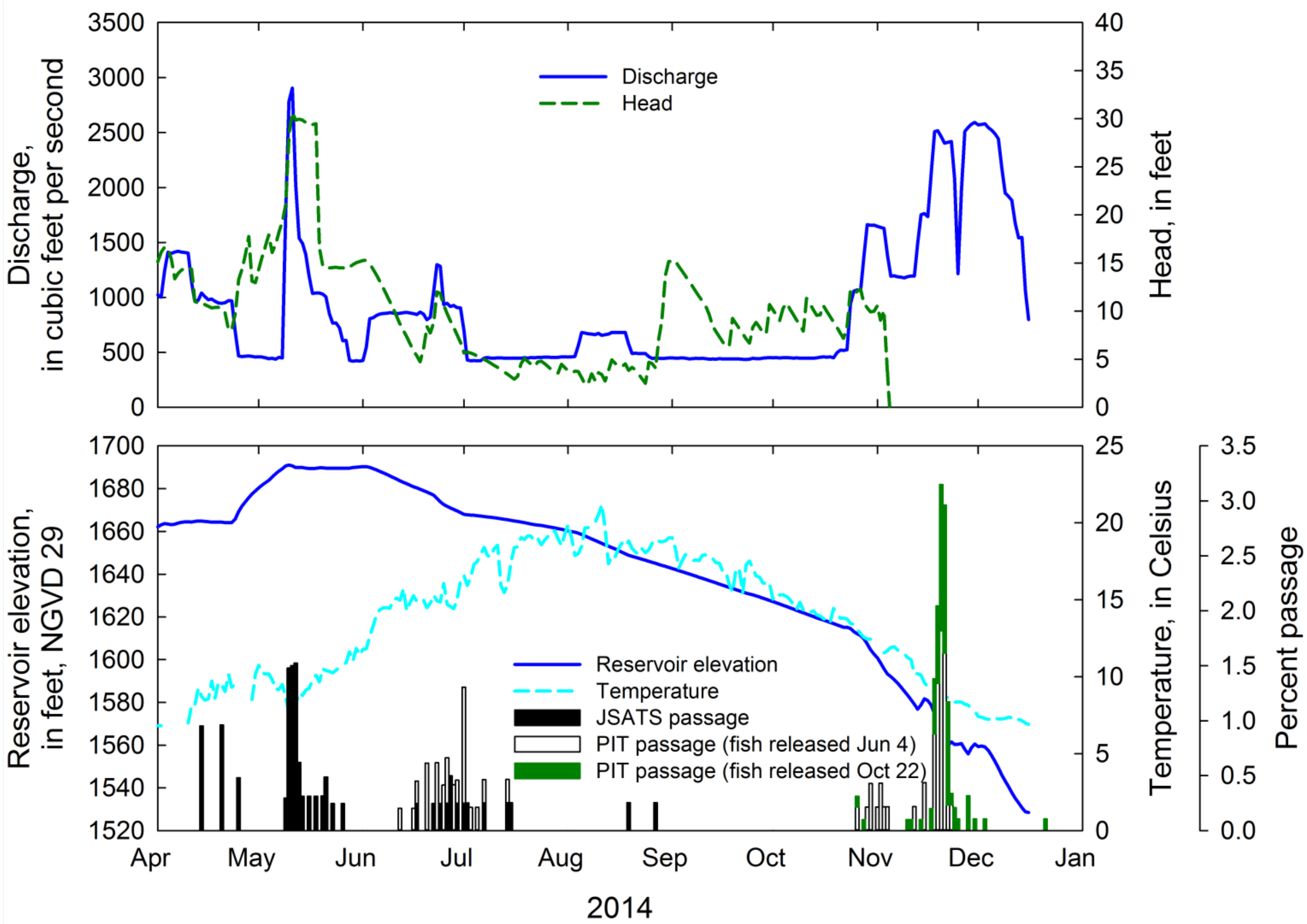

Figure 10. Graphs of mean daily project discharge and head over the weir gates (top), and reservoir elevation and water temperature (bottom) at Cougar Reservoir, Oregon, April 9–December 16, 2014. Water temperature is the average of the upper 13–19 feet of the water column near the water temperature control tower. Additionally, the bottom graph shows daily passage of juvenile Chinook salmon through the water temperature control tower and portable floating fish collector of as a percentage of fish in the reservoir available to pass (vertical bars).

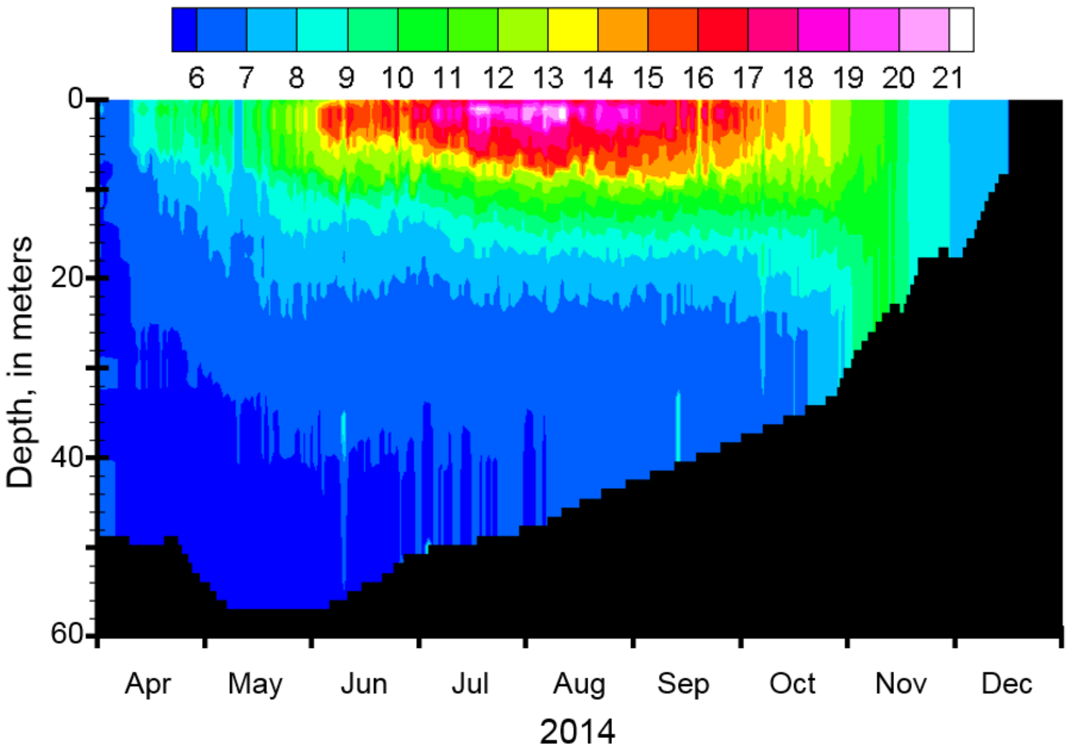

Figure 11. Contour plot of hourly temperature in degrees Celsius by water depth of the sensors at the water temperature control tower between April 1 and December 16, 2014, at Cougar Reservoir, Oregon, 2014.

Operation and Hydraulic Indicators of PFFC Performance

Operating Conditions and Treatment Schedule

The two-treatment block schedule was adhered to with the following exceptions (table 5). The High treatment used a setting of 90 percent (of maximum speed of the attraction pumps) during block 1 and was changed to 85 percent to reduce vibration for much of the remainder of the study, except when the weir ramp was removed during December 11–15 and the High treatment was changed to 75 percent. Attraction pump settings for the Low treatment included 60 percent for block 1 and 50 percent for all other blocks. The trap was off when crews performed maintenance, worked up the collected animals, modified the weir for changing the treatment, or during power outages. During the Low operation in block 2, the operation was changed to High overnight during June 19–20 to allow the USGS to conduct water velocity measurements using an ADV. In block 8, the Low treatment was extended two days (to 9 days) and in block 9 the Low treatment was reduced by two days (to 5 days). Block 10 consisted of 13.75 days of High treatment and no Low treatment. The High treatment in block 11 was 9 days and the Low treatment was 6 days. Block 15 was 6 days total with 2 days of Low and 4 days of High treatment. The PFFC was temporarily off due to power outages during blocks 6 (16 hours), 11 (39 hours), 13 (122.5 hours), and between blocks 6 and 7 (4 hours). Appendix F lists the mean observed reservoir elevation, distance from the tower, pump configuration, weir configuration, and water temperatures when the USACE crew worked at the PFFC.

Table 5. Actual portable floating fish collector operations at Cougar Reservoir, Oregon, during the randomized-block treatment schedule, 2014.

[Periods when the portable floating fish collector was off for sampling or maintenance during a treatment period are included in the associated start and end times, but were omitted in the duration estimates]

Block	Treatment	Attraction pump percentage	Start	End	Treatment duration (days)
1	Low	60	05/27/2014 11:35	06/03/2014 14:00	6.75
	High	90	06/03/2014 14:00	06/10/2014 11:56	6.40
2	High	85	06/10/2014 00:00	06/17/2014 12:30	6.99
	Low	50	06/17/2014 12:30	06/19/2014 14:30	2.07
	High	85	06/19/2014 14:30	06/20/2014 11:40	0.84
	Low	50	06/20/2014 11:40	06/24/2014 12:43	4.00
3	High	85	06/24/2014 12:43	07/01/2014 11:08	6.80
	Low	50	07/01/2014 11:08	07/08/2014 11:08	6.94
4	High	85	07/08/2014 11:08	07/15/2014 11:35	6.94
	Low	50	07/15/2014 00:00	07/22/2014 12:00	6.94
5	Low	50	07/22/2014 12:00	07/29/2014 11:07	6.89
	High	85	07/29/2014 11:07	08/05/2014 12:40	7.00
6	Low	50	08/05/2014 12:40	08/12/2014 14:50	6.33
	High	85	08/12/2014 14:50	08/19/2014 12:19	6.82
7	High	85	08/19/2014 16:00	08/26/2014 13:00	6.76
	Low	50	08/26/2014 13:00	09/02/2014 10:30	6.85
8	High	85	09/02/2014 10:30	09/09/2014 11:50	6.99
	Low	50	09/09/2014 11:50	09/18/2014 11:55	8.92
9	High	85	09/18/2014 11:55	09/25/2014 11:00	6.91
	Low	50	09/25/2014 11:00	09/30/2014 13:30	5.00
10	High	85	09/30/2014 13:30	10/14/2014 15:16	13.75
11	High	85	10/14/2014 15:16	10/23/2014 14:26	7.01
	Low	50	10/23/2014 14:26	10/29/2014 14:09	5.89
12	High	85	10/29/2014 14:09	11/06/2014 10:44	7.64
	Low	50	11/06/2014 10:44	11/12/2014 14:56	6.01
13	High	85	11/17/2014 17:35	11/18/2014 15:15	0.78
	Low	50	11/18/2014 15:15	11/25/2014 14:41	6.42
14	High	85	11/25/2014 14:41	12/02/2014 13:03	6.73
	Low	50	12/02/2014 13:03	12/09/2014 12:00	6.85
15	Low	50	12/09/2014 12:00	12/11/2014 14:00	0.97
	High	75/90	12/11/2014 14:00	12/15/2014 14:30	4.68

Water Velocities

The ADV data showed that the inward (downstream) velocities were greater during the High treatment than during the Low treatment, but there also were differences in the gradients and acceleration profiles between the treatments (fig. 12A–12B). During the High treatment, the highest velocity (1.87 ft/s) occurred at the flume opening, and the highest gradient ((0.28 ft/s/ft) and acceleration (0.28 ft/s^2) were from 6 to 3 ft outside the flume opening. Inside the flume, the velocity, gradient, and acceleration decreased and increased twice before passing through the PIT antenna and the knife gate (fig. 12C). During the Low treatment, gradient (0.09–0.00 ft/s/ft) and acceleration (0.05–0.00 ft/s^2) gradually decreased from outside the flume to just prior to the knife gate, and velocity increased from 0.42 ft/s over the same distance to a maximum of 1.07 ft/s (fig. 12C). The highest velocity (1.41 ft/s), gradient (0.11ft/s/ft), and acceleration (0.14 ft/s^2) during the Low treatment were from 19 to 22 ft inside the opening of the flume near the PIT antenna and the knife gate).

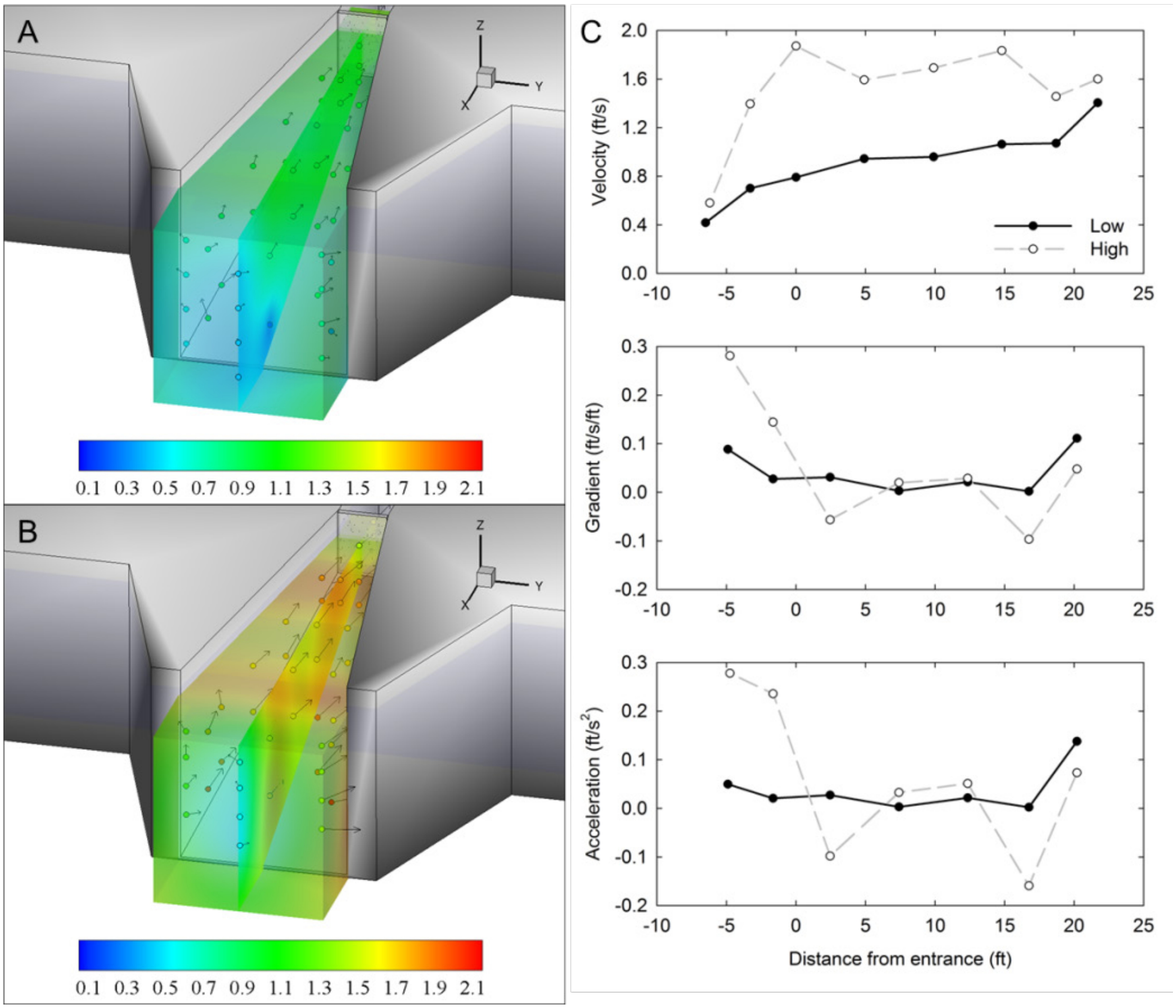

Figure 12. Three-dimensional view of interpolated velocity magnitude (ft/s) and velocity vectors for the (A) Low (attraction pumps at 50 percent), and (B) High (attraction pumps at 85 percent) treatments; and (C) velocity, gradient, and acceleration profiles for portable floating fish collector at Cougar Reservoir, Oregon, June 18–20, 2014.

Overall Fish Collection by the PFFC

Collection by the PFFC varied by species and time. The collection of juvenile Chinook salmon primarily was composed of subyearling fish that entered the reservoir in 2014. Juvenile Chinook salmon were collected from May 28 through July 3 and September 2 to December 15, 2014 (fig. 13). Collection from July to September was dominated by dace and largemouth bass and devoid of Chinook salmon. bluegill, rainbow trout (*Oncorhynchus mykiss*), sculpin, and amphibians also were captured at the PFFC, but in small numbers (fig. 14). A total of 156 juvenile Chinook salmon were collected: 148 subyearling and 8 yearling; there also was one adult captured. The combined catch of Chinook salmon was similar between treatments: 80 fish were collected during the Low treatment and 76 were collected during the High treatment; however, more than one-half of the collection during the Low treatment was captured during the first block and the treatments were not all of the same length. Over the study period, the catch of Chinook salmon by block and treatment (essentially weekly) ranged from 1 to 45.

The mean CPUE of Chinook salmon ranged from 0 to 6.77 per 24 hours among the treatment and block combinations, and treatment differences in CPUE were negligible except for blocks 1 and 13 (fig. 15). Block 10 had only a High treatment and was excluded from the CPUE analyses. A significant interaction between the effects of treatment and block on CPUE indicated that the two effects were dependent ($P = 0.032$). When block 1 was removed from this analysis, the effect of block on CPUE was significant ($P < 0.001$), and the treatment effect and the interaction were not significant ($P = 0.194$ and $P = 0.279$). A one-way ANOVA for block 1 only indicated that mean CPUE was significantly higher for the Low treatment than for the High treatment ($P = 0.042$).

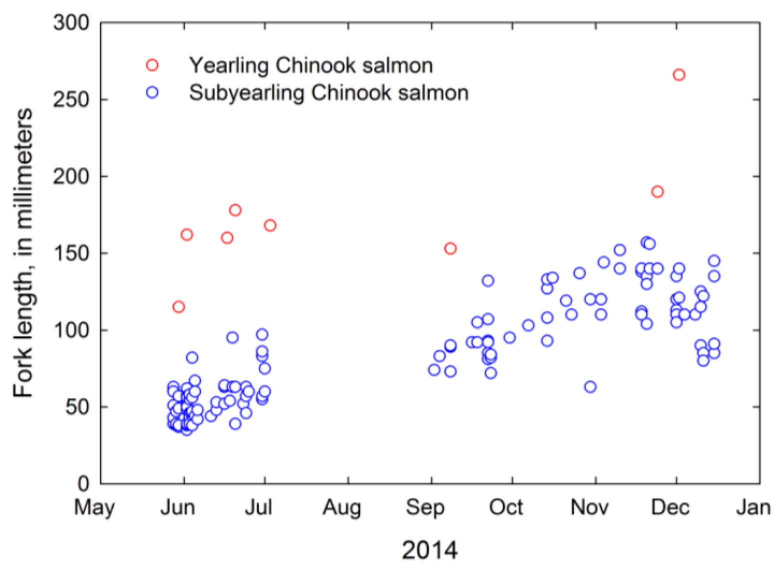

Figure 13. Graph of fork lengths of juvenile Chinook salmon collected at the portable floating fish collector, Cougar Reservoir, Oregon, 2014.

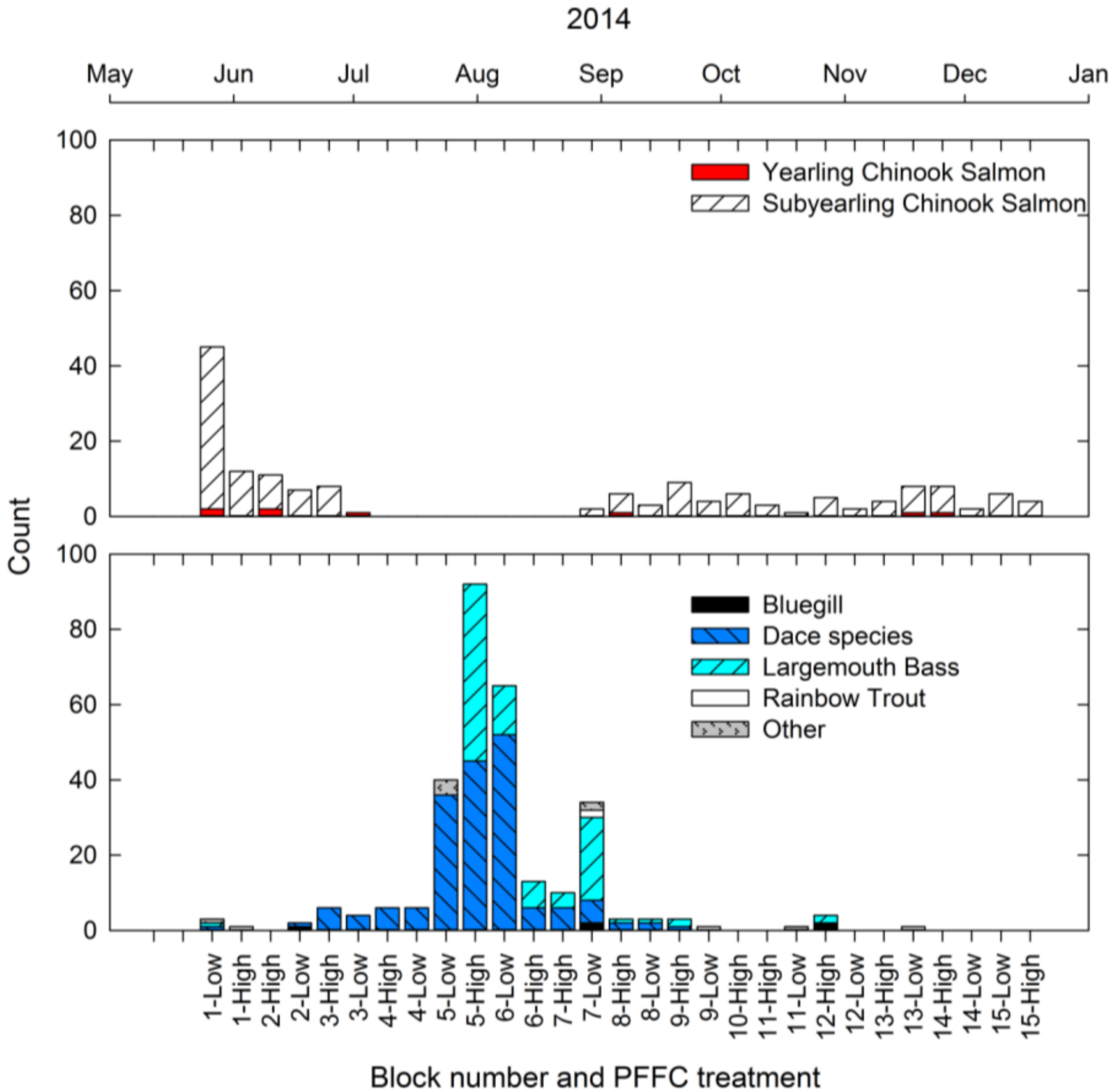

Figure 14. Graphs showing frequency of juvenile Chinook salmon (top) and bycatch (bottom) captured by block and treatment at the portable floating fish collector (PFFC), Cougar Reservoir, Oregon, 2014.

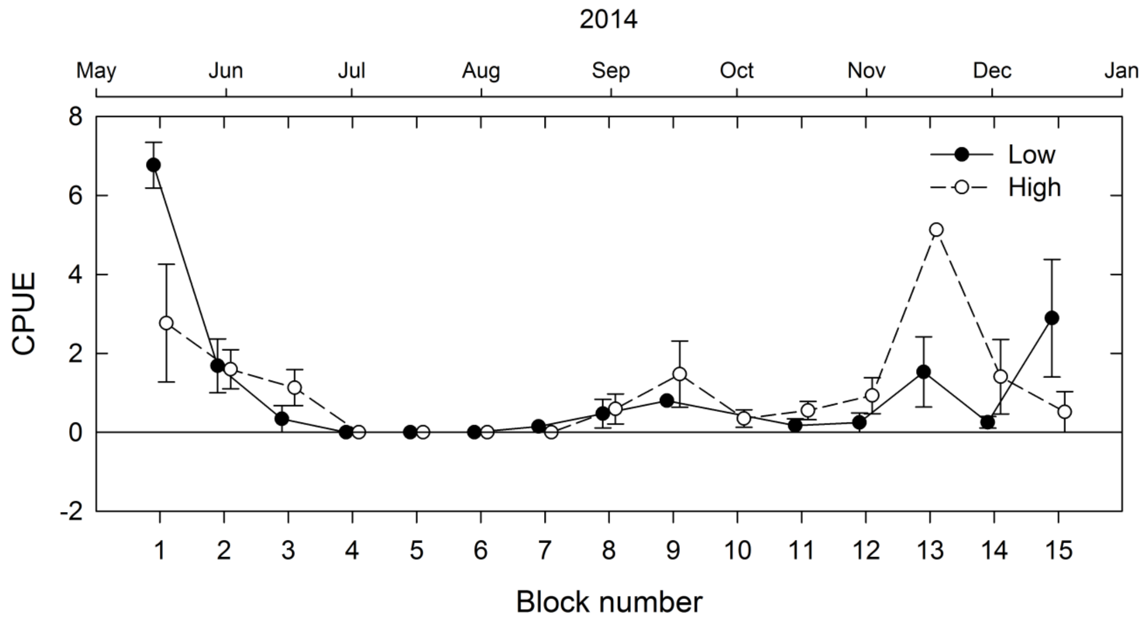

Figure 15. Graph of juvenile Chinook salmon mean catch per unit effort (CPUE) per 24 hours of trap operation by block and treatment at portable floating fish collector, Cougar Reservoir, Oregon, 2014. Whiskers represent the standard error.

The mortality of juvenile Chinook salmon collected by the PFFC was high and varied over treatment and block. Total mortality of the 148 subyearling Chinook salmon collected was 27.6 percent during the Low treatment, 36.1 percent during the High treatment, and 31.8 percent over both treatments combined (table 6). About 81 percent (38 of 47) of the total mortality was categorized as trap mortality (prior to staff handling the collected fish), indicating poor holding conditions, fish with compromised health status, or both. The rest of the mortality (about 19 percent of the total mortality; 6.1 percent of the fish collected) was attributed to handling. There was one mortality of the four yearling Chinook salmon collected during the Low treatment (a trap mortality) and no mortality of the four collected during the High treatment.

Table 6. Summary of mortality of subyearling Chinook salmon collected in the portable floating fish collector, Cougar Reservoir, Oregon, May 27–December 16, 2014.

[Mortality is divided into Trap (dead upon examination of collection) and Handling (died between time of examination and release). *N*, number of fish]

Treatment	Total collected	Mortality					
		Trap		Handling		Total	
		N dead	Percent	*N* dead	Percent	*N* dead	Percent
Low	76	17	22.4	4	5.3	21	27.6
High	72	21	29.2	5	6.9	26	36.1
Combined	148	38	25.7	9	6.1	47	31.8

Tagged Fish

Handling, Tagging, and Release

During the spring, 430 hatchery Chinook salmon, 4 wild Chinook salmon collected in the Lampara seine, and 1 wild Chinook salmon collected by the PFFC were implanted with acoustic and PIT tags and released. Data from all tagged fish were grouped together for analysis. The hatchery Chinook salmon were tagged and released between April 9 and May 21, 2014. We deployed the Lampara seine for 56 sets and collected 7 wild Chinook salmon. Four of these fish were tagged and released during April 21–24, 2014, and the other three were post-tag mortalities. On June 18, 2014, the one wild Chinook salmon collected in the PFFC was tagged and released the next day. The mean fork lengths were 164.2 mm (range 115–180 mm) for the hatchery Chinook salmon and 114.3 mm (range 104–135 mm) for the wild Chinook salmon from the Lampara seine (table 7). The wild Chinook salmon captured in the PFFC had a fork length of 160.0 mm. The mean tag-weight-to-body weight ratio (based on the 0.53-g weight of the acoustic transmitter plus the PIT tag) was 1.3 percent for the hatchery Chinook salmon (range 0.8–3.7 percent) and 3.8 percent (range 2.2–4.6 percent) for the wild Chinook salmon from the Lampara seine. The tag-weight-to-body weight ratio of the single wild Chinook salmon tagged and released after capture by the PFFC was 1.1 percent. The pre-tag holding times ranged from 17.9 to 19.4 hours for the hatchery Chinook salmon, 18.2 to 25.1 hours for the fish from the Lampara seine, and 27.3 hours for the fish from the PFFC. Post-tag holding times were 18.0–23.4 hours for the hatchery fish, 19.1–28.9 hours for the fish from the Lampara seine, and 18.1 hours for the fish from the PFFC.

Table 7. Summary statistics of fork length and weight of acoustic and passive integrated transponder (PIT) tagged hatchery and wild juvenile Chinook salmon at Cougar Reservoir, Oregon, 2014.

[*N*, number of fish; SD, standard deviation; NA, not applicable; PIT, passive integrated transponder; PFFC, portable floating fish collector]

Fish origin	Tag type	*N*	Fork length (millimeters)			Weight (grams)		
			Mean	SD	Range	Mean	SD	Range
Spring								
Hatchery[1]	Acoustic	430	164.2	12.8	115–180	45.3	10.3	14.4–68.7
Wild, Lampara seine	Acoustic	4	114.3	12.3	104–135	15.2	12.2	11.6–23.9
Wild, PFFC[2]	Acoustic	1	160.0	NA	NA	46.7	NA	NA
Hatchery	PIT	495	76.7	6.1	65–93	5.1	1.4	1.9–10.6
Fall								
Hatchery	PIT	1,010	154.5	22.1	71–180	42.0	14.8	3.6–71.2

[1]Eight of the hatchery acoustic-tagged fish were removed from acoustic data analyses because of indication of predation or shed acoustic tags.

[2]The wild PFFC fish was released after the acoustic tag died and, therefore, was removed from any acoustic data analyses.

In addition to the JSATS tagging, hatchery Chinook salmon also were held and PIT-tagged at FPGL. During the spring, 495 fish were tagged and released with a mean fork length of 76.7 mm and, in the fall, 1,010 fish were tagged and released with a mean fork length of 154.5 mm (table 7). The mean tag-weight-to-body weight ratio (based on the 0.10 g weight of the PIT tag) was 2.1 percent (range 0.9–5.3) for the spring fish and 0.3 percent (range 0.1–2.8) for the fall fish.

There was mortality and PIT-tag loss during the post-tag holding periods. In the first delivery of hatchery Chinook salmon on March 13, 2014, there was a 6.3 percent (36 of 575) mortality rate during pre-tag holding that occurred at Leaburg Hatchery. After the second delivery of hatchery Chinook salmon on April 24, 2014, there was a 6.2 percent mortality rate during pre-tag holding (23 of 370). The overall post-tagging mortality rate of acoustic +PIT-tagged fish during the entire tagging season was 0.7 percent (3 of 438; all from the Lampara seine). During the PIT-tag-only tag and release period in the spring, there was a 0.4 percent mortality rate (2 of 502) and, during the fall, there was a 0.5 percent mortality rate (5 of 1,024). During both the spring and fall, when fish were held 6–20 days after tagging, some hatchery Chinook salmon shed their PIT tags. In the spring, 1.0 percent (5 of 502) of hatchery Chinook salmon shed their PIT tags and, in the fall, 0.9 percent (9 of 1,024) of fish shed their PIT tags.

We omitted nine acoustic+PIT-tagged fish from analyses because the acoustic tag was dead prior to release (*N*=1; wild fish collected by PFFC) or the positions in the cul-de-sac indicated predation, shed tag, or egregious positions (*N*=8). The total number of fish with acoustic tags used in analyses was 426.

Travel Times

Travel time varied by area of the reservoir. The median travel time from release to the first detection at the log boom array was 2.2 days for the 93.2 percent of fish that were detected at the log boom (397 of 426; fig. 16). Of the Chinook salmon detected at the log boom after PFFC operations began, 97.6 percent (207 of 212) were detected within 10 m of the tower face within the remaining life of the acoustic transmitter. In contrast, 87.7 percent (186 of 212) of fish were detected near the PFFC entrance after detection at the log boom after PFFC operations began. Median travel time from the log boom was 0.9 days to the tower face and 5.2 days to the PFFC entrance. The mean number of trips each fish made from the log boom to within 10 m of the PFFC was 3.6 (range 1–16). The mean number of trips each fish made from the log boom to within 10 m of the tower was approximately double that of the trips to the PFFC (mean 7.6, range 1–23).

One acoustic+PIT-tagged fish was collected in the PFFC. This fish was first detected at the PFFC entrance on May 30, 2014, and made four trips to the PFFC entrance (each trip defined by a detection at the log boom) prior to capture on June 15, 2014. The four trips from the log boom to within 10 m of the PFFC ranged from 32 minutes to just over 8 hours in duration and consisted of detections in three PFFC Low operation treatments and one PFFC High operation treatments. The total time from first detection near the PFFC entrance to the last JSATS detection was 35.6 days. This hatchery Chinook salmon was collected in the PFFC during a Low treatment.

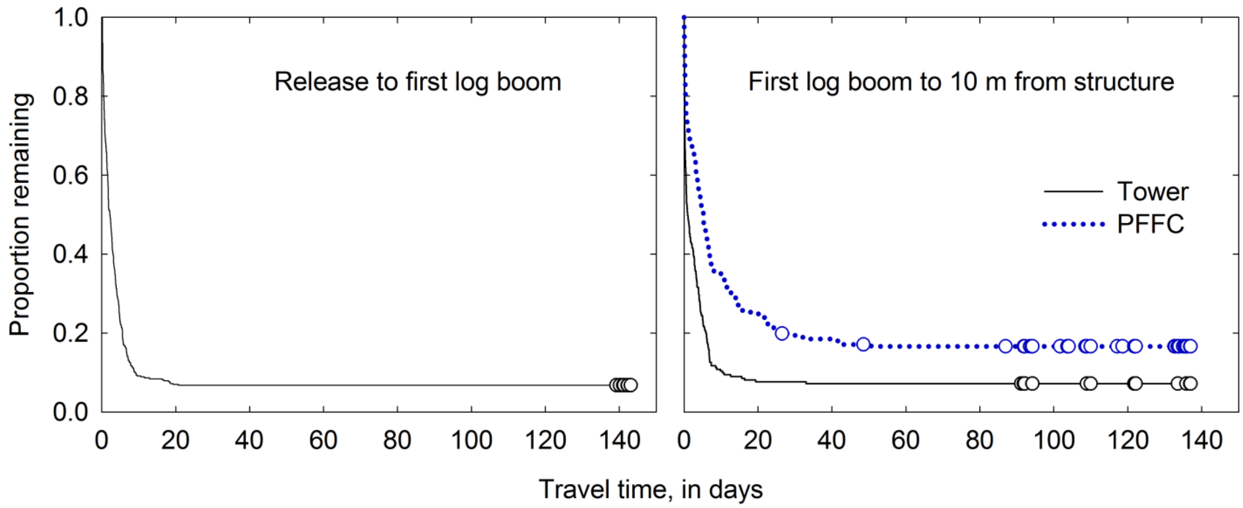

Figure 16. Graphs of travel time (days) from release of Chinook salmon to first detection at the log boom and from the log boom to within 10 meters (m) of the entrance to the water temperature control tower (Tower) or the portable floating fish collector (PFFC) after May 27, 2014, Cougar Reservoir, Oregon, 2014. Open circles indicate censored observations.

Depths in the Cul-de-Sac

Depths of fish positioned within 20 m of the PFFC and tower varied by month and generally were deeper at night than during the day. The mean of the median hourly depths of each fish near the tower and PFFC ranged from 1.4 to 11.5 m in May and June, but ranged from 7.2 to 28.3 m in July and August as sample sizes decreased. Fish were deeper during the night than during the day in May and June, but not later in the study when fewer tagged fish were present (table 8; figs. 17 and 18).

Table 8. Summary of the mean of the median hourly depths (in meters) of each fish positioned within 20 meters of the water temperature control tower (Tower) and portable floating fish collector (PFFC) from May 27 to the 90th percentile of each acoustic tag in Cougar Reservoir, Oregon.

[*N*, sample size; SE, standard error]

Month	Diel period	PFFC			Tower		
		N	Depth	SE	*N*	Depth	SE
May	Overall	140	6.3	6.7	154	4.7	5.6
	Day	105	2.0	3.5	121	2.0	3.1
	Night	100	8.6	4.6	99	6.9	5.4
June	Overall	198	7.4	5.9	199	6.7	6.0
	Day	192	4.5	3.6	191	3.3	2.5
	Night	193	9.2	4.5	193	8.4	4.1
July	Overall	116	9.5	4.8	116	9.9	5.5
	Day	96	9.3	4.5	83	9.0	4.9
	Night	99	8.6	3.4	99	8.9	3.3
August	Overall	44	11.7	5.3	41	12.2	6.5
	Day	30	12.5	4.8	25	12.6	7.7
	Night	32	9.8	3.1	36	9.8	3.5
September	Overall	16	8.7	6.1	15	11.6	7.6
	Day	11	12.6	4.9	10	12.5	6.6
	Night	11	7.4	4.0	12	7.2	2.8
October	Overall	2	16.6	7.8	2	18.9	6.1
	Day	1	20.0	0.0	1	23.1	0.0
	Night	2	10.4	0.4	2	13.7	3.5

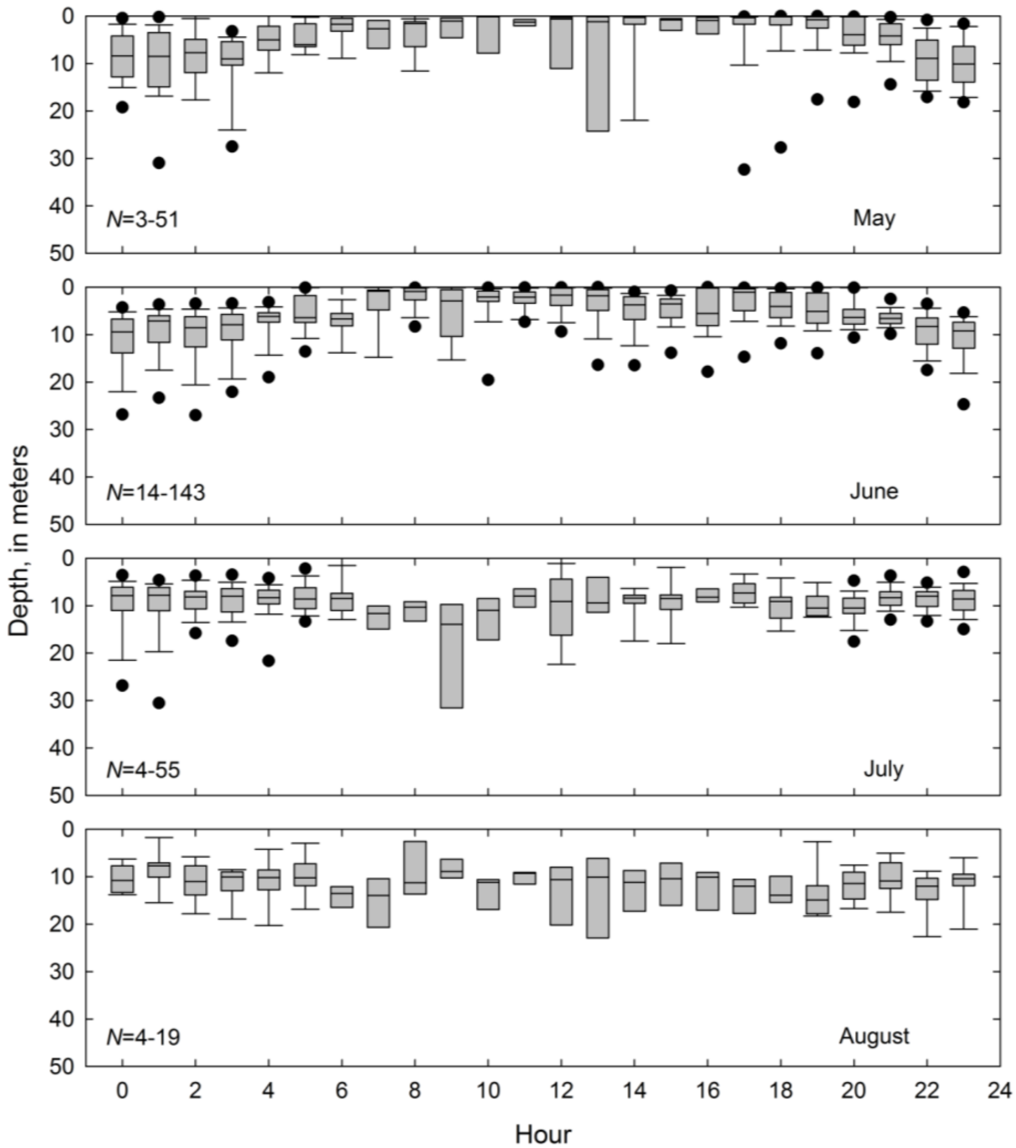

Figure 17. Boxplots of the hourly depths (in meters) of acoustic+PIT-tagged juvenile Chinook salmon with position estimates within 20 meters of the portable floating fish collector (PFFC) in Cougar Reservoir, Oregon, 2014. Data summarized are the median hourly depths of each fish present at the month indicated during the PFFC operation period. Boxes range from the 25th to the 75th percentiles with a line indicating the median, whiskers represent the 10th and 90th percentiles, and dots represent the 5th and 95th percentiles. Boxes without whiskers or dots contained insufficient data for them to be estimated. Sample sizes represent the number of fish (*N*) in the hourly boxes.

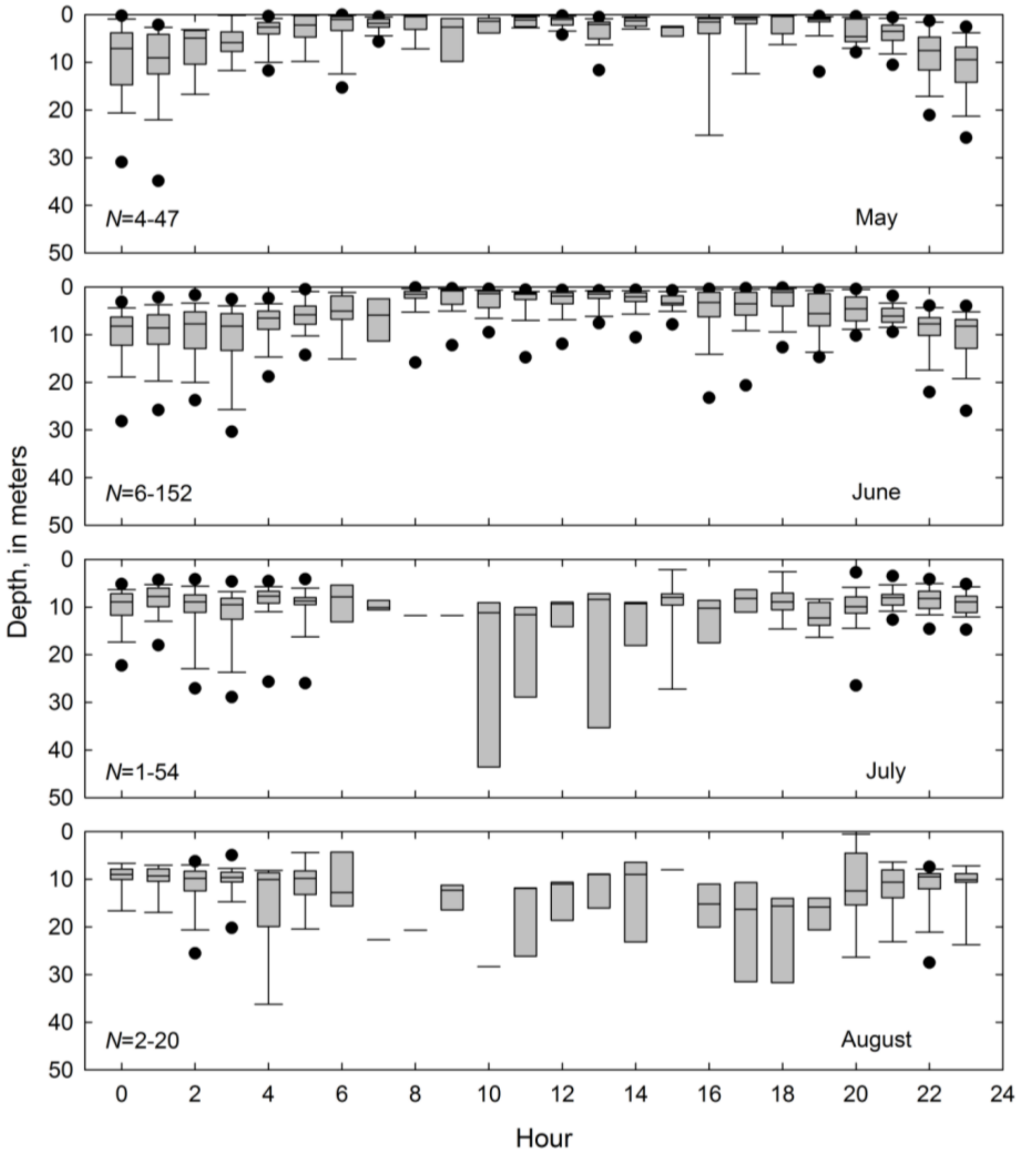

Figure 18. Boxplots of the hourly depths (in meters) of acoustic+PIT-tagged juvenile Chinook salmon with position estimates within 20 meters of the water temperature control tower in Cougar Reservoir, Oregon, 2014. Data summarized are the median hourly depths of each fish present at the month indicated during the portable floating fish collector operation period. Boxes range from the 25th to the 75th percentiles with a line indicating the median, whiskers represent the 10th and 90th percentiles, and dots represent the 5th and 95th percentiles. Boxes without whiskers or dots contained insufficient data for them to be estimated. Sample sizes represent the number of fish (*N*) in the hourly boxes.

Temperature Selection

The depths of acoustic+PIT-tagged fish near the tower and PFFC primarily were in a narrow range of the available water temperatures, suggesting they may have selected their depth based on temperature. The water temperatures at the mean daily fish depths generally were between 10 and 13 °C, and seasonal changes in fish depths were similar to vertical changes in temperatures in that range (fig. 19). The trend is supported from the beginning of the data in late May to about mid-August, when sample sizes of tagged fish decrease to less than about 10 fish per day and the daily depth data are much more variable. The results from data from fish within 20 m of the PFFC entrance (fig. 19, top graph) are similar to those within 20 m of the tower entrance (fig. 19, bottom graph).

The standardized resource selection indices support the premise that the acoustic+PIT-tagged fish preferentially selected depths based on water temperature. This was most evident in data from within 20 m of the PFFC entrance in the months of June, July, and August, when the selection index increased gradually from low levels at 6 or 7 °C, peaked at 13–15 °C depending on the month, and then decreased gradually to low levels at temperatures greater than about 16° C (fig. 20, top graph). The data from within 20 m of the tower entrance were similar to those near the PFFC entrance, but show peaks at slightly warmer temperatures (fig. 20, bottom graph). Few of the estimated fish depths were at temperatures warmer than 14 °C during June (29 percent), July (9 percent), and August (5 percent), and only 3 percent were at temperatures greater than 16° C.

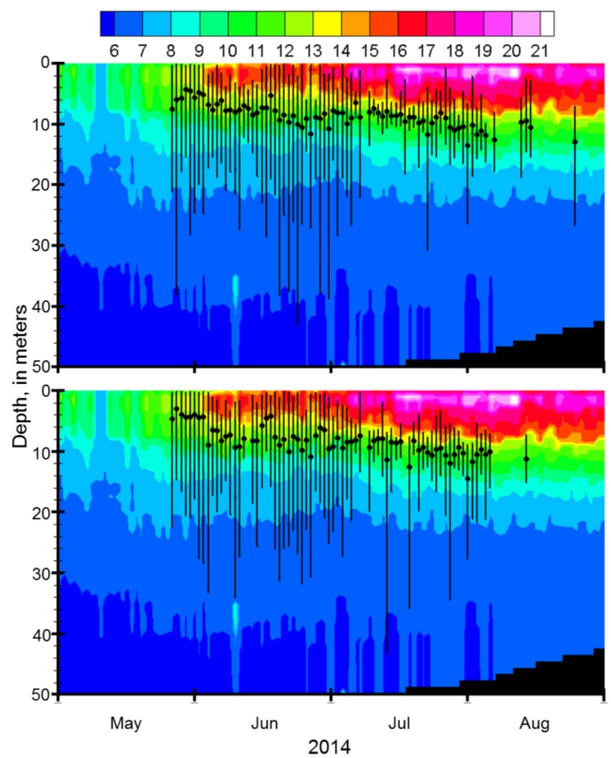

Figure 19. Graphs of mean daily fish depth (solid circles) within 20 meters of the portable floating fish collector entrance (top) and within 20 meters of the water temperature control tower entrance (bottom) and hourly water temperatures (in degrees Celsius) in Cougar Reservoir, Oregon, 2014. Vertical lines represent the daily minimum and maximum fish depths.

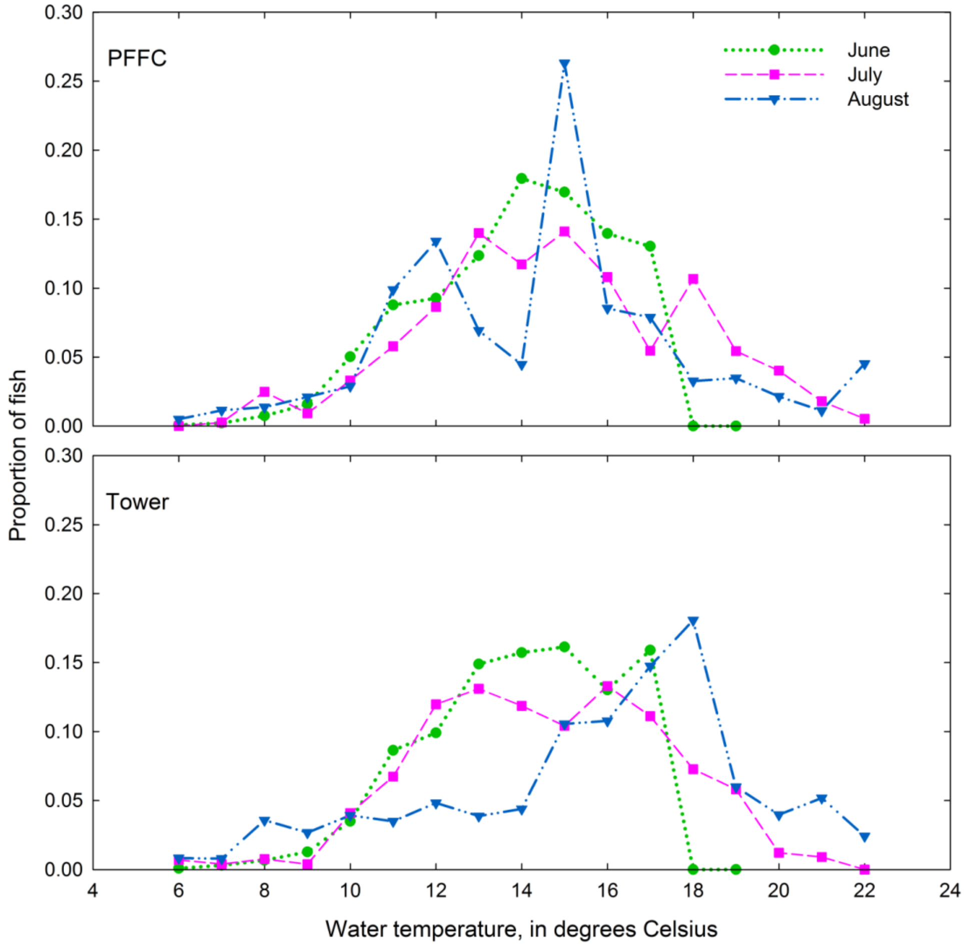

Figure 20. Graphs of the standardized resource selection index for fish positioned within 20 meters of the portable floating fish collector (PFFC) entrance (top) and within 20 meters of the water temperature control tower (Tower) entrance (bottom) at Cougar Reservoir, Oregon, 2014.

Spatial Intensity of Use

In the Cul-de-sac

Most fish positioned within the cul-de-sac were used in estimates of utilization distributions (UDs). There were a total of 267 tagged fish positioned in the cul-de-sac, and the number of fish used in UDs ranged from 9 to 205 depending on the strata with a median of 115 fish among strata. The number of positions per fish ranged from 16 to 23,992, and the number of bursts (trips) per fish ranged from 1 to 19 with an average of 3 among strata.

The tagged fish were present throughout the area monitored in the cul-de-sac, but used the area between the PFFC and the temperature control tower most intensely. We focus here on results of fish in the 0–3 and 3–6 m depth bins, because the PFFC entrance was about 3 m deep; however, plots of UDs for all strata are shown in appendix D.

Fish were dispersed throughout the area monitored in the cul-de-sac, but the distributions of the 0–3 m UDs indicated that fish use was often lowest near the PFFC entrance and highest near the tower. This trend was most apparent during the day, when the most intense use was near the southwestern corner of the tower and slightly upstream of the PFFC (fig. 21A–C). During the night, there was little difference between treatments (fig. 21 D–F) and the distributions were more diffuse than during the day. The 0–3 m UD values were negligible underneath the PFFC, but this was expected because of the volume occupied by the structure.

The major trends in the 3–6 m UDs were similar to those of the 0–3 m UDs, but indicated more similarity between treatments. As in the 0–3 m UDs, fish use during the day was greatest near the southwestern corner of the PFFC and in small areas near the upstream corners of the PFFC (fig. 22A–B). During the night, the UDs were more dispersed than during the day and the areas of greatest fish use were between the PFFC and the tower (both treatments) and slightly upstream of the PFFC (High treatment only; fig. 22D–F).

The UDs prior to the PFFC treatment schedule and during PFFC off periods generally were similar to those during the treatment schedule. The 0–3 and 3–6 m UDs during the 11 days before the PFFC treatments began on May 27, 2014, often were similar to those of the Low treatment (appendix D). This is most evident for the 0–3 and 3–6 m UDs during the day and all UDs during the night, when sample sizes are highest. The areas with the highest UDs prior to the PFFC treatment schedule were between the stern of the PFFC and the tower during the day and near the stern of the PFFC at night. There was no record of the PFFC operating conditions prior to the treatment schedule. The 0–3 and 3–6 m UDs when the PFFC was off (primarily during treatment changes in the day) were greatest between the stern of the PFFC and the tower and near the southwestern corner of the PFFC. The PFFC was rarely off during the night so UD data from that condition were not examined.

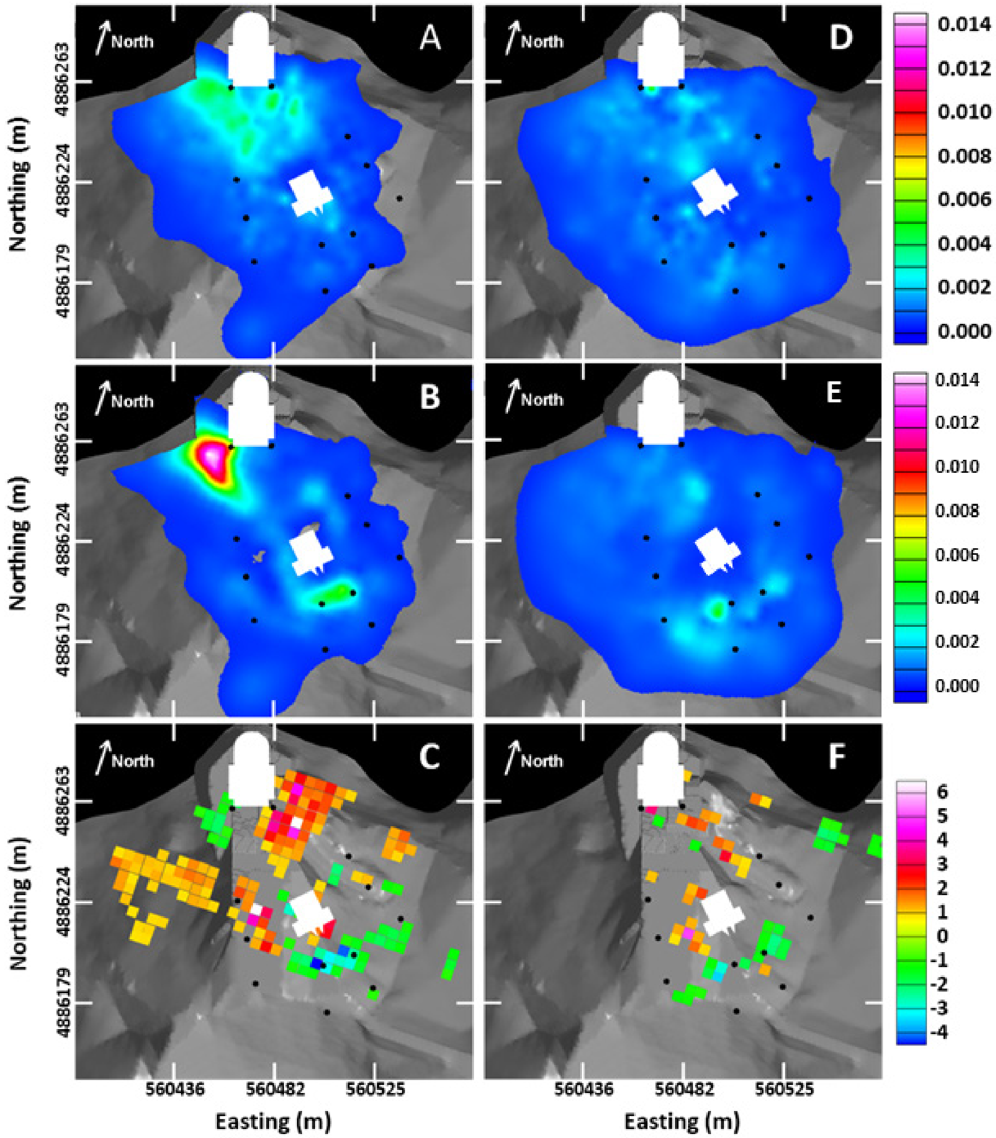

Figure 21. Graphs of the utilization distributions (UDs) of acoustic+PIT-tagged juvenile Chinook salmon in the 0–3 m depth bin at Cougar Reservoir, Oregon, 2014. Graphs in the left column show UDs in the day during the Low (A) and High (B) treatments, and their difference (C). Graphs in the right column show UDs of the same strata at night. Positive differences show where Low treatment UDs exceed High treatment UDs. Negative differences show where High treatment UDs exceed Low treatment UDs. The portable floating fish collector is shown near the center of each graph and the water temperature control tower is near the top center of each graph. Black circles indicate the relative position of the hydrophones.

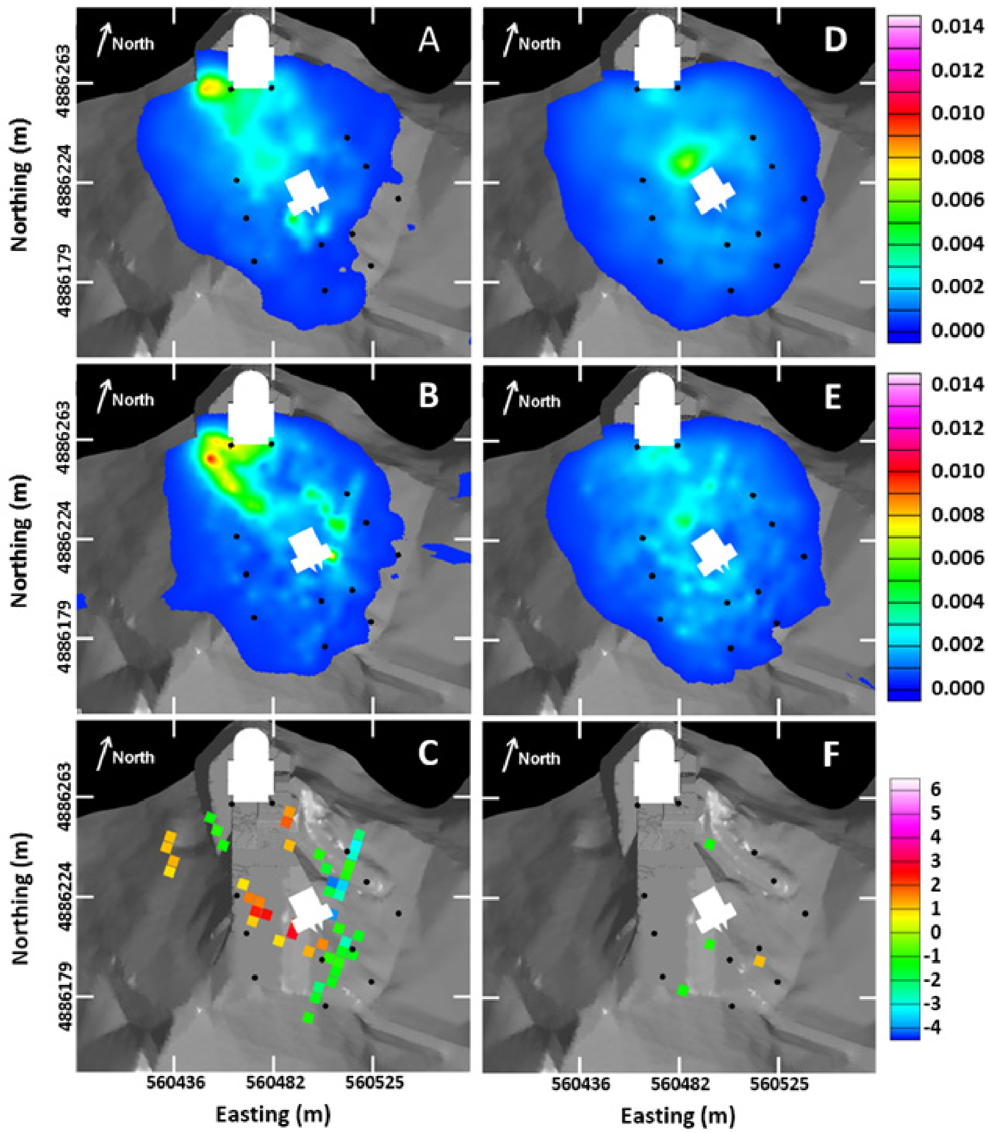

Figure 22. Graphs of the utilization distributions (UDs) of acoustic+PIT-tagged juvenile Chinook salmon in the 3–6 m depth bin at Cougar Reservoir, Oregon, 2014. Graphs in the left column show UDs in the day during the Low (A) and High (B) treatments, and their difference (C). Graphs in the right column show UDs of the same strata at night. Positive differences show where Low treatment UDs exceed High treatment UDs. Negative differences show where High treatment UDs exceed Low treatment UDs. The portable floating fish collector is shown near the center of each graph and the water temperature control tower is near the top center of each graph. Black circles indicate the relative position of the hydrophones.

Near the PFFC Entrance

A total of 203 tagged fish were positioned in a volume defined by a 20-m radius from the center of the PFFC entrance and 0–6 m deep. The number of fish used in the calculation of the individual UDs ranged from 40 to 157. The 0–3 and the 3–6 m UDs indicate a low intensity of use within about 5 m of the PFFC entrance during both treatments (figs. 23 and 24). The intensity of use was greatest in an arc about 10 m from the PFFC entrance. The PFFC entrance was encompassed by the 80-percent contours only in the 3–6 m UDs during the day (fig. 24A–B). Other differences among UDs were negligible.

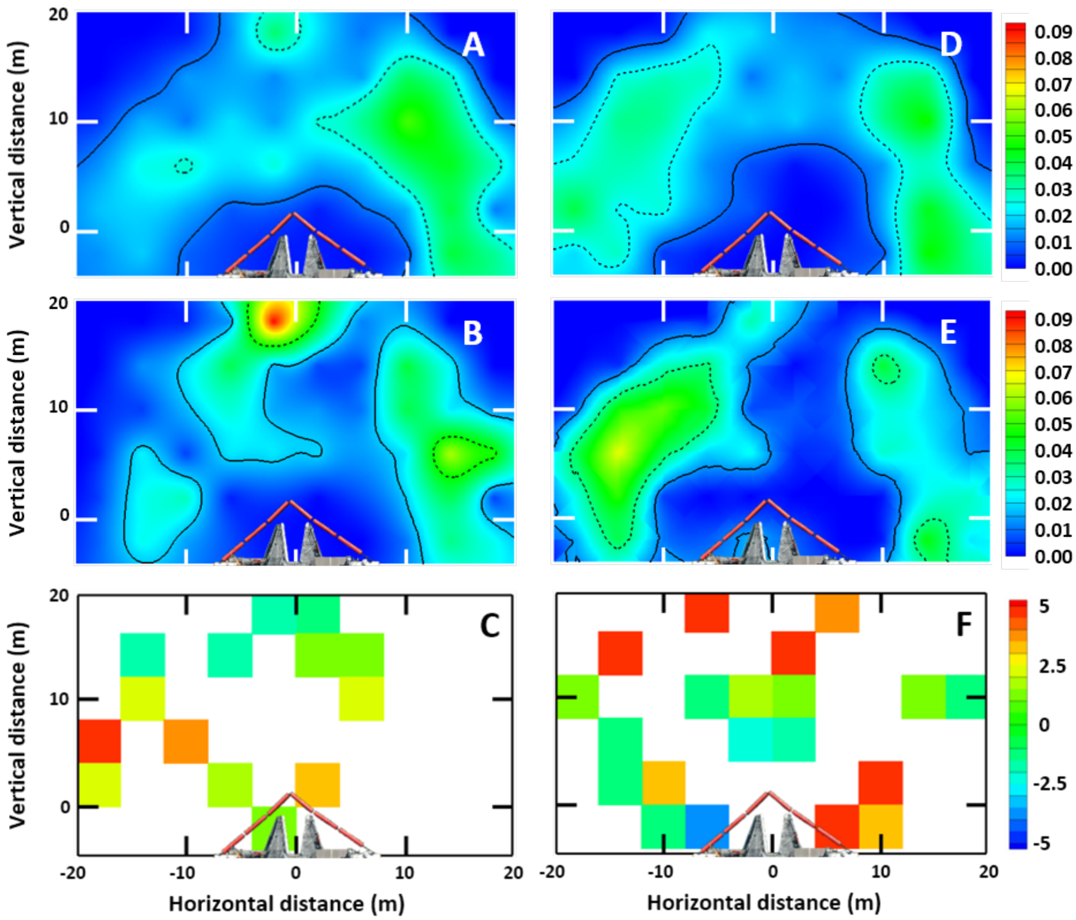

Figure 23. Graphs of the utilization distributions (UDs) of acoustic+PIT-tagged juvenile Chinook salmon near the portable floating fish collector (PFFC) in the 0–3 m depth bin at Cougar Reservoir, Oregon, 2014. Graphs in the left column show UDs in the day during the Low (A) and High (B) treatments, and their difference (C). Graphs in the right column show UDs of the same strata at night. Positive differences show where Low treatment UDs exceed High treatment UDs. Negative differences show where High treatment UDs exceed Low treatment UDs. The PFFC entrance is shown at the bottom of each graph.

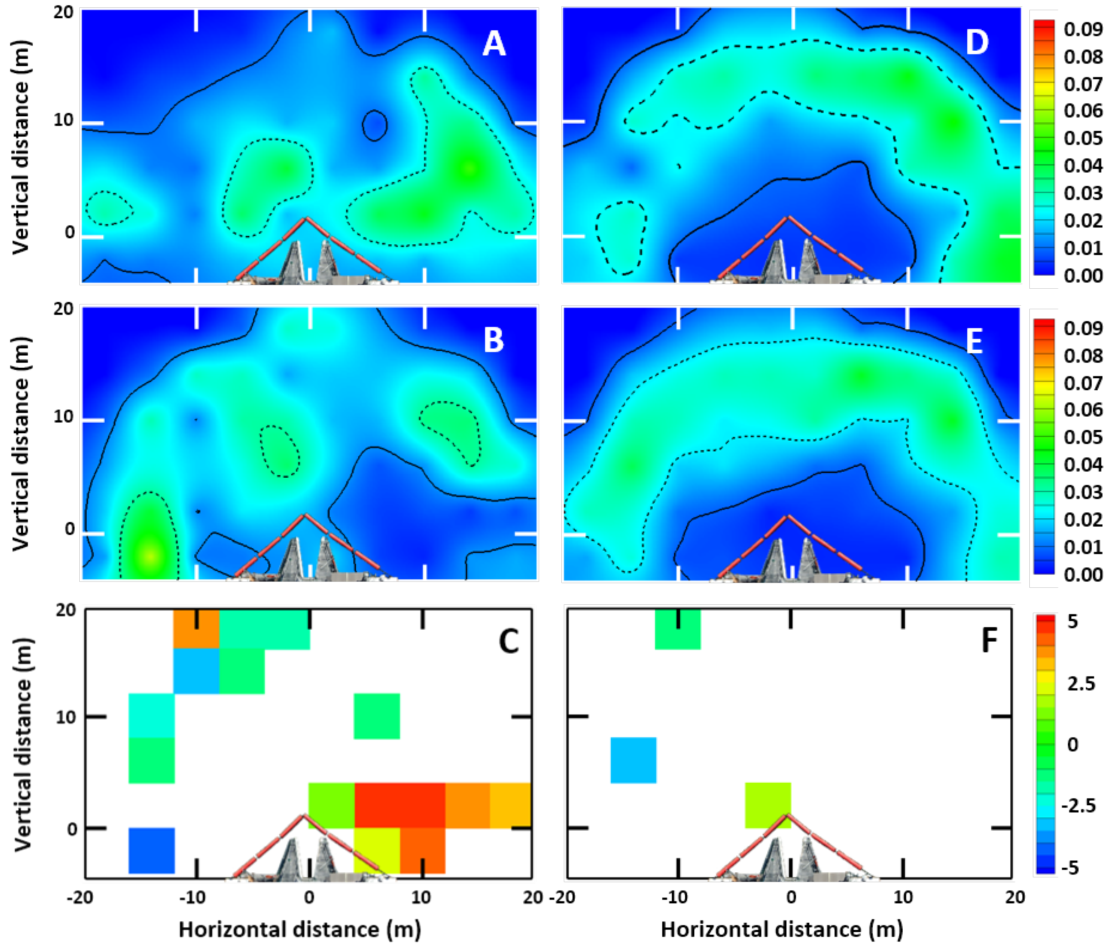

Figure 24. Graphs of the utilization distributions (UDs) of acoustic+PIT-tagged juvenile Chinook salmon near the portable floating fish collector (PFFC) in the 3–6 m depth bin at Cougar Reservoir, Oregon, 2014. Graphs in the left column show UDs in the day during the Low (A) and High (B) treatments, and their difference (C). Graphs in the right column show UDs of the same strata at night. Positive differences show where Low treatment UDs exceed High treatment UDs. Negative differences show where High treatment UDs exceed Low treatment UDs. The PFFC entrance is shown at the bottom of each graph.

Behaviors near the PFFC Entrance

A total of 179 tagged fish were positioned in front of the PFFC within 10 m of the entrance and at depths of 0–6 m. The number of fish in the individual treatment, photoperiod, and depth strata ranged from 17 to 104. The mean bearings (directions) of the trajectories of fish positioned within the ten 4 × 5 m cells for each strata are shown in figures 25–28.

Low numbers of tagged fish near the PFFC in the 0–3 m depth bin made meaningful comparisons between treatments difficult during both the day and the night (figs. 25 and 26). The Low treatment in the day was the only strata with a substantial number of cells with a sample size of 10 or more. During this condition, fish 5–10 m from the entrance most often had trajectory directions that were nonuniform (*P*s ≤ 0.009) and directed to the southwest, nearly parallel to the PFFC (fig. 25 A and F–J). In contrast, fish within 5 m of the entrance had trajectory directions that were statistically random, indicating no preferred direction of travel (fig. 25B–D; *P*s > 0.451). All other strata in the 0–3 depth group had fewer than five cells that met the sample size criterion and are not described further.

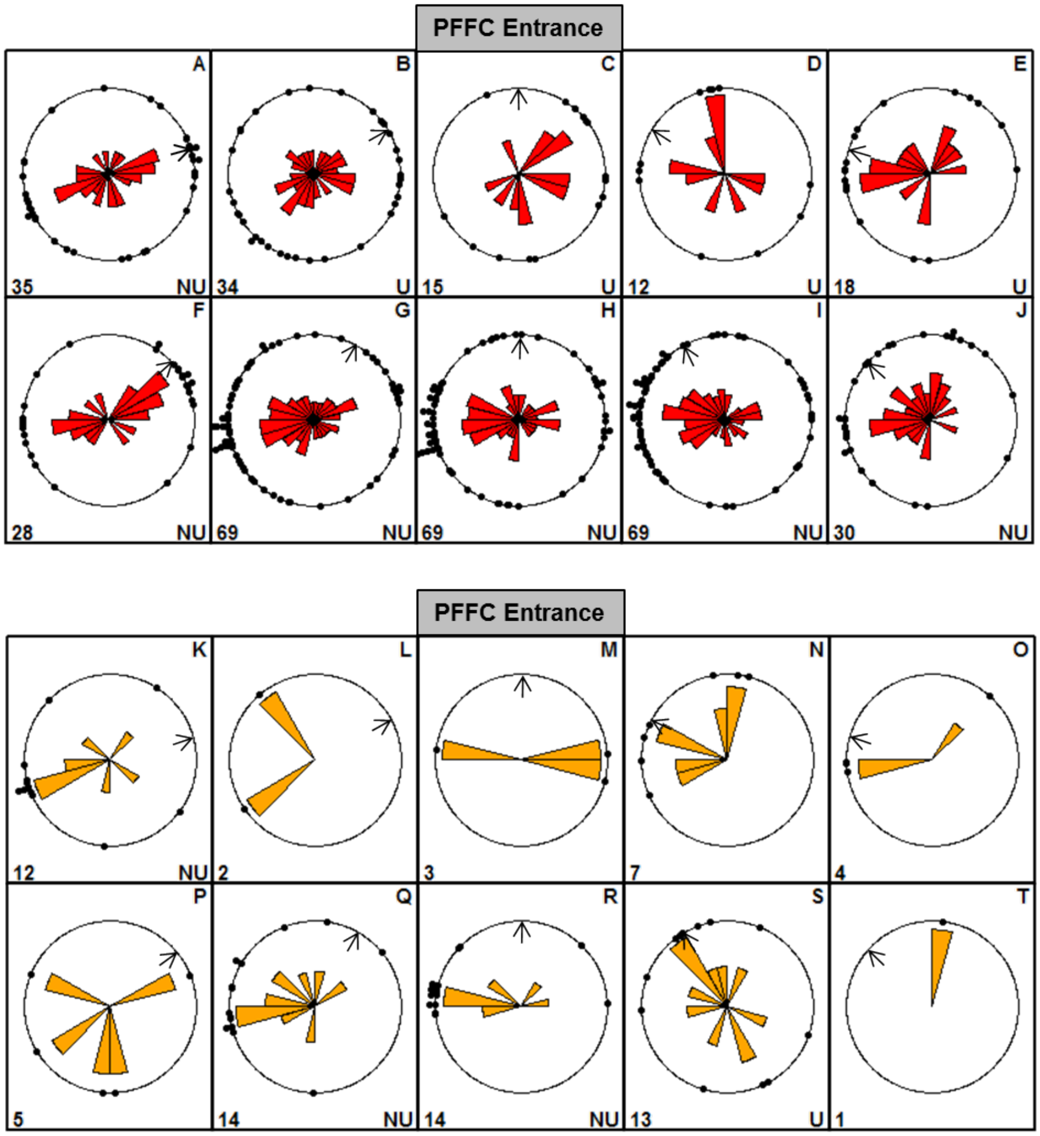

Figure 25. Rose diagrams showing mean bearings of acoustic+PIT-tagged juvenile Chinook salmon in front of the portable floating fish collector (PFFC) entrance at 0–3 meter depths during the day, Cougar Reservoir, Oregon, 2014. Figure parts A–J and K–T (indicated in the upper right corner of each part) show the Low and High treatment, respectively. Arrows indicate the direction from the center of each cell to the center of the collector entrance. Points on the plot circumferences are mean bearings for each fish and are stacked when multiple fish have the same bearing. Sample sizes are indicated in the lower left corner of each figure part and the results of Moore's second-order test of uniformity are given in the lower right corner for sample sizes greater than 9 (U=hypothesis of uniformly distributed bearings accepted, NU=hypothesis of uniformly distributed bearings rejected, α=0.05).

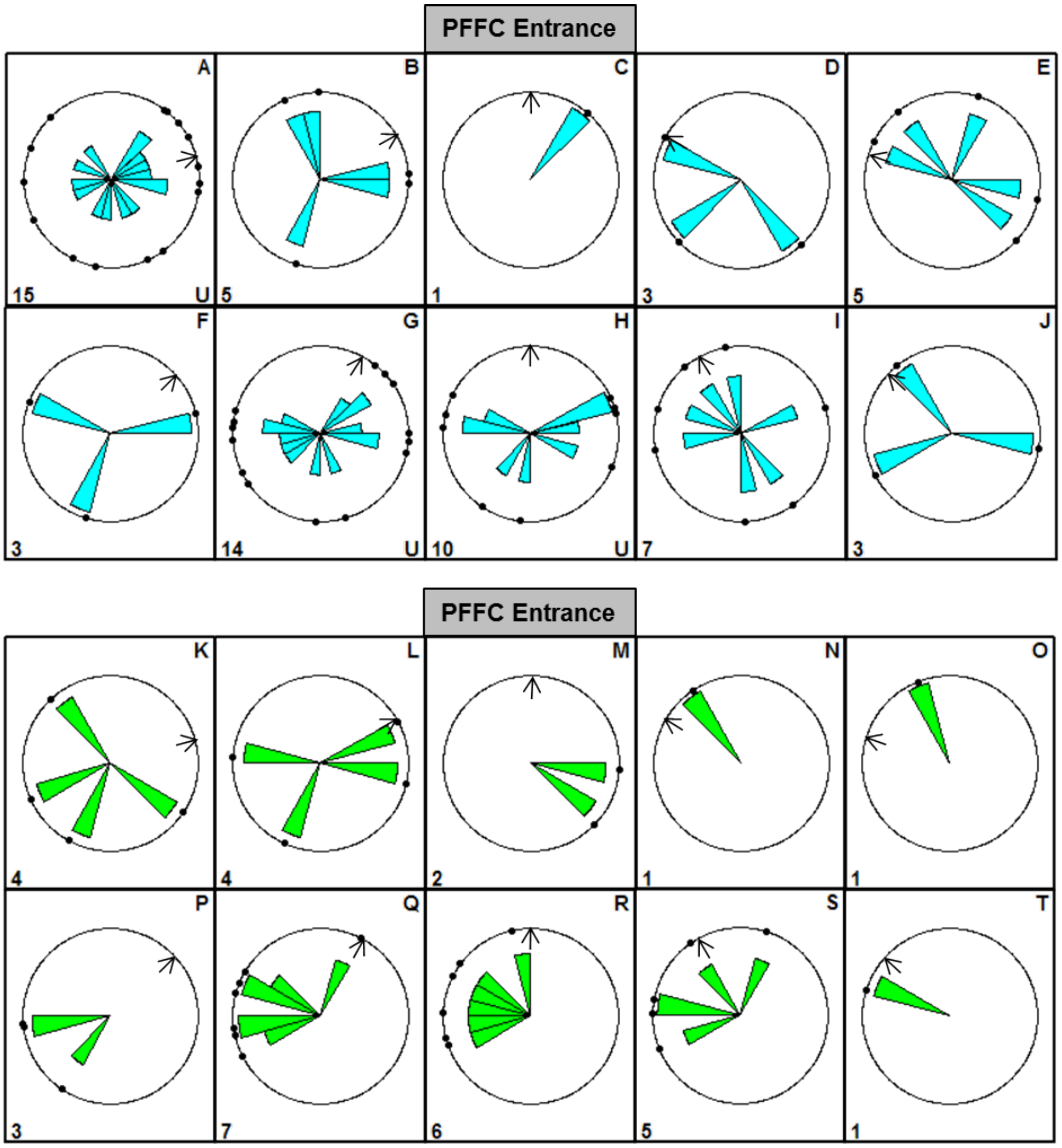

Figure 26. Rose diagrams showing mean bearings of acoustic+PIT-tagged juvenile Chinook salmon in front of the portable floating fish collector (PFFC) entrance at 0–3 meter depths during the night, Cougar Reservoir, Oregon, 2014. Figure parts A–J and K–T (indicated in the upper right corner of each part) show the Low and High treatment, respectively. Arrows indicate the direction from the center of each cell to the center of the collector entrance. Points on the plot circumferences are mean bearings for each fish and are stacked when multiple fish have the same bearing. Sample sizes are indicated in the lower left corner of each figure part and the results of Moore's second-order test of uniformity are given in the lower right corner for sample sizes greater than 9 (U=hypothesis of uniformly distributed bearings accepted, NU=hypothesis of uniformly distributed bearings rejected, α=0.05).

Fish positioned in the 3–6 m depth bin generally were present in higher numbers than the 0–3 m group, but the distributions of the directions of the fish trajectories were not significantly different from random for 27 out of 34 cells with sufficient sample sizes (figs. 27 and 28). In the cases where the fish directions were not random, the directions were widely scattered with no strong preference for the PFFC entrance.

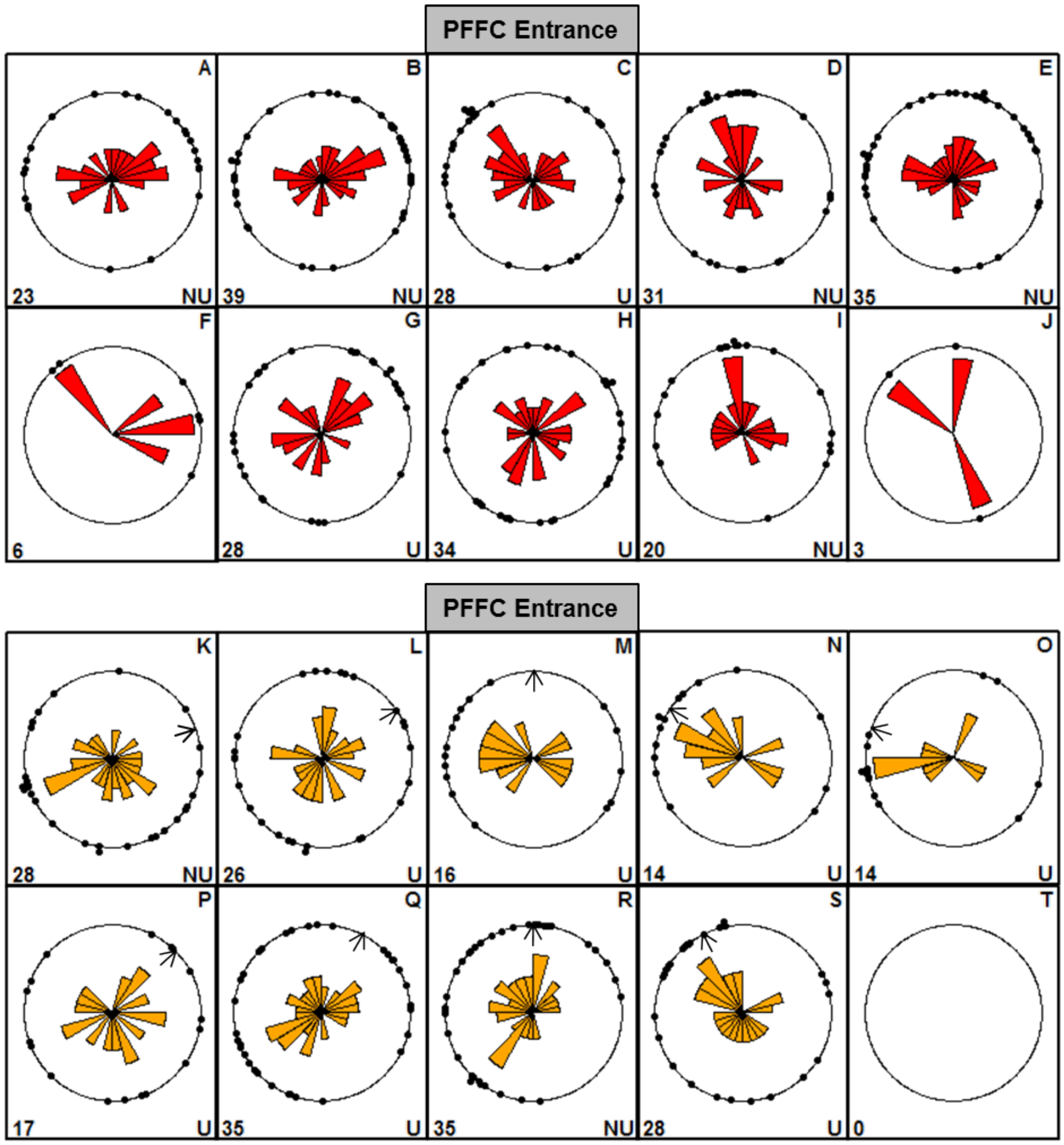

Figure 27. Rose diagrams showing mean bearings of acoustic+PIT-tagged juvenile Chinook salmon in front of the portable floating fish collector (PFFC) entrance at 3–6 meter depths during the day, Cougar Reservoir, Oregon, 2014. Figure parts A–J and K–T (indicated in the upper right corner of each part) show the Low and High treatment, respectively. Arrows indicate the direction from the center of each cell to the center of the collector entrance. Points on the plot circumferences are mean bearings for each fish and are stacked when multiple fish have the same bearing. Sample sizes are indicated in the lower left corner of each figure part and the results of Moore's second-order test of uniformity are given in the lower right corner for sample sizes greater than 9 (U=hypothesis of uniformly distributed bearings accepted, NU=hypothesis of uniformly distributed bearings rejected, α=0.05).

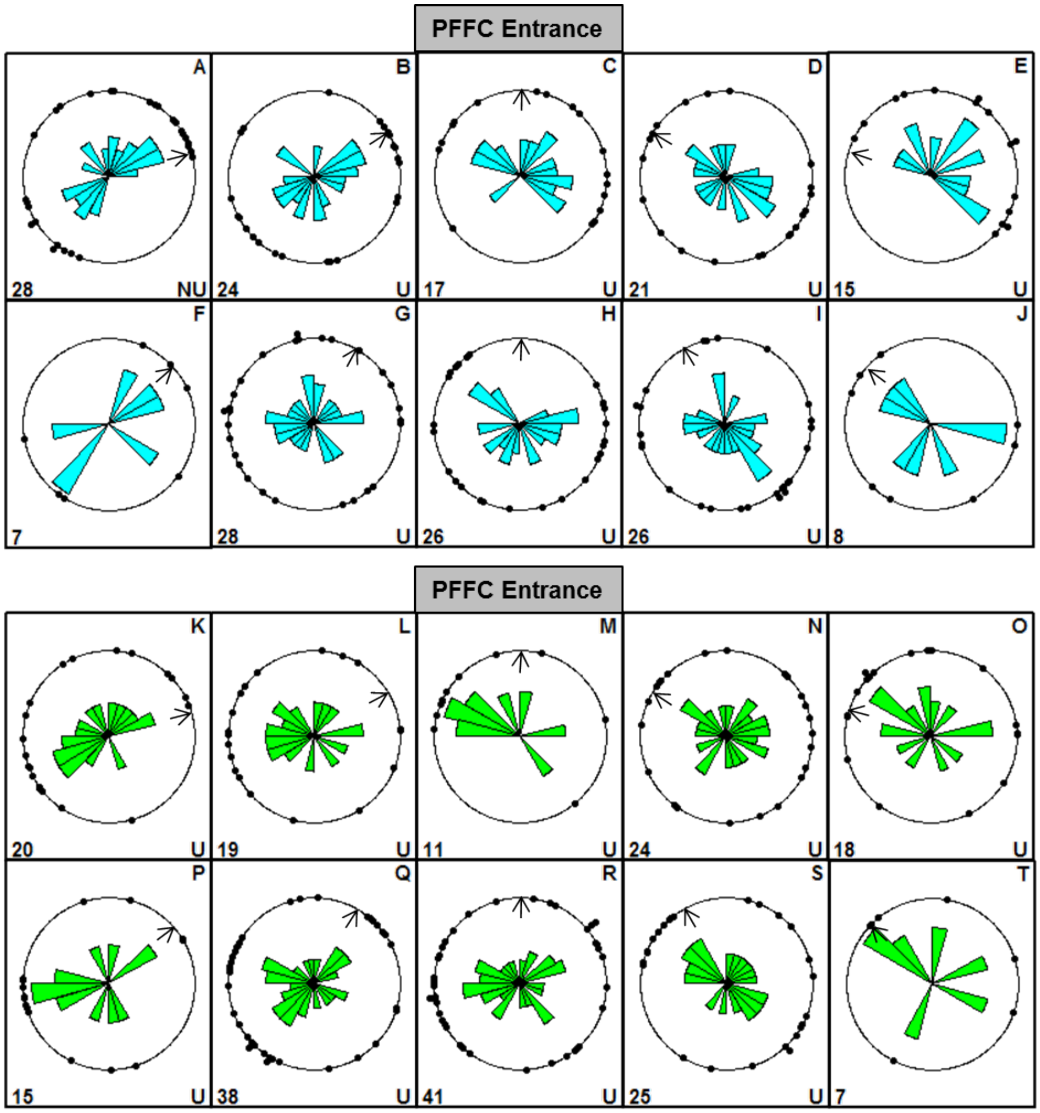

Figure 28. Rose diagrams showing mean bearings of acoustic+PIT-tagged juvenile Chinook salmon in front of the portable floating fish collector (PFFC) entrance at 3–6 meter depths during the night, Cougar Reservoir, Oregon, 2014. Figure parts A–J and K–T (indicated in the upper right corner of each part) show the Low and High treatment, respectively. Arrows indicate the direction from the center of each cell to the center of the collector entrance. Points on the plot circumferences are mean bearings for each fish and are stacked when multiple fish have the same bearing. Sample sizes are indicated in the lower left corner of each figure part and the results of Moore's second-order test of uniformity are given in the lower right corner for sample sizes greater than 9 (U=hypothesis of uniformly distributed bearings accepted, NU=hypothesis of uniformly distributed bearings rejected, α=0.05).

A sample of eight random fish trajectories during the Low treatment in the day reflect the data used to estimate UDs and fish movements near the PFFC (fig. 29). Although these fish approached between 5 and 10 m of the PFFC entrance, few fish approached closer than about 5 m. The trajectories often were relatively short (fig. 29A–D) and parallel to the PFFC (fig. 29 C–D, G, and H), but some fish milled briefly about 10 m from the PFFC entrance before moving out of the area (fig. 29F–H).

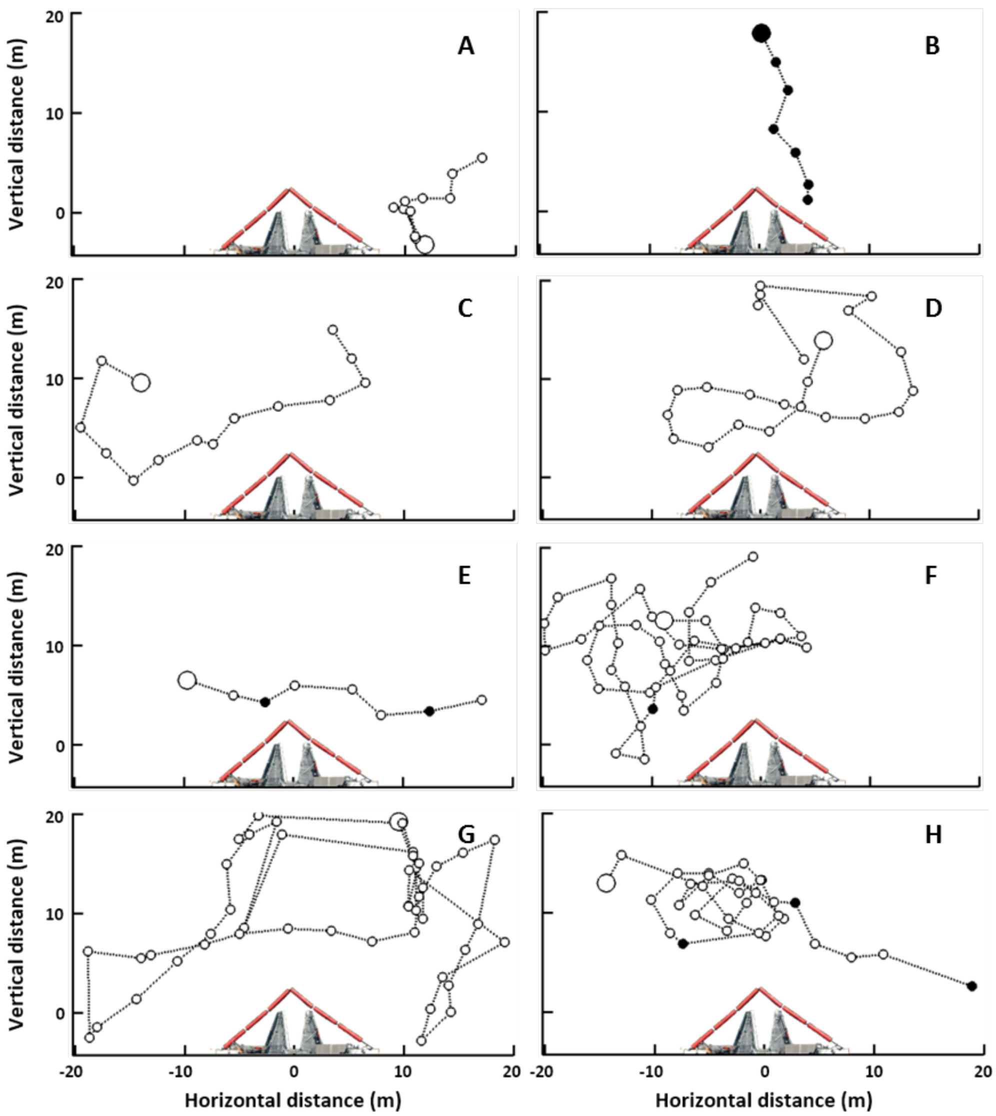

Figure 29. Graphs of movements of eight randomly selected acoustic+PIT-tagged juvenile Chinook salmon near the portable floating fish collector (PFFC; figure parts A–H) during the Low treatment during the day at Cougar Reservoir, Oregon, 2014. Fish were selected from a pool of fish with at least two positions within 10 m of the PFFC entrance. The large circle is the first position of each track, open circles are positions less than or equal to 3 m deep, filled circles are positions greater than 3 m in deep. The PFFC entrance is shown at the bottom of each plate.

Collection in the PFFC and Dam Passage

Most of the acoustic+PIT-tagged fish that passed Cougar Dam did so prior to the beginning of PFFC treatments on May 27, 2014. Of the 426 fish released, 10.1 percent (*N*=43) were assigned passage through the tower or PFFC within the 90th percentile of the acoustic tag life. A total of 65.1 percent of those fish (*N*=28) passed through the tower prior to PFFC operations on May 27, 2014, with most passing during a period of high discharge between May 10 and 12, 2014 (see fig. 10 in section, "Dam Operations and Environmental Conditions"). During the PFFC treatments, six acoustic+PIT-tagged fish passed the tower during each of the High and Low treatments and two were last detected on the acoustic telemetry system when the PFFC was off. One tagged hatchery Chinook salmon was collected in the PFFC on July 2, 2014, during the Low treatment and transported to the tailrace for release. Of the 43 fish assigned passage, 42 were of hatchery origin and one was of wild origin (initially collected with the Lampara seine). The PIT tag of one additional wild fish collected with the Lampara seine was detected downstream of Cougar Dam after the 90th percentile of the acoustic tag life. The wild fish was detected by the PIT interrogators at Leaburg Dam on November 4, 2014, at the Walterville Canal on November 8, 2014, and at Willamette Falls on November 13, 2014. In all, 44 acoustic+ PIT-tagged fish were assigned passage.

Most of the acoustic+PIT-tagged fish were detected in the cul-de-sac and near the PFFC or tower, but few entered a passage route. Over 93 percent of tagged fish were detected at the log boom (reservoir passage efficiency, RPE) and most fish detected at the log boom were subsequently detected in the cul-de-sac, resulting in a forebay passage efficiency (FBE) of 0.955 (table 9) The season-wide dam passage efficiency (DPE) was 0.108 (table 9). The DPE during the PFFC treatment period (DPE_{TREAT}) was 0.024 (6 of 245) during the Low treatment, 0.027 during the High treatment (6 of 226), and 0.057 overall (table 9). The Discovery Efficiency (DE) at the PFFC was significantly greater during the Low treatment than the High treatment (ratio = 1.574, 95-percent confidence interval [CI] 1.033–2.399; $P = 0.034$) (table 10). The DEs at the tower did not differ significantly between treatments ($P = 0.182$), but were greater than those at the PFFC (table 10). The entrance efficiency (EE) and fish collection efficiency [FCE] through the PFFC were less than 1 percent during each treatment. FCEs based on a denominator of fish numbers in the forebay (FBE_{FB}) or in the cul-de-sac (FCE_{CDS}) were similar because of the high FBE. Two of the acoustic+PIT-tagged fish were detected by the PFFC PIT interrogator, but only one of them was collected in the PFFC. The EE at the tower was 0.025 during the Low treatment and 0.032 during the High treatment. Fish collection effectiveness (FCF) of the two routes was at or near zero during both treatments. An alternate method to estimate effectiveness is to divide route passage by passage through all routes (PFFC and tower), resulting in an estimate of the proportion of passage afforded by each route. The FCF calculated using the alternate method for the PFFC was 0.167 for Low treatment and 0.000 for the High treatment. Corresponding estimates for the tower were 0.833 for the Low treatment and 1.000 for the High treatment.

Table 9. Reservoir passage efficiency, forebay passage efficiency, and dam passage efficiency from acoustic-tagged juvenile Chinook salmon at Cougar Reservoir, Oregon, 2014.

[Metrics RPE, DPE, and FBE were calculated over the entire study period (April 9–December 16, 2014) and DPE_{TREAT} was calculated from data beginning when portable floating fish collector (PFFC) treatments began on May 27, 2014. Sample size, number of tagged fish in the denominator of the estimate; RPE, reservoir passage efficiency; FBE, forebay passage efficiency; DPE, dam passage efficiency; Treat, time period during PFFC treatments; 95-percent CI, 95-percent lower and upper confidence intervals]

Metric	Sample size	Estimate	95-percent CI
RPE	426	0.932	0.904, 0.952
FBE	221	0.955	0.919, 0.975
DPE	397	0.108	0.081, 0.143
DPE_{TREAT}	246	0.057	0.028, 0.086

Table 10. Passage metric estimates and lower and upper 95-percent confidence intervals during portable floating fish collector treatments from acoustic-tagged juvenile Chinook salmon at Cougar Reservoir, Oregon, 2014.

[Sample size, number of tagged fish in the denominator of the estimate; 95-percent CI, 95-percent lower and upper confidence intervals; *P*, probability; CDS, cul-de-sac; DE, discovery efficiency; FB, forebay; PFFC, portable floating fish collector; EE, entrance efficiency; FCE, fish collection efficiency; FCF, fish collection effectiveness; Tower, water temperature control tower; NA, not applicable]

Metric	PFFC Low			PFFC High			Difference		
	Sample size	Estimate	95-percent CI	Sample size	Estimate	95-percent CI	Odds ratio	95-percent CI	*P*
				PFFC					
DE	208	0.736	0.672, 0.791	202	0.639	0.570, 0.702	1.574	1.033, 2.399	0.034
EE	153	0.007	0.000, 0.019	129	0.000	0.000, 0.000	NA	NA	NA
FCE_{FB}	245	0.004	0.000, 0.012	226	0.000	0.000, 0.000	NA	NA	NA
FCE_{CDS}	210	0.005	0.000, 0.014	204	0.000	0.000, 0.000	NA	NA	NA
FCF	NA	0.007	NA	NA	0.000	NA	NA	NA	NA
				Tower					
DE	208	0.957	0.920, 0.977	202	0.926	0.881, 0.955	1.774	0.758, 4.150	0.182
EE	199	0.025	0.003, 0.047	187	0.032	0.007, 0.057	0.777	0.233, 2.592	0.681
FCE_{FB}	245	0.020	0.003, 0.038	226	0.027	0.001, 0.048	0.764	0.223, 2.538	0.659
FCE_{CDS}	210	0.024	0.003, 0.044	204	0.029	0.006, 0.053	0.805	0.242, 2.680	0.723
FCF	NA	0.000	NA	NA	0.000	NA	NA	NA	NA

Some of the acoustic+PIT-tagged fish passing Cougar Dam were detected as far downstream as Portland, Oregon. A total of 39.5 percent (*N*=17) of the 43 tagged juvenile Chinook salmon passing Cougar Dam within the life of the acoustic transmitter were detected at acoustic telemetry or PIT sites downstream of Cougar Dam. Of those fish, 70.6 percent (*N*=12) were detected at the acoustic telemetry sites in the tailraces (9 below the powerhouse, 2 below the RO, 1 at both places), 47.1 percent (*N*=8) were detected at the acoustic telemetry site at the USGS stream gage on the South Fork McKenzie River (stream gage number 14159410), and 35.3 percent (*N*=6) were detected at the Leaburg Dam complex. Detection at the powerhouse or RO tailrace does not necessarily indicate passage route because fish can move between tailraces after passage (Beeman and others, 2014a). Three fish were detected at the acoustic telemetry sites in the Willamette River (Salem, Wilsonville, and Portland).

Some of the juvenile Chinook salmon tagged solely with PIT tags were detected at the PFFC interrogator or downstream of Cougar Dam. A total of 12.7 percent (63 of 495) of the fish released in the spring and 6.2 percent (63 of 1,010) of those released in the fall were detected at downstream PIT sites. None of the fish released in the spring and two released in the fall were collected in the PFFC, indicating that the rest passed through the tower. Six percent (61 of 1,010) of the fish released in the fall passed through the tower. Some fish were detected multiple times on the PIT interrogator, sometimes over multiple days, indicating the antenna was located in an area without complete fish entrainment. After accounting for the detection probability of the PIT interrogator and fish that left the reservoir through the tower, the PFFC fish collection efficiency of PIT-tagged fish was 0.000 in the spring and 0.002 in the fall.

Untagged Fish

Outside the PFFC

Fish Abundance

Data from the acoustic camera indicated that fish abundance upstream of the PFFC was less than 500 fish per day (fig. 30). The predominant size category was large fish (90–250 mm), with peak abundances observed during late-May and late-September. Abundance increased again in late-October near the time data collection ended. The daily abundance trends of predator-size fish (>300 mm) generally mimicked that of the large fish (90–250 mm), with a maximum observation of 107 predator-sized fish in mid-October. No fish in the 30–60 mm size category were observed, and a few medium-sized fish (60–90 mm) were observed in late-October.

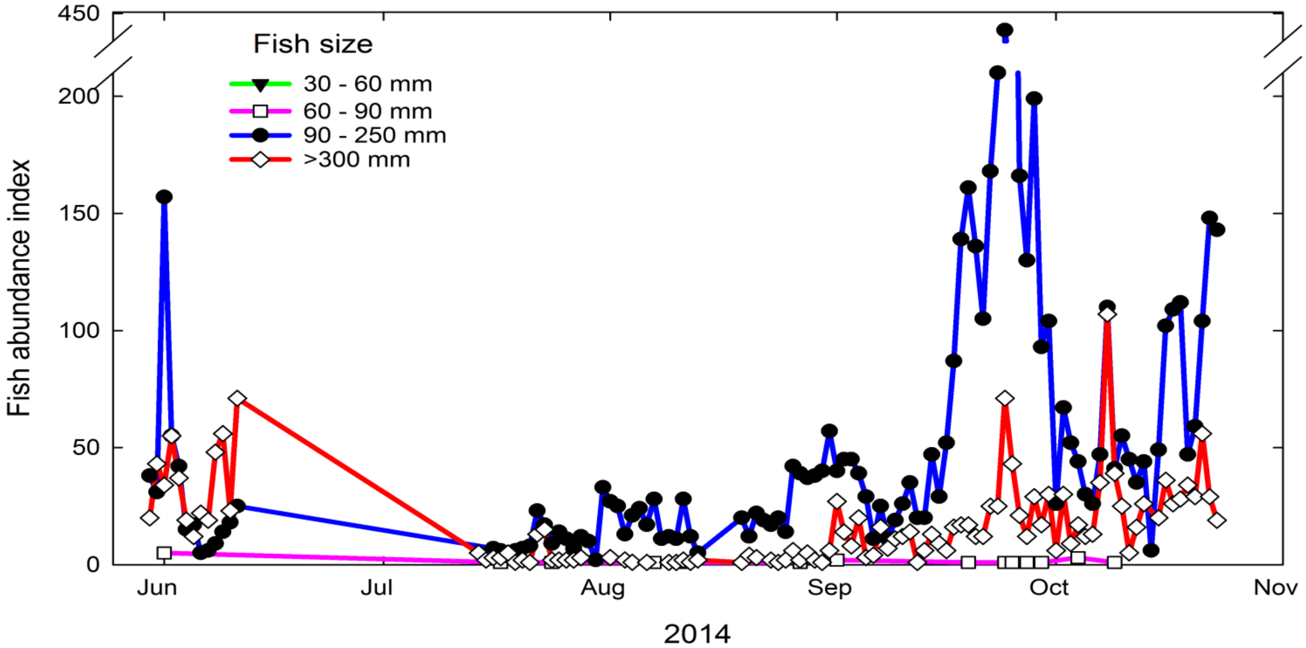

Figure 30. Graph showing date of detection of fish by size category using the acoustic camera outside the portable floating fish collector at Cougar Reservoir, Oregon, 2014.

Fish Movements

Fish Directions

When the PFFC was on, the direction of fish movement immediately upstream appeared to be influenced more by photoperiod than by PFFC treatment (table 11). No small fish (30–60 mm) were observed in the acoustic beam, and there were insufficient numbers of medium fish (60–90 mm; *N*=17) to accurately describe directions of movement during either photoperiod or PFFC treatment (fig. 31). However, for the large fish (90–250 mm) during the day, rose diagrams showed that they appeared to move away from the entrance to the PFFC regardless of treatment (fig. 32). During the night, movements of the large fish were lateral to the entrance to the PFFC. The directions of movement for large fish during both the Low and High treatments had a diametrically bimodal distribution.

The direction of movement for predator-size fish (> 300 mm; fig. 33) was similar to that of large fish (90–250 mm). When the PFFC was on, the predator-size fish appeared to move away from the entrance during the day and lateral to the entrance during the night. When the PFFC was off, fish movements appeared to be random across all fish sizes and for both day and night.

Table 11. Mean travel directions and concentration parameters by size category for fish detected using the acoustic camera outside the portable floating fish collector at Cougar Reservoir, Oregon, 2014.

[The heading to the entrance of the PFFC is normalized to 0°. *N*, sample size; *μ*, mean travel direction (in degrees) of the fish; SE, standard error; *κ*, concentration parameter; mm, millimeter; NA, not applicable; >, greater than. Note: Sample size is the number of fish observation events with the acoustic camera, not necessarily the number of individual fish, because a given fish could be observed more than once]

Fish size category (type)	*N*	*μ* (SE)	*κ* (SE)
PFFC off, Day			
30 60 mm (small fish)	0	NA	NA
60–90 mm (medium fish)	0	NA	NA
90–250 mm (large fish)	65	6.64 (51.74)	0.20 (0.18)
>300 mm (predators)	97	253.18 (24.29)	0.34 (0.15)
PFFC off, Night			
30–60 mm (small fish)	0	NA	NA
60–90 mm (medium fish)	0	NA	NA
90–250 mm (large fish)	80	267.45 (18.39)	0.50 (0.17)
>300 mm (predators)	19	247.62 (39.88)	0.47 (0.34)
Low treatment, Day			
30–60 mm (small fish)	0	NA	NA
60–90 mm (medium fish)	8	181.96 (27.79)	1.10 (0.61)
90–250 mm (large fish)	425	202.82 (31.17)	0.13 (0.07)
>300 mm (predators)	274	162.37 (56.09)	0.09 (0.09)
Low treatment, Night			
30–60 mm (small fish)	0	NA	NA
60–90 mm (medium fish)	4	7.38 (74.26)	0.56 (0.75)
90–250 mm (large fish)	1,563	104.79/284.79 (3.67)	0.56 (0.04)
>300 mm (predators)	195	131.07/311.07 (4.58)	1.34 (0.14)
High treatment, Day			
30–60 mm (small fish)	0	NA	NA
60–90 mm (medium fish)	1	26.14 (NA)	NA (NA)
90–250 mm (large fish)	377	212.79 (16.22)	0.26 (0.07)
>300 mm (predators)	725	231.41(25.44)	0.12 (0.05)
High treatment, Night			
30–60 mm (small fish)	0	NA	NA
60–90 mm (medium fish)	4	83.23 (11.00)	7.33 (4.97)
90–250 mm (large fish)	3,150	104.70/284.70 (2.69)	0.55 (0.03)
>300 mm (predators)	378	144.75/324.75 (3.90)	1.16 (0.09)

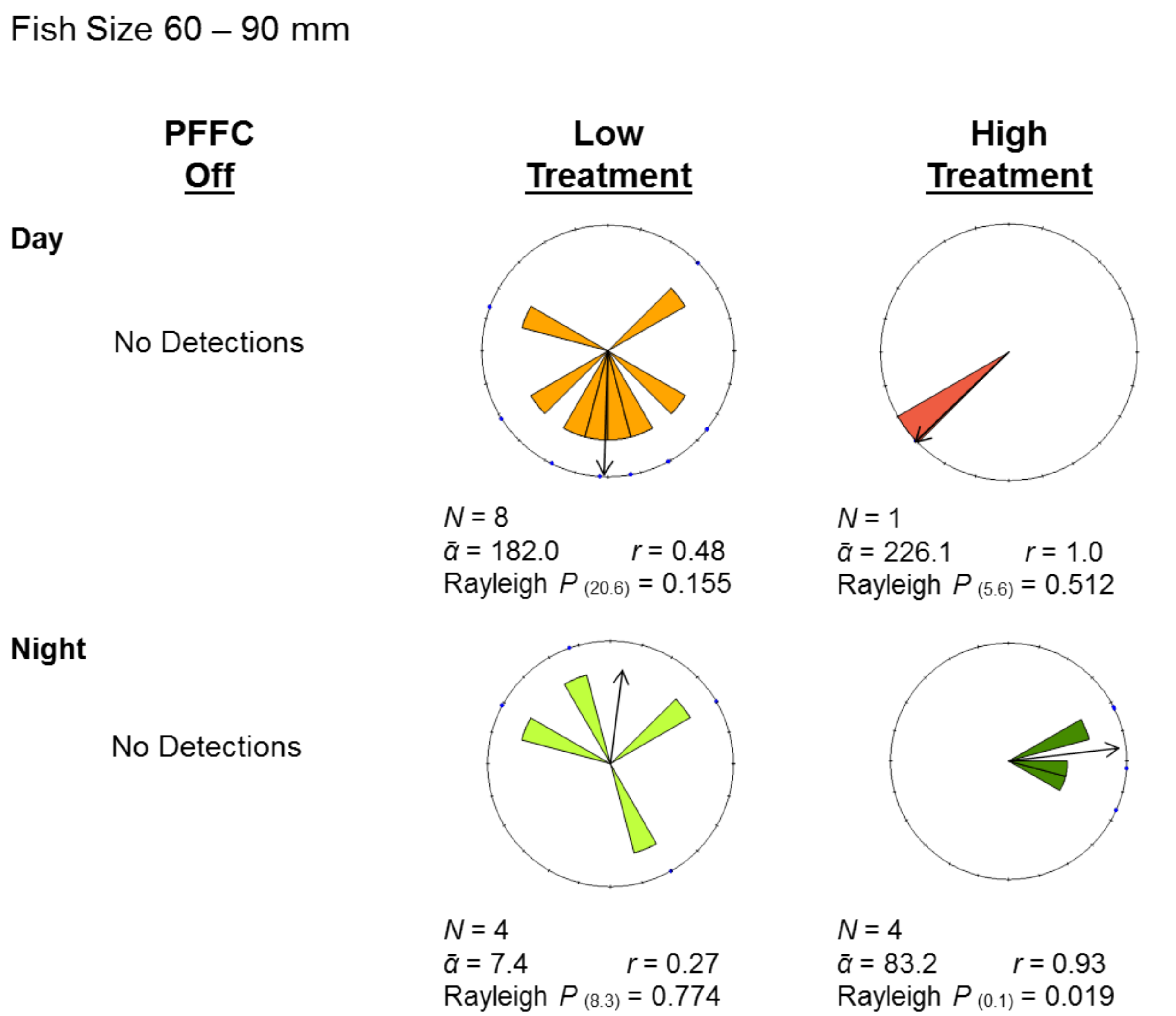

Figure 31. Rose diagrams of mean travel directions (in degrees) by diel period (Day or Night) and portable floating fish collector (PFFC) condition (PFFC Off, Low Treatment, or High Treatment) for the 60–90 millimeter (mm) size category of fish detected using the acoustic camera outside the PFFC at Cougar Reservoir, Oregon, 2014. The heading to the entrance of the PFFC is normalized to 0° (top). Sample sizes represent the number of fish (*N*) observed during each period. The mean vector ($\bar{\alpha}$) and mean vector resultant length (*r*) are described by the arrows. The Rayleigh *P* indicates the significance level according to the Rayleigh *z* test statistic (in parenthesis).

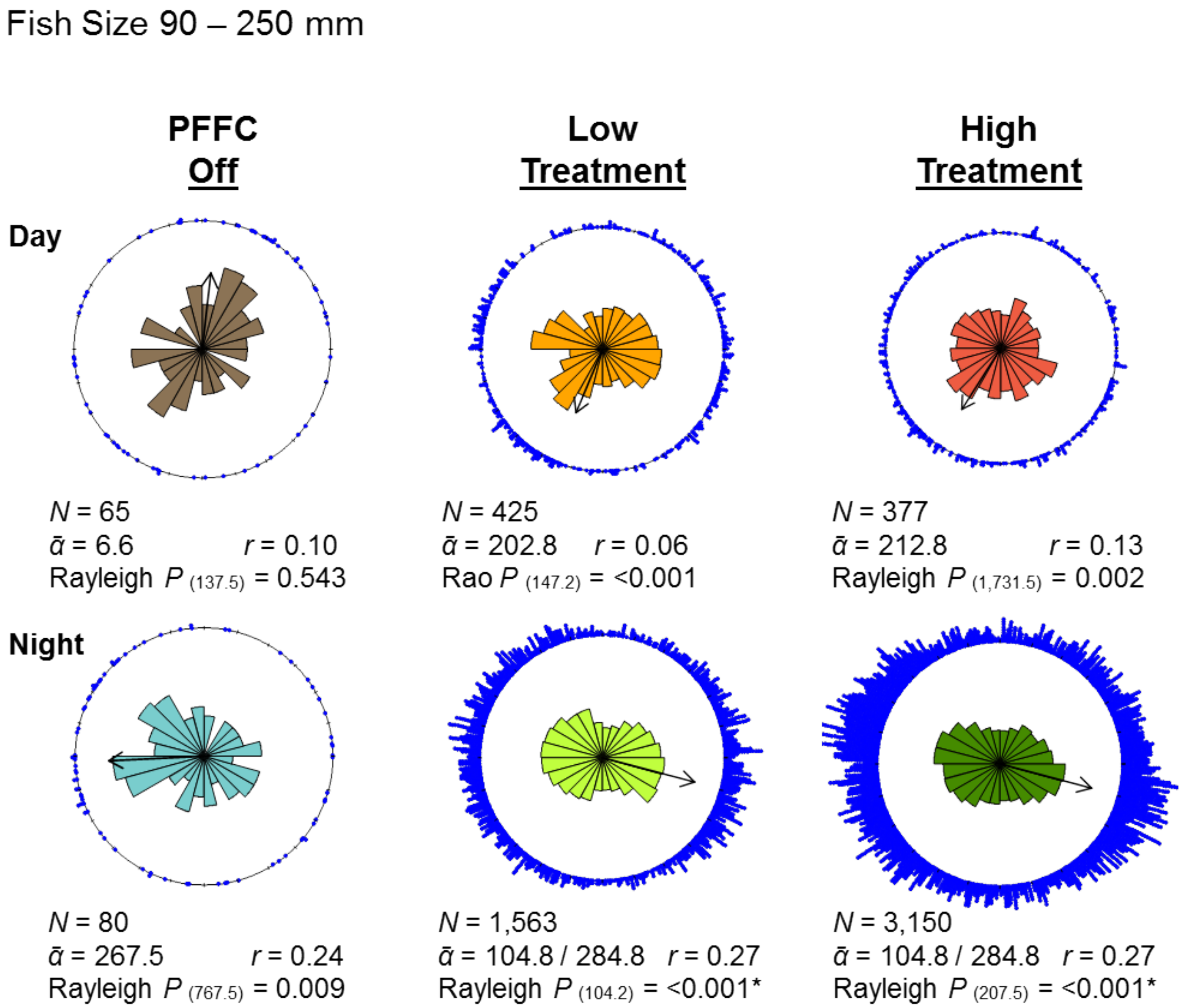

Figure 32. Rose diagrams of mean travel directions (in degrees) by diel period (Day or Night) and portable floating fish collector (PFFC) condition (PFFC Off, Low Treatment, or High Treatment) for the 90–250 millimeter (mm) size category of fish detected using the acoustic camera outside the PFFC at Cougar Reservoir, Oregon, 2014. The heading to the entrance of the PFFC is normalized to 0° (top). Sample sizes represent the number of fish (N) observed during each period. The mean vector ($\bar{\alpha}$) and mean vector resultant length (r) are described by the arrows. The Rayleigh P indicates the significance level according to the Rayleigh z test statistic (in parenthesis). A Rao P was calculated when the data failed to follow a von Mises distribution or was multi-modal. *Because of a bimodal distribution, the data were transformed (not shown) in accordance with Zar (1999).

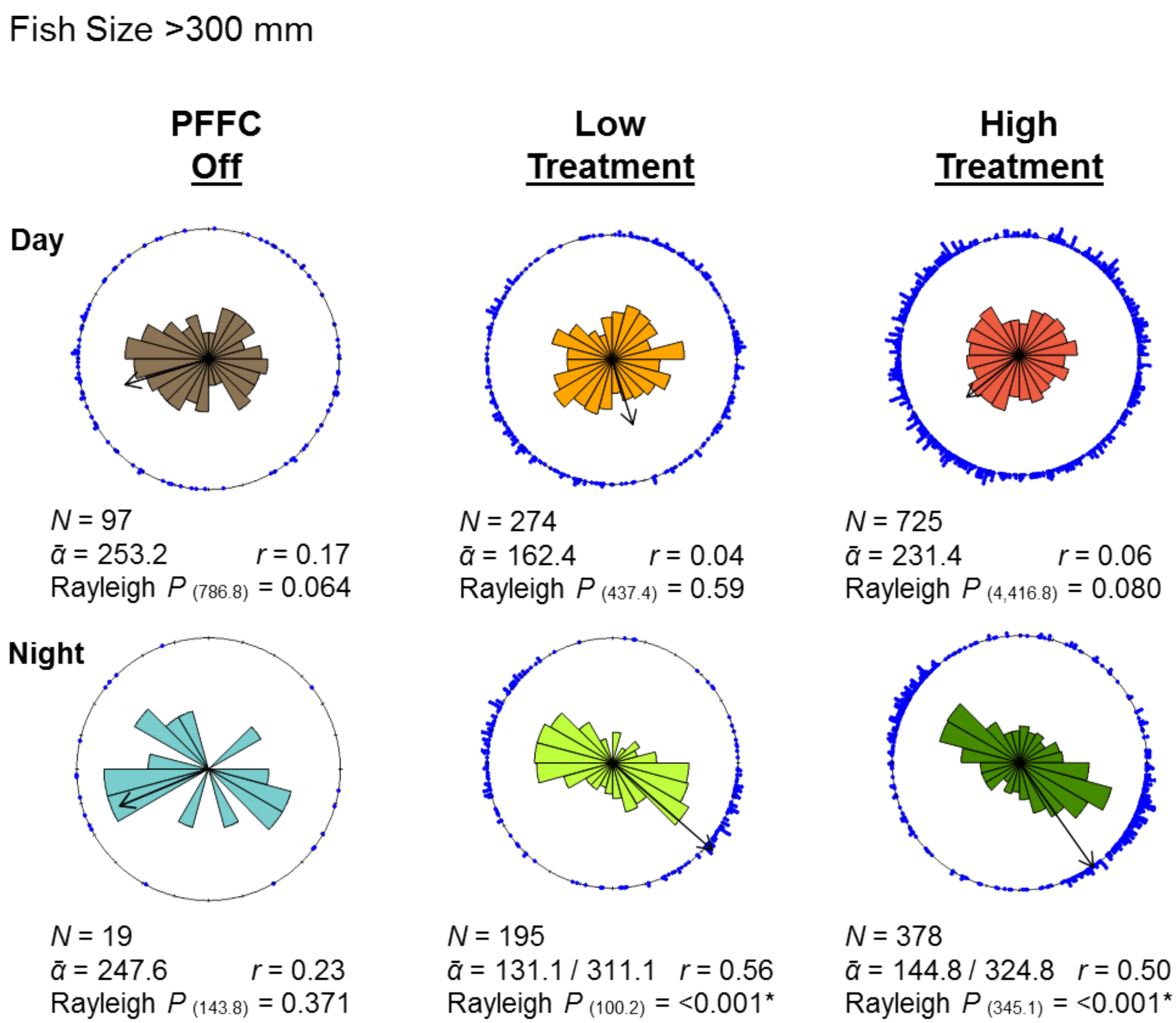

Figure 33. Rose diagrams of mean travel directions (in degrees) by diel period (Day or Night) and portable floating fish collector (PFFC) condition (PFFC Off, Low Treatment, or High Treatment) for the greater than (>) 300 millimeter (mm) size category of fish detected using the acoustic camera outside the PFFC at Cougar Reservoir, Oregon, 2014. The heading to the entrance of the PFFC is normalized to 0° (top). Sample sizes represent the number of fish (*N*) observed during each period. The mean vector ($\bar{\alpha}$) and mean vector resultant length (*r*) are described by the arrows. The Rayleigh *P* indicates the significance level according to the Rayleigh *z* test statistic (in parenthesis). *Because of a bimodal distribution, the data were transformed (not shown) in accordance with Zar (1999).

Fish Speed and Duration of Observation

The speed at which fish traveled in the area upstream of the PFFC was not influenced by the PFFC treatment. For example, the mean travel speed of fish was 0.48 ft/s (interquartile range (IQR) = 0.50) when the PFFC was off, 0.54 ft/s (IQR = 0.45) during the Low treatment, and 0.53 ft/s (IQR = 0.50) during the High treatment (table 12). These differences in fish travel speed were not significant between treatments (ANOVA; $F_{2, 5674} = 1.987$, $P = 0.137$).

Although fish speed was not influenced by PFFC treatment, the duration of time fish were observed in the acoustic beam was influenced by treatment (table 12). An ANOVA on the score yielded significant variation among the treatments ($F_{2, 5674} = 3.870$, $P = 0.021$). A post hoc Tukey HSD test showed that fish that were observed when the PFFC was off had significantly longer durations than both the Low and the High treatment groups ($P < 0.020$), whereas the Low and the High treatment groups were not significantly different from each other ($P = 0.989$). In comparison to the Low and High treatments, travel times tended to be longer and travel speeds slower when the PFFC was off.

Table 12. Summary statistics for the travel speeds and duration of detection of fish observed using the acoustic camera outside the portable floating fish collector at Cougar Reservoir, Oregon, 2014.

[*N*, sample size; SD, standard deviation; IQR, interquartile range; ft/s, feet per second; s, seconds; PFFC, portable floating fish collector; <, less than. Note: Sample size is the number of fish observation events with the acoustic camera, not necessarily the number of individual fish, because a given fish could be observed more than once]

Condition	*N*	Mean	SD	IQR	Minimum	2.5th percentile	50th percentile	97.5th percentile	Maximum
					Travel speed (ft/s)				
PFFC off	145	0.48	0.36	0.50	0.03	0.05	0.44	1.16	2.68
Low treatment	2,000	0.54	0.34	0.45	<0.01	0.06	0.48	1.30	2.10
High treatment	3,532	0.53	0.34	0.50	<0.01	0.06	0.48	1.28	1.76
					Duration in acoustic beam (s)				
PFFC off	145	10.68	20.66	7.43	0.60	0.77	5.55	69.95	170.22
Low treatment	2,000	7.35	13.57	5.83	0.50	0.77	4.67	27.08	303.57
High treatment	3,532	7.40	14.10	6.15	0.50	0.66	4.51	29.45	340.42

Tortuosity

The tortuosity index indicated that fish tracks immediately upstream of the PFFC entrance were essentially linear regardless of treatment or fish size. For all three groups, the median tortuosity index (50th percentile) values ranged from 1.10 to 1.12 (table 13). The only observable differences between the treatment groups were that the maximum values increased as the amount of water entering the PFFC increased, but these differences were not significant (ANOVA; $F_{2,5674} = 0.710$, $P = 0.492$).

Table 13. Summary statistics for the tortuosity index of fish observed using the acoustic camera outside the portable floating fish collector at Cougar Reservoir, Oregon, 2014.

[*N*, sample size; SD standard deviation; PFFC, portable floating fish collector. Note: Sample size is the number of fish observation events with the acoustic camera, not necessarily the number of individual fish, because a given fish could be observed more than once]

Condition	*N*	Mean	SD	Minimum	25th percentile	50th percentile	75th percentile	Maximum
PFFC off	145	1.72	2.00	1.00	1.03	1.12	1.48	15.43
Low treatment	2,000	1.59	1.76	1.00	1.03	1.10	1.35	34.83
High treatment	3,532	1.66	1.52	1.00	1.03	1.10	1.35	56.12

Timing of Detection

Peaks in the number of fish detected upstream of the PFFC coincided with the crepuscular periods. Detections for medium fish (60–90 mm) were greatest at approximately 6:00 a.m. and 8:00 a.m. and again at 7:00 p.m., but low sample numbers resulted in several hours lacking any observations for fish of that size category. For larger fish (90–250 mm), the percentage of fish detections peaked in the morning at about 3:00 a.m., and then generally was low throughout the day until approximately 6:00 p.m. when fish detections began to increase again (fig. 34). The percentage of detections of predator-size fish (> 300 mm) was the opposite of that of the smaller fish (< 250 mm), with the peak number of observations occurring later in the day at about 3:00 p.m.

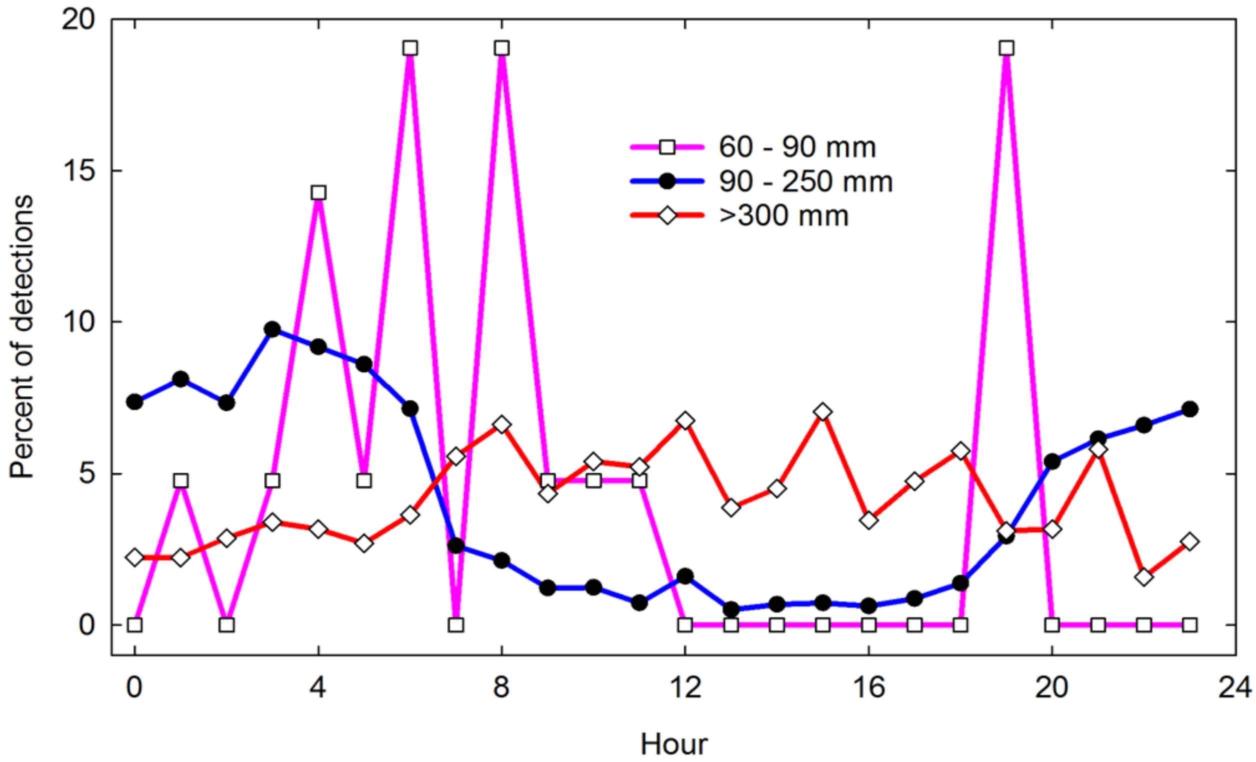

Figure 34. Graph showing hour of detection of fish by size category (in millimeters [mm]) using the acoustic camera outside the portable floating fish collector at Cougar Reservoir, Oregon, 2014.

Within and Near the PFFC

Fish Abundance

The abundance of fish at the entrance of the PFFC peaked in late-June/early-July and then remained low until abundance increased again in late-October (fig. 35). The most abundant size category was the 90–250 mm large fish with a predominant peak in late-June to early-July and minor peaks in the late-October to early-November periods. The daily abundance of predator-size fish (>300 mm) was low during the spring and summer relative to the large fish, but increased in the fall with abundances similar to those of the large fish. Daily observations for fish in the 30–60 and 60–90 mm size categories peaked in early-July, with few fish from either size category being observed as the season progressed.

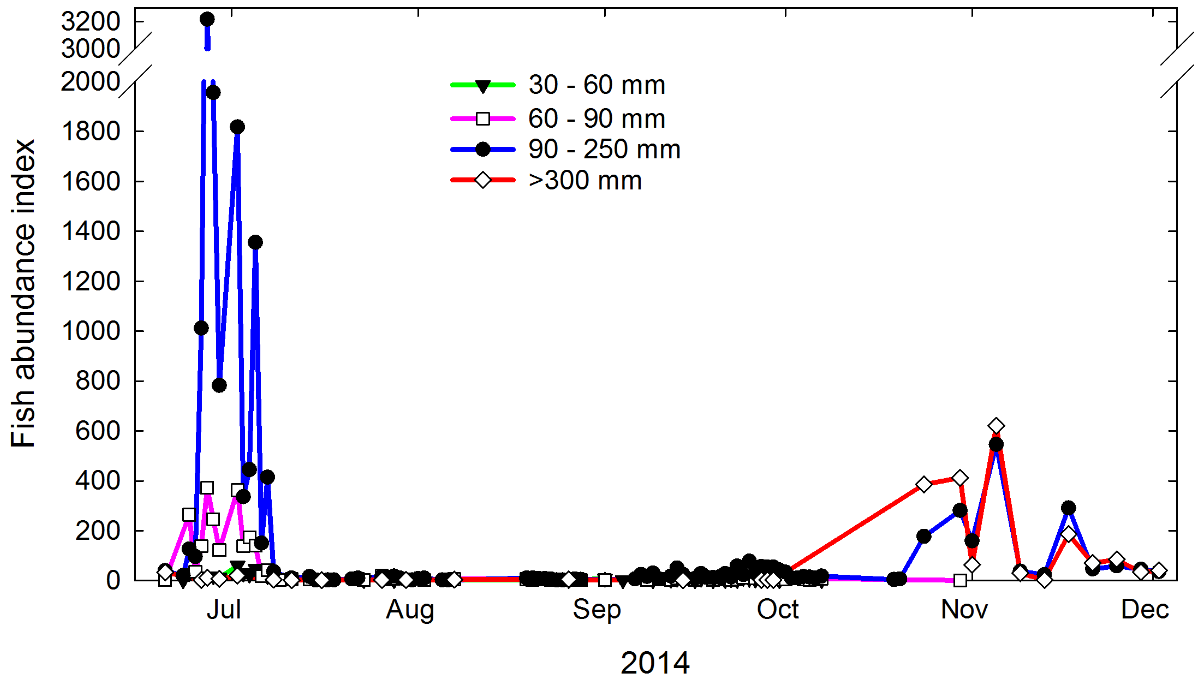

Figure 35. Graph showing date of detection of fish by size category (in millimeters [mm]) using the acoustic cameras inside the portable floating fish collector at Cougar Reservoir, Oregon, 2014.

Fish Movements

Fish Directions

Data collected by cameras mounted inside the PFFC showed that fish movements were directed inward when the PFFC was on regardless of fish size, photoperiod, or PFFC treatment (table 14; figs. 36–39; appendix G). Although there were no significant differences in the direction of movements, there were significantly more fish observed inside the PFFC during the day compared to the night for all sizes of fish. When the PFFC was off, there were few fish observed inside and their movements were random.

Table 14. Mean travel directions (in degrees) and concentration parameters by size category of fish observed inside the entrance to the portable floating fish collector (PFFC) using acoustic cameras inside the PFFC at Cougar Reservoir, Oregon, 2014.

[The heading to the entrance of the PFFC is normalized to 0°. *N*, sample size; μ, mean direction (in degrees) of the fish; SE, standard error; κ, concentration parameter; mm, millimeter; NA, not applicable; >, greater than. Note: Sample size is the number of fish observation events with the acoustic camera, not necessarily the number of individual fish, because a given fish could be observed more than once]

Fish size category (type)	*N*	μ (SE)	κ (SE)
PFFC off, Day			
30–60 mm (small fish)	0	NA	NA
60–90 mm (medium fish)	4	83.02 (51.80)	0.81 (0.80)
90–250 mm (large fish)	14	91.67 (31.86)	0.70 (0.41)
>300 mm (predators)	21	78.50 (88.24)	0.20 (0.31)
PFFC off, Night			
30–60 mm (small fish)	0	NA	NA
60–90 mm (medium fish)	0	NA	NA
90–250 mm (large fish)	2	341.88 (22.92)	3.68 (3.28)
>300 mm (predators)	0	NA	NA
Low treatment, Day			
30–60 mm (small fish)	37	35.23 (44.23)	0.30 (0.24)
60–90 mm (medium fish)	90	49.21 (12.09)	0.73 (0.16)
90–250 mm (large fish)	256	49.35 (4.47)	1.23 (0.11)
>300 mm (predators)	199	43.11 (7.05)	0.85 (0.11)
Low treatment, Night			
30–60 mm (small fish)	9	36.98 (41.94)	0.66 (0.51)
60–90 mm (medium fish)	23	59.47 (14.27)	1.29 (0.39)
90–250 mm (large fish)	53	54.67 (9.51)	1.28 (0.25)
>300 mm (predators)	27	43.30 (10.43)	1.73 (0.43)
High treatment, Day			
30–60 mm (small fish)	23	38.43 (27.04)	0.64 (0.32)
60–90 mm (medium fish)	62	27.38 (6.25)	1.97 (0.31)
90–250 mm (large fish)	225	47.04 (3.50)	1.81 (0.15)
>300 mm (predators)	100	51.66 (6.76)	1.31 (0.19)
High treatment, Night			
30–60 mm (small fish)	4	5.57 (18.97)	2.86 (1.74)
60–90 mm (medium fish)	9	61.02 (28.65)	1.00 (0.60)
90–250 mm (large fish)	24	43.07 (16.73)	1.05 (0.35)
>300 mm (predators)	9	16.20 (21.14)	1.42 (0.65)

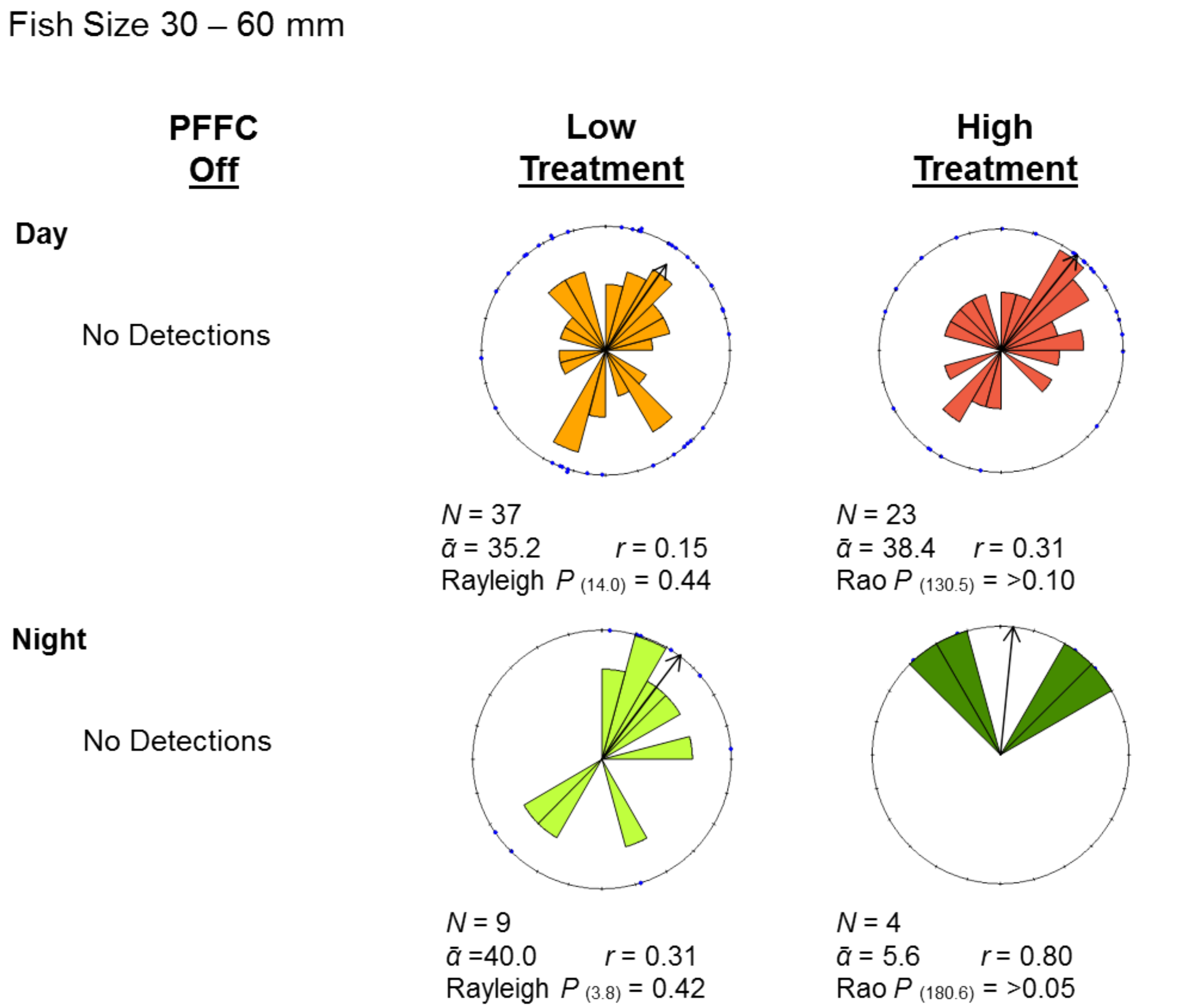

Figure 36. Rose diagrams of mean travel directions (in degrees) by diel period (Day or Night) and portable floating fish collector (PFFC) condition (PFFC Off, Low Treatment, or High Treatment) for the 30–60 millimeter (mm) size category of fish detected within the entrance of the PFFC using acoustic cameras inside the PFFC at Cougar Reservoir, Oregon, 2014. The heading to the entrance of the PFFC is normalized to 0° (top). Sample sizes represent the number of fish (*N*) observed during each period. The mean vector ($\bar{\alpha}$) and mean vector resultant length (*r*) are described by the arrows. The *P*-value indicates the significance level according to either the Rayleigh *z* or Rao *U* test statistic (in parenthesis).

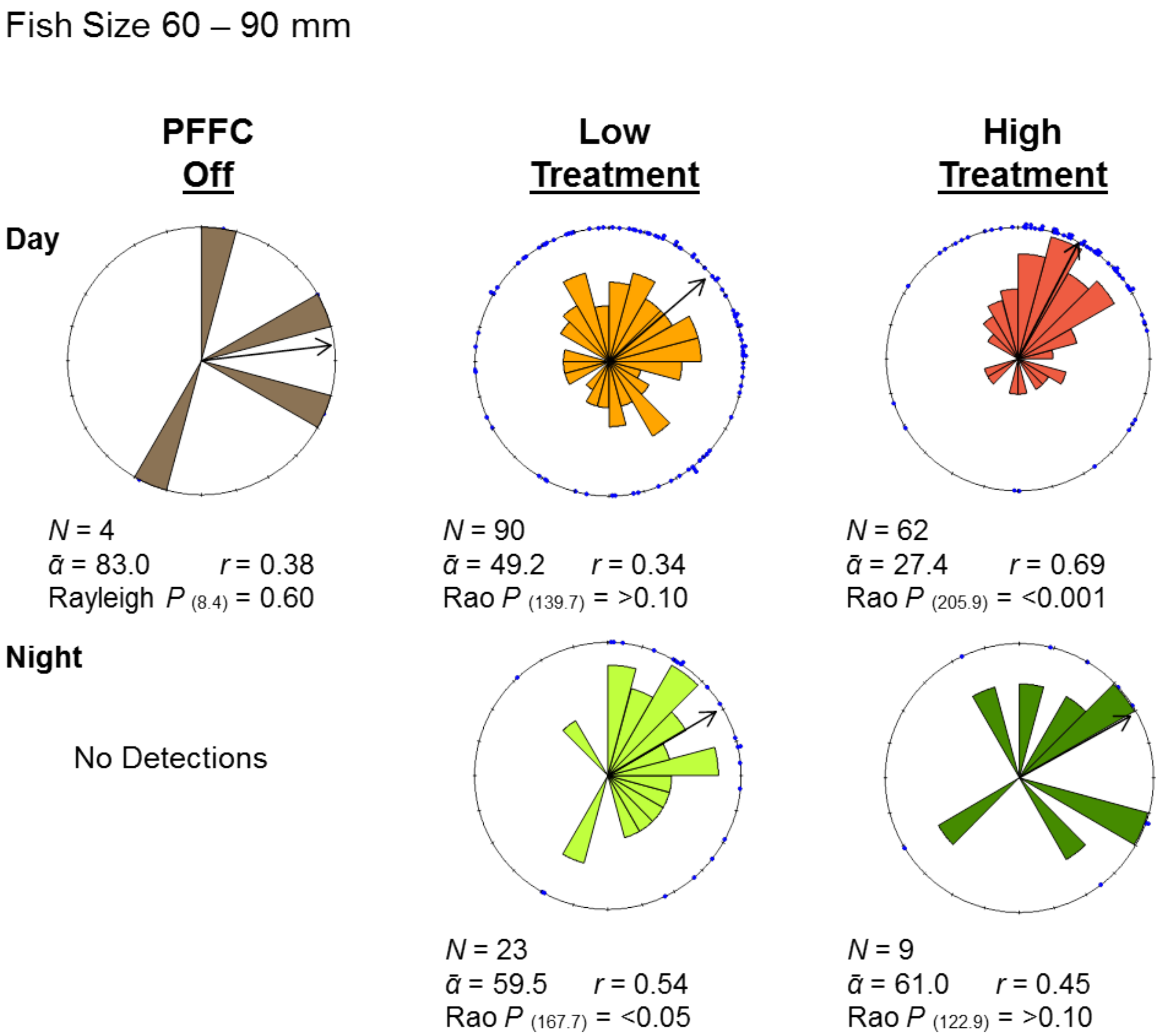

Figure 37. Rose diagrams of mean travel directions (in degrees) by diel period (Day or Night) and portable floating fish collector (PFFC) condition (PFFC Off, Low Treatment, or High Treatment) for the 60–90 millimeter (mm) size category of fish detected within the entrance of the PFFC using acoustic cameras inside the PFFC at Cougar Reservoir, Oregon, 2014. The heading to the entrance of the PFFC is normalized to 0° (top). Sample sizes represent the number of fish (*N*) observed during each period. The mean vector ($\bar{\alpha}$) and mean vector resultant length (*r*) are described by the arrows. The *P*-value indicates the significance level according to either the Rayleigh *z* or Rao *U* test statistic (in parenthesis).

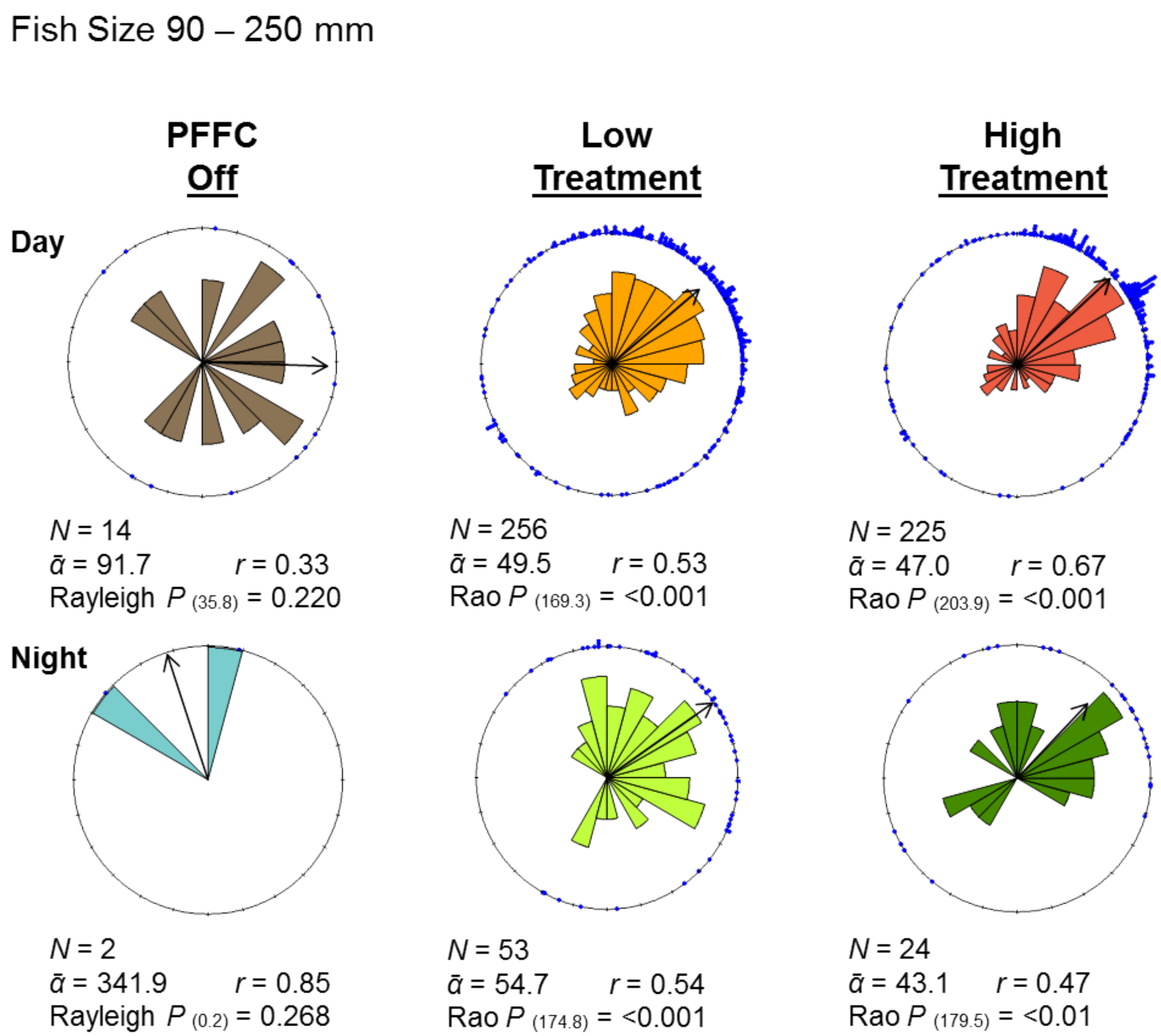

Figure 38. Rose diagrams of mean travel directions (in degrees) by diel period (Day or Night) and portable floating fish collector (PFFC) condition (PFFC Off, Low Treatment, or High Treatment) for the 90–250 millimeter (mm) size category of fish detected within the entrance of the PFFC using acoustic cameras inside the PFFC at Cougar Reservoir, Oregon, 2014. The heading to the entrance of the PFFC is normalized to 0° (top). Sample sizes represent the number of fish (*N*) observed during each period. The mean vector ($\bar{\alpha}$) and mean vector resultant length (*r*) are described by the arrows. The *P*-value indicates the significance level according to either the Rayleigh *z* or Rao *U* test statistic (in parenthesis).

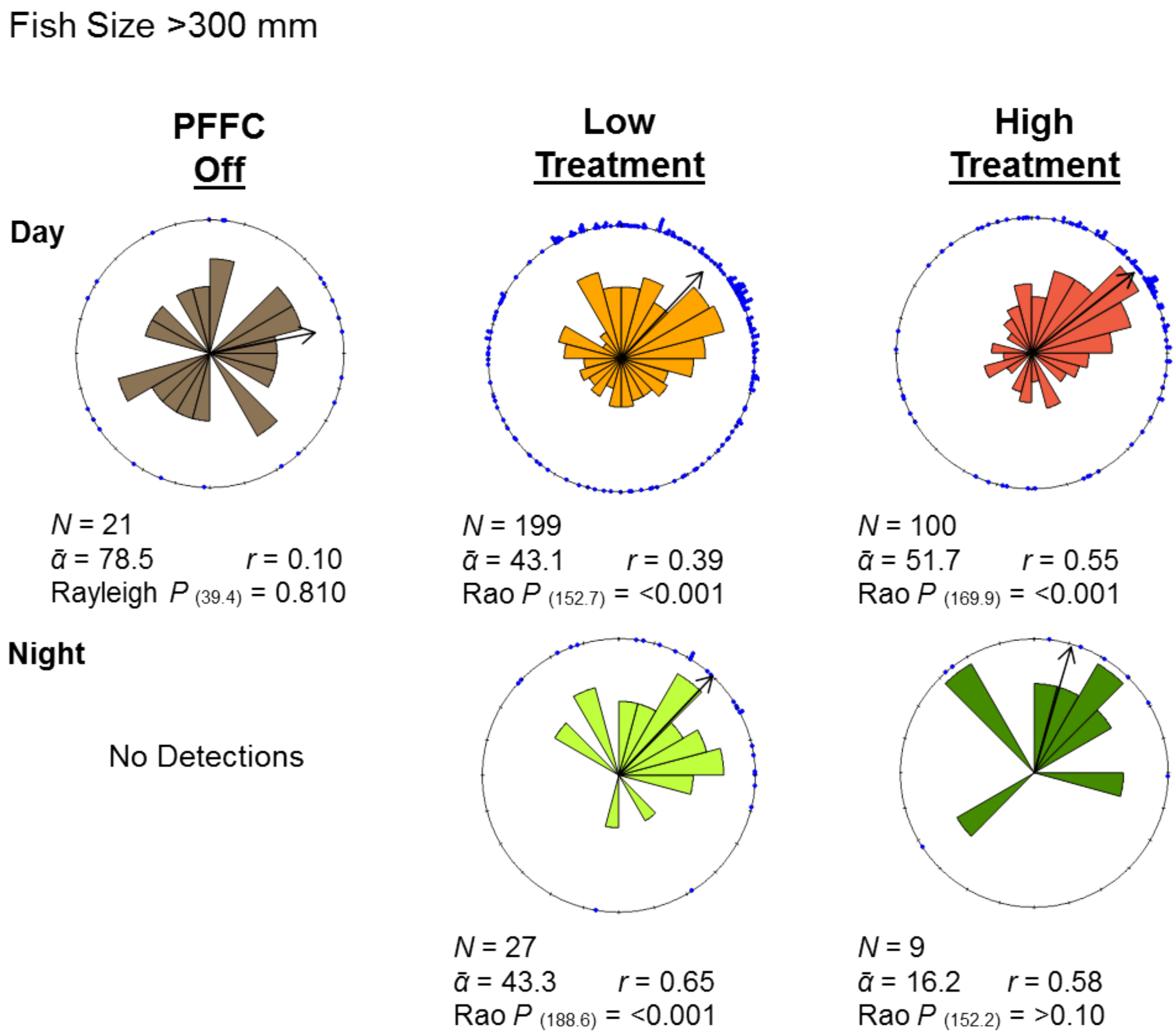

Figure 39. Rose diagrams of mean travel directions (in degrees) by diel period (Day or Night) and portable floating fish collector (PFFC) condition (PFFC Off, Low Treatment, or High Treatment) for the greater than (>) 300 millimeter (mm) size category of fish detected within the entrance of the PFFC using acoustic cameras inside the PFFC at Cougar Reservoir, Oregon, 2014. The heading to the entrance of the PFFC is normalized to 0° (top). Sample sizes represent the number of fish (*N*) observed during each period. The mean vector ($\bar{\alpha}$) and mean vector resultant length (*r*) are described by the arrows. The *P*-value indicates the significance level according to either the Rayleigh *z* or Rao *U* test statistic (in parenthesis).

Fish of all sizes observed outside the PFFC flume had circular distributions that were significantly directed, but the directions were not always toward the PFFC. Small sample sizes for fish less than 90 mm likely resulted in some inconsistent results (table 15; figs. 40 and 41). However, for the large size class (90–250 mm), which had a relatively large sample size, fish observed when the PFFC was off during the day were directed to the west of the PFFC, whereas during the PFFC treatments, fish traveled primarily to the east of the PFFC entrance (fig. 42). At night, large fish had axially bimodal travel paths during all treatments, with the direction of travel mostly to the east and away from the PFFC. The direction of movement for predator-size fish (>300 mm) again was similar to that of large fish. During the day, predator-size fish observed during the Low treatment showed no difference from a uniform direction, whereas fish during the High treatment presented a multi-modal pattern of movement both toward and away from the PFFC (fig. 43). At night, the predator-size fish had axially bimodal directions, with most of the movement away from the PFFC during both Low and High treatments. Predator-size fish observed when the PFFC was off during both photoperiods had significant directionality of movement (Rao $P < 0.001$), but generally not toward the PFFC. The only significant result for fish less than 90 mm was during the day during the Low treatment, when medium size fish had significant (Rayleigh $P < 0.001$) axially-bimodal directions of travel at 125.7° and 305.7°. During the High treatment for medium size fish, the direction of movement was significant (Rao $P < 0.001$) for movement toward the east side of the PFFC entrance.

Table 15. Mean travel directions and concentration parameters by size category of fish observed outside the entrance to the portable floating fish collector (PFFC) using the acoustic camera outside the PFFC at Cougar Reservoir, Oregon, 2014.

[The heading to the entrance of the PFFC is normalized to 0°. *N*, sample size; μ, mean travel direction of the fish; SE, standard error; κ, concentration parameter; mm, millimeter; NA, not applicable; >, greater than. Note: Sample size is the number of fish observation events with the acoustic camera, not necessarily the number of individual fish, because a given fish could be observed more than once]

Fish size category (type)	*N*	μ (SE)	κ (SE)
		PFFC off, Day	
30–60 mm (small fish)	0	NA	NA
60–90 mm (medium fish)	0	NA	NA
90–250 mm (large fish)	76	290.62 (26.18)	0.36 (0.17)
>300 mm (predators)	175	301.33 (32.03)	0.19 (0.11)
		PFFC off, Night	
30–60 mm (small fish)	0	NA	NA
60–90 mm (medium fish)	0	NA	NA
90–250 mm (large fish)	176	107.50/287.50 (5.79)	1.13 (0.13)
>300 mm (predators)	51	122.61 (7.16)	1.87 (0.33)
		Low treatment, Day	
30–60 mm (small fish)	3	238.59 (256.23)	0.18 (0.82)
60–90 mm (medium fish)	46	125.70/305.70 (14.15)	0.88 (0.24)
90–250 mm (large fish)	480	60.96 (3.90)	1.01 (0.08)
>300 mm (predators)	303	54.15 (19.94)	0.23 (0.08)
		Low treatment, Night	
30–60 mm (small fish)	1	30.30 (NA)	NA
60–90 mm (medium fish)	6	72.31 (32.66)	1.08 (0.70)
90–250 mm (large fish)	220	130.00/310.00 (4.81)	1.24 (0.12)
>300 mm (predators	146	132.00/312.00 (5.96)	1.22 (0.15)
		High treatment, Day	
30 – 60 mm (small fish)	3	65.78 (56.61)	0.86 (0.93)
60 – 90 mm (medium fish)	86	55.93 (10.31)	0.89 (0.18)
90 – 250 mm (large fish)	1,269	51.21 (3.78)	0.62 (0.04)
>300 mm (predators)	973	48.01 (5.73)	0.46 (0.05)
		High treatment, Night	
30–60 mm (small fish)	0	NA	NA
60–90 mm (medium fish)	1	109.55 (NA)	NA
90–250 mm (large fish)	379	140.60/320.60 (4.07)	1.09 (0.09)
>300 mm (predators)	109	135.00/315.00 (6.19)	1.39 (0.18)

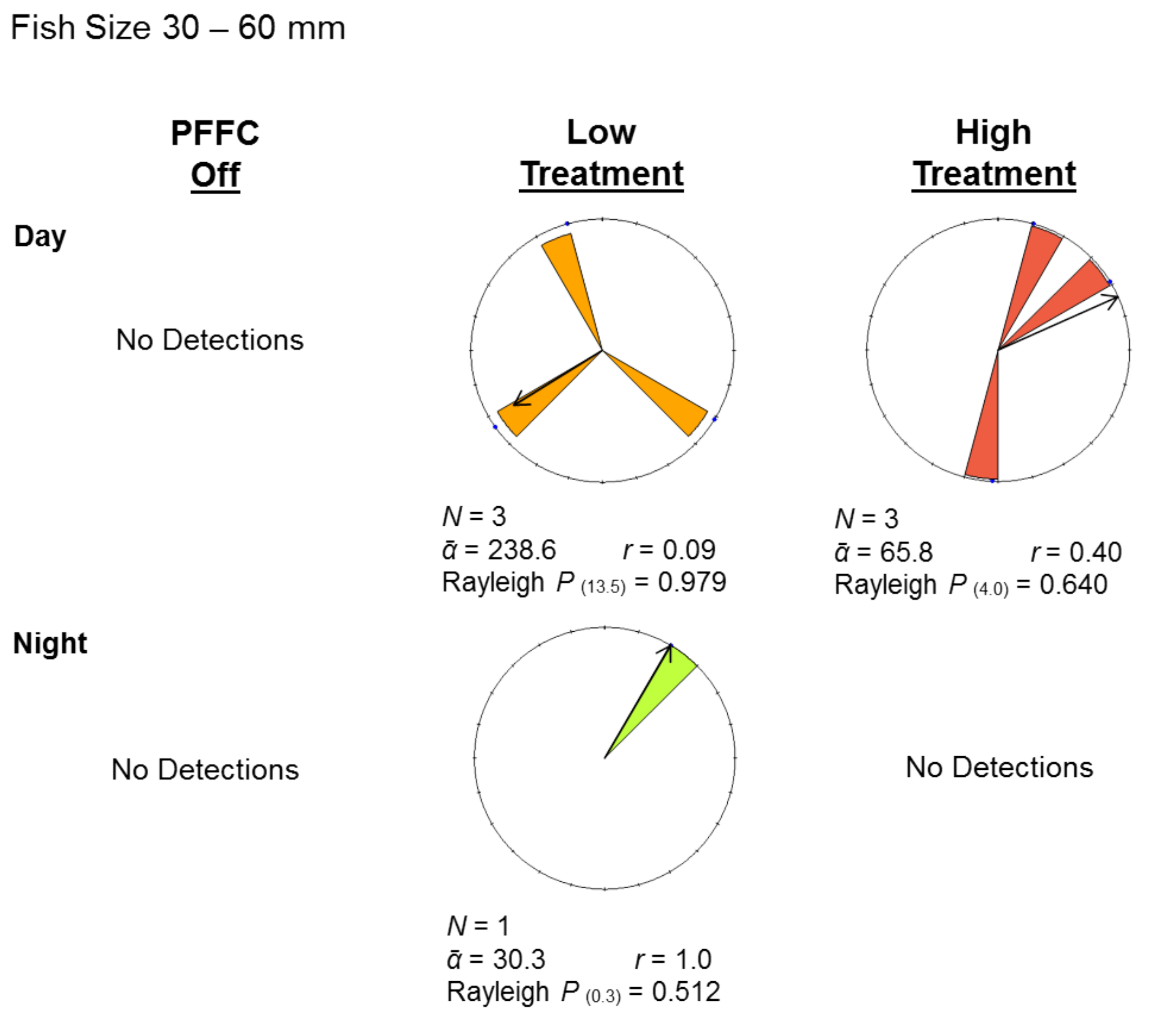

Figure 40. Rose diagrams of mean travel directions (in degrees) by diel period (Day or Night) and portable floating fish collector (PFFC) condition (PFFC Off, Low Treatment, or High Treatment) for the 30–60 millimeter (mm) size category of fish detected outside the entrance of the PFFC using an acoustic camera outside the PFFC at Cougar Reservoir, Oregon, 2014. The heading to the entrance of the PFFC is normalized to 0° (top). Sample sizes represent the number of fish (*N*) observed during each period. The mean vector (ᾱ) and mean vector resultant length (*r*) are described by the arrows. The *P*-value indicates the significance level according to either the Rayleigh *z* or Rao *U* test statistic (in parenthesis).

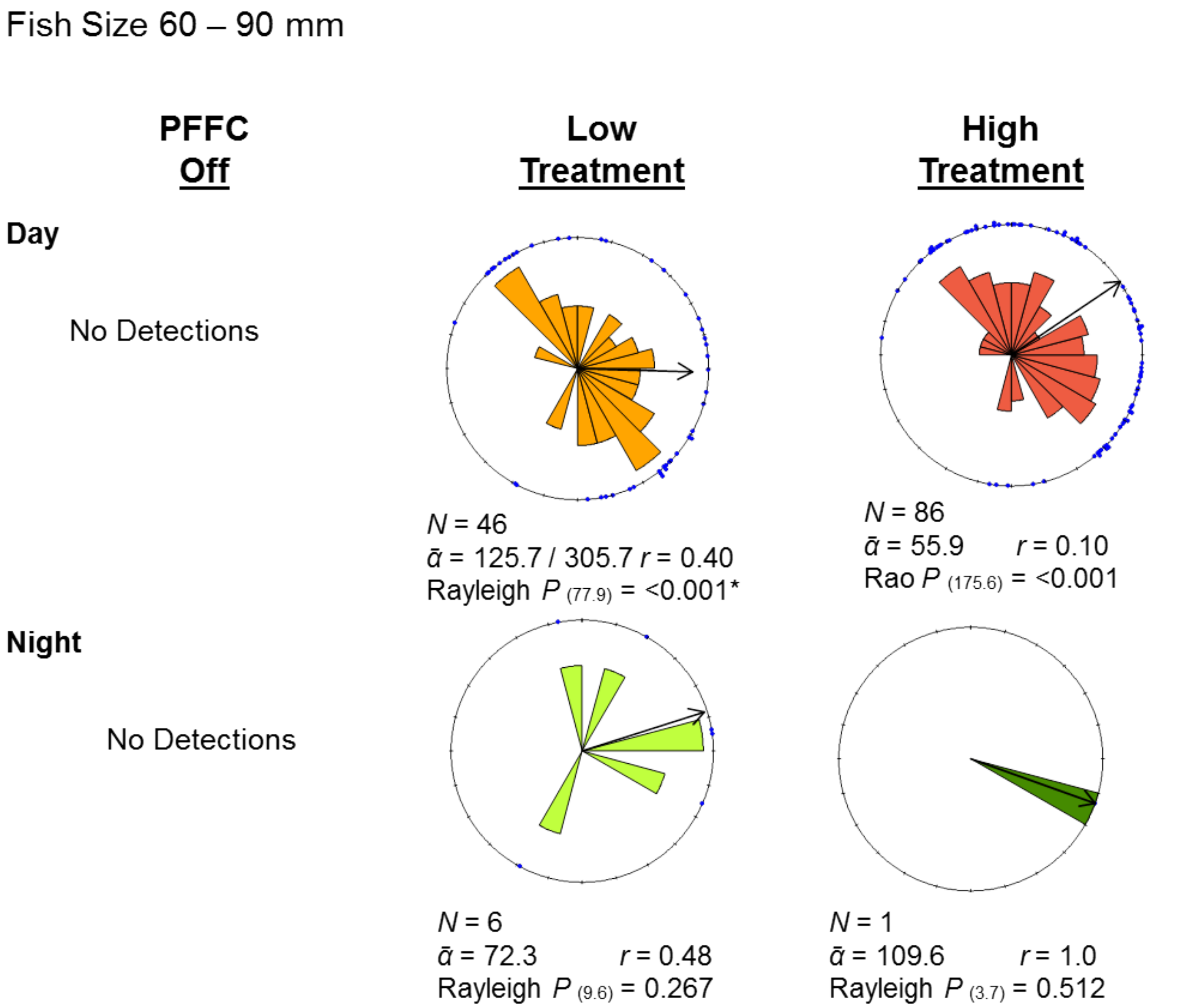

Figure 41. Rose diagrams of mean travel directions (in degrees) by diel period (Day or Night) and portable floating fish collector (PFFC) condition (PFFC Off, Low Treatment, or High Treatment) for the 60–90 millimeter (mm) size category of fish detected outside the entrance of the PFFC using an acoustic camera outside the PFFC at Cougar Reservoir, Oregon, 2014. The heading to the entrance of the PFFC is normalized to 0° (top). Sample sizes represent the number of fish (*N*) observed during each period. The mean vector ($\bar{\alpha}$) and mean vector resultant length (*r*) are described by the arrows. The *P*-value indicates the significance level according to either the Rayleigh *z* or Rao *U* test statistic (in parenthesis). *Because of a bimodal distribution, the data were transformed (not shown) in accordance with Zar (1999).

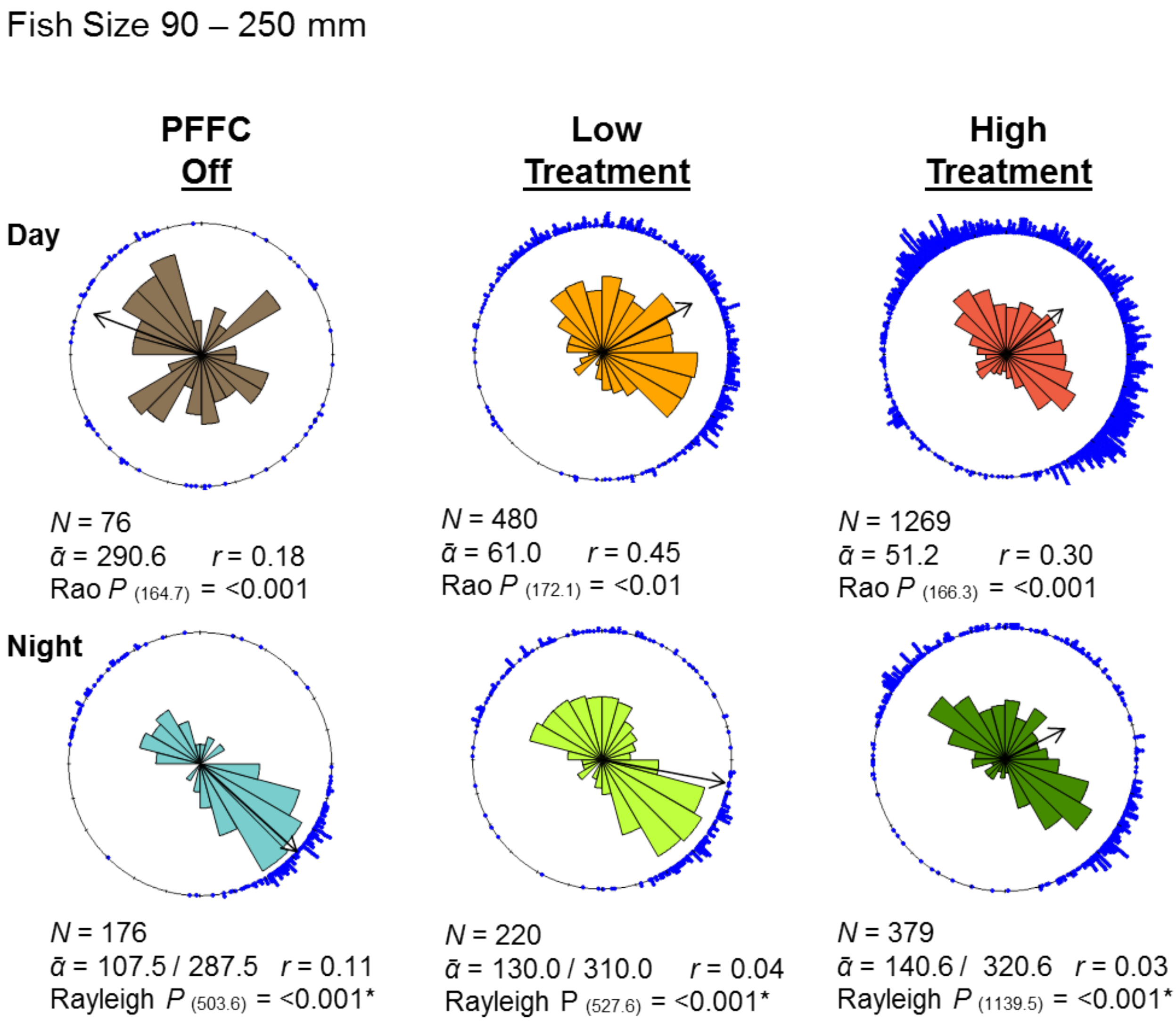

Figure 42. Rose diagrams of mean travel directions (in degrees) by diel period (Day or Night) and portable floating fish collector (PFFC) condition (PFFC Off, Low Treatment, or High Treatment) for the 90–250 millimeter (mm) size category of fish detected outside the entrance of the PFFC using an acoustic camera outside the PFFC at Cougar Reservoir, Oregon, 2014. The heading to the entrance of the PFFC is normalized to 0° (top). Sample sizes represent the number of fish (*N*) observed during each period. The mean vector (ᾱ) and mean vector resultant length (*r*) are described by the arrows. The *P*-value indicates the significance level according to either the Rayleigh *z* or Rao *U* test statistic (in parenthesis). *Because of a bimodal distribution, the data were transformed (not shown) in accordance with Zar (1999).

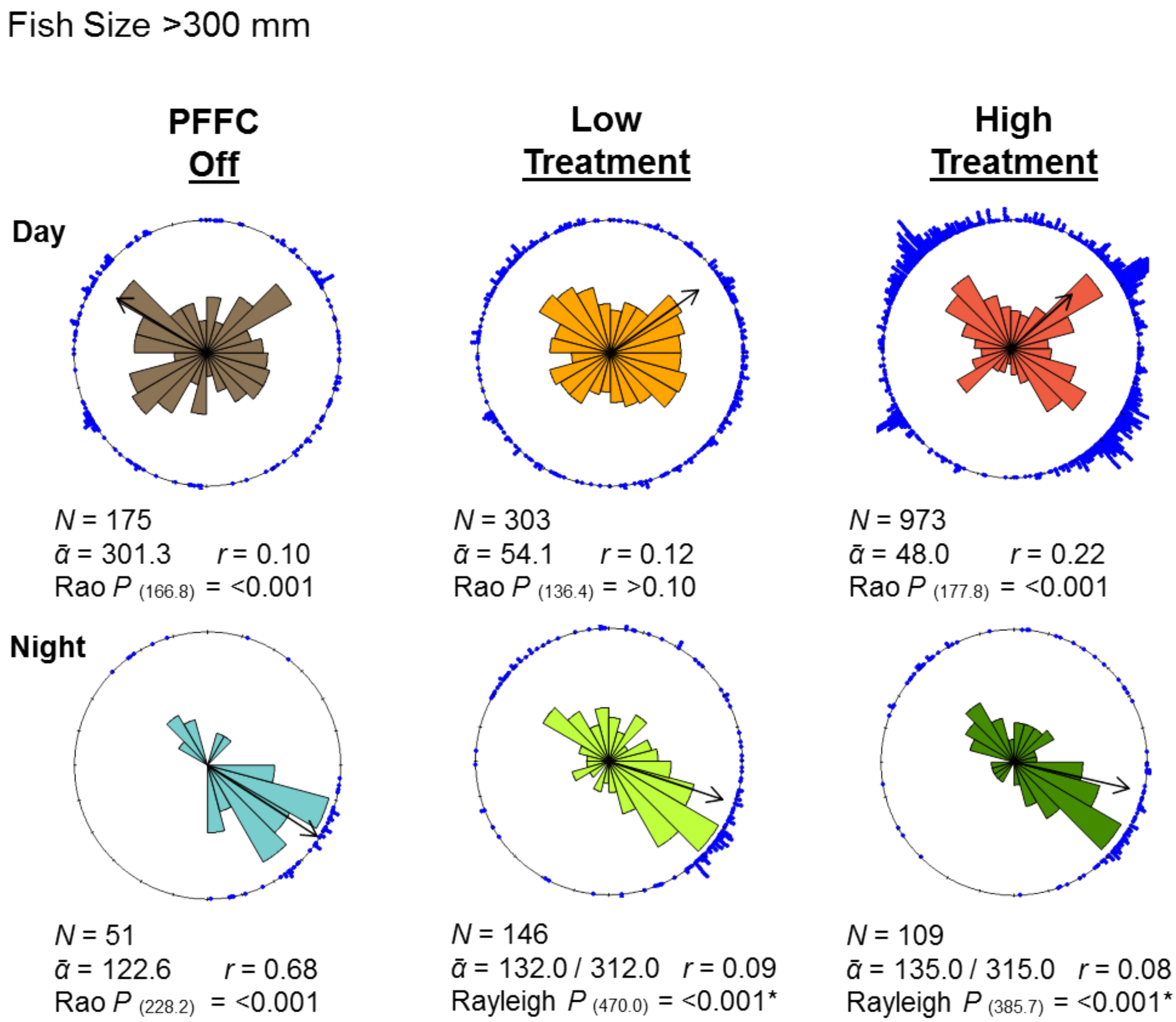

Figure 43. Rose diagrams of mean travel directions (in degrees) by diel period (Day or Night) and portable floating fish collector (PFFC) condition (PFFC Off, Low Treatment, or High Treatment) for the greater than (>) 300 millimeter (mm) size category of fish detected outside the entrance of the PFFC using an acoustic camera outside the PFFC at Cougar Reservoir, Oregon, 2014. The heading to the entrance of the PFFC is normalized to 0° (top). Sample sizes represent the number of fish (*N*) observed during each period. The mean vector ($\bar{\alpha}$) and mean vector resultant length (*r*) are described by the arrows. The *P*-value indicates the significance level according to either the Rayleigh *z* or Rao *U* test statistic (in parenthesis). *Because of a bimodal distribution, the data were transformed (not shown) in accordance with Zar (1999).

Fish Speed and Duration of Observations

The travel speed of fish observed using acoustic cameras inside the entrance of the PFFC increased with inflow rate. The mean travel speed of fish was 0.24 ft/s (IQR = 0.31 ft/s) when the PFFC was off, 0.55 ft/s (IQR = 0.51 ft/s) during the Low treatment, and 0.74 ft/s (IQR = 0.75 ft/s) during the High treatment (table 16). The travel speed differed significantly among conditions (ANOVA; $F_{2, 832} = 27.77$, $P < 0.001$). The Tukey HSD test showed that the travel speeds of all three groups differed significantly from each other at $P < 0.01$.

Fish travel speeds outside the PFFC also varied with PFFC operating condition. The mean travel speed of fish was 0.28 ft/s (IQR = 0.22 ft/s) when the PFFC was off, 0.39 ft/s (IQR = 0.31 ft/s) during the Low treatment, and 0.35 ft/s (IQR = 0.25 ft/s) during the High treatment (table 16). The differences among conditions were statistically significant (ANOVA, $F_{2, 2743} = 18.75$, $P < 0.001$). Additionally, the Tukey HSD test showed that the travel speeds of all three groups significantly differed from each other at $P < 0.001$.

Differences between the travel speeds of fish observed inside compared to those observed outside the entrance varies with PFFC operating condition. Fish travel speeds inside compared to outside the PFFC differed significantly during both the Low (ANOVA; $F_{1, 1219} = 70.76$, $P < 0.001$) and High (ANOVA; $F_{1, 2077} = 430.0$, $P < 0.001$) treatment, but were not significantly different when the PFFC was off (ANOVA; $F_{1, 270} = 0.976$, $P = 0.324$).

Table 16. Summary statistics for the travel speeds (feet per second) of fish observed either inside or outside the portable floating fish collector (PFFC) entrance using acoustic cameras inside the PFFC at Cougar Reservoir, Oregon, 2014.

[*N*, sample size; SD, standard deviation; IQR, interquartile range; <, less than. Note: Sample size is the number of fish observation events with the acoustic camera, not necessarily the number of individual fish, because a given fish could be observed more than once]

Condition	*N*	Mean	SD	IQR	Minimum	2.5th percentile	50th percentile	97.5th percentile	Maximum
Inside PFFC Entrance									
PFFC off	20	0.24	0.27	0.31	0.04	0.04	0.08	0.91	1.04
Low treatment	468	0.55	0.36	0.51	<0.01	0.05	0.47	1.36	1.99
High treatment	347	0.74	0.52	0.75	0.03	0.08	0.58	1.97	2.35
Outside PFFC Entrance									
PFFC off	252	0.28	0.16	0.22	<0.01	0.05	0.26	0.63	0.90
Low treatment	756	0.39	0.29	0.31	<0.01	0.05	0.31	1.14	2.22
High treatment	1,738	0.35	0.27	0.25	<0.01	0.06	0.28	1.12	2.35

Fish located inside the entrance of the PFFC remained within the beams of the acoustic cameras for a longer duration as the volume of water entering the structure decreased, indicating less fish movement. The median duration of observation of fish (50th percentile) was 3.98 seconds (mean 22.21 seconds; IQR = 6.36) during the High treatment, 4.90 seconds (mean 18.94 seconds; IQR = 7.03 seconds) during the Low treatment, and 25.16 seconds (mean 42.19 seconds; IQR = 38.31 seconds) when the PFFC was off (table 17). These differences were not statistically significant between groups (ANOVA; $F_{2, 832} = 0.613$, $P = 0.542$).

Immediately upstream of the entrance of the PFFC, the duration of time fish observed in the acoustic beam varied little when the volume of water entering the PFFC changed. The median duration of observation of fish (50th percentile) was 4.58 seconds (mean 6.36 seconds; IQR = 6.76 seconds) when the PFFC was off, 4.09 seconds (mean 17.76 seconds; IQR = 6.90 seconds) during the Low treatment, and 3.85 seconds (mean 15.13 seconds; IQR = 5.82 seconds) during the High treatment (table 17). These differences were not statistically significant between groups (ANOVA; $F_{2, 2743} = 1.069$, $P = 0.343$).

Differences between the duration of time for fish observed inside of the entrance to the PFFC to the duration of time for fish observed immediately upstream of the entrance varied depending on PFFC treatment. The duration of fish observations was significantly different when the PFFC was off (ANOVA; $F_{1, 270} = 58.99$, $P < 0.001$) and during the High (ANOVA; $F_{1, 2077} = 13.47$, $P < 0.001$) treatment between fish observed inside and immediately upstream of the entrance to the PFFC. During the Low treatment, the duration of observation for fish observed either inside or outside of the PFFC entrance was not significantly different (ANOVA; $F_{1, 1219} = 0.16$, $P = 0.689$).

Table 17. Summary statistics for the duration in the acoustic beam (in seconds) of fish that were observed either inside or outside the portable floating fish collector (PFFC) entrance with the acoustic cameras inside the PFFC at Cougar Reservoir, Oregon, 2014.

[*N*, sample size; SD, standard deviation; IQR, interquartile range. Note: Sample size is the number of fish observation events with the acoustic camera, not necessarily the number of individual fish, because a given fish could be observed more than once]

Condition	*N*	Mean	SD	IQR	Minimum	2.5th percentile	50th percentile	97.5th percentile	Maximum
Inside PFFC Entrance									
PFFC off	20	42.19	72.58	38.31	1.44	2.00	25.16	215.49	332.19
Low treatment	468	18.94	99.93	7.03	0.72	0.99	4.90	81.47	900.00
High treatment	347	22.21	93.17	6.36	0.52	0.81	3.98	167.71	900.00
Outside PFFC Entrance									
PFFC off	252	6.36	5.91	6.76	0.50	0.71	4.58	20.88	42.90
Low treatment	756	17.76	97.24	6.90	0.50	0.72	4.09	79.78	900.00
High treatment	1,738	15.13	18.50	5.82	0.50	0.69	3.85	49.38	900.00

Tortuosity

The swimming paths of fish inside the PFFC were more variable than the paths of fish upstream of the entrance. For fish observed inside the PFFC entrance, the median tortuosity index (50th percentile) values ranged from 1.36 to 2.38, and differed significantly between PFFC treatments (ANOVA; $F_{2, 829} = 7.53$, $P < 0.001$; table 18; fig. 44). The Tukey HSD test showed that the tortuosity of each of the three groups significantly differs from that of the others at $P < 0.05$. Tortuosity values were greatest when the PFFC was off, which is to be expected, as fish must reverse direction to exit the PFFC because there is no other outlet available when the PFFC is turned off.

For fish observed immediately upstream of the PFFC entrance, the tortuosity index values were similar to the values obtained from the data collected with the acoustic camera outside the PFFC. The median tortuosity index values ranged from 1.08 to 1.31, indicating that fish tracks primarily were linear (table 18, fig. 44). Maximum values for each group increased significantly (ANOVA; F2, 2737 = 10.2, P <0.001) as the volume of water entering the PFFC increased from when the PFFC was off to the Low and High treatments. Tests between the groups showed that the tortuosity of fish observed when the PFFC was off significantly differed from when the PFFC was running (Tukey HSD; $P < 0.03$), whereas there was no difference in tortuosity between the Low and High treatment groups (Tukey HSD; $P = 0.65$).

Differences between the tortuosity for fish observed inside the entrance compared to outside the entrance differed depending on PFFC treatment. The tortuosity of fish was significantly different when the PFFC was off (ANOVA; $F_{1, 270} = 77.81$, $P < 0.001$) and for the High (ANOVA; $F_{1, 2077} = 7.53$, $P = 0.006$) treatment between fish observed inside and outside the entrance to the PFFC. During the Low treatment, the tortuosity of fish observed inside and outside the PFFC entrance was not significantly different (ANOVA; $F_{1, 1219} = 0.008$, $P = 0.929$).

Table 18. Summary statistics for the tortuosity index by treatment of fish that were observed either inside or outside the portable floating fish collector (PFFC) entrance using the acoustic cameras inside the PFFC at Cougar Reservoir, Oregon, 2014.

[*N*, sample size; SD, standard deviation. Note: Sample size is the number of fish observation events with the acoustic camera, not necessarily the number of individual fish, because a given fish could be observed more than once]

Condition	*N*	Mean	SD	Minimum	25th percentile	50th percentile	75th percentile	Maximum
Inside PFFC Entrance								
PFFC off	20	10.16	15.66	1.01	1.51	2.38	10.55	63.87
Low treatment	468	2.51	3.43	1.00	1.11	1.38	2.49	31.19
High treatment	347	4.42	15.26	1.00	1.12	1.36	2.33	148.76
Outside PFFC Entrance								
PFFC off	252	1.42	1.01	1.00	1.02	1.08	1.30	11.63
Low treatment	756	2.49	4.17	1.00	1.08	1.26	2.10	57.48
High treatment	1,738	3.04	6.45	1.00	1.08	1.31	2.37	125.55

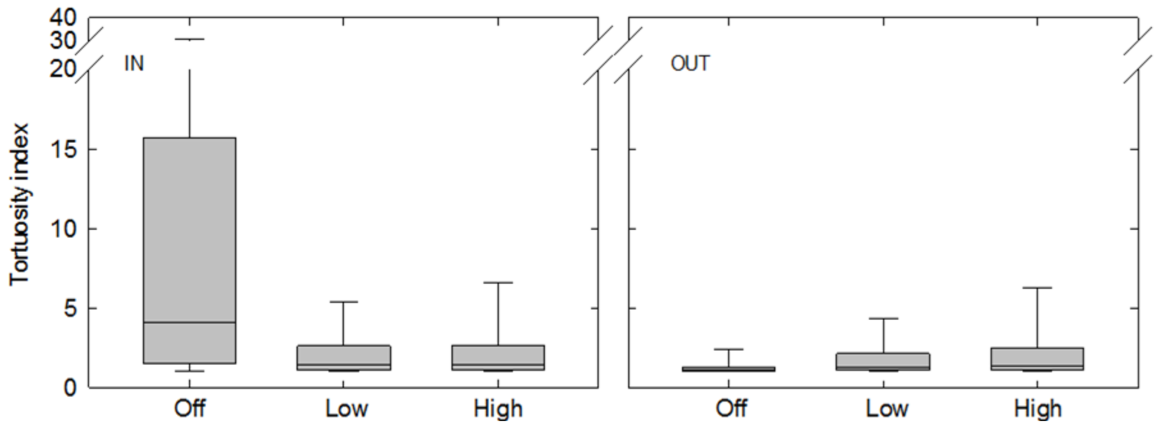

Figure 44. Box and whisker plots of the tortuosity index by condition for fish observed inside or outside the portable floating fish collector (PFFC) entrance with the acoustic cameras inside the PFFC at Cougar Reservoir, Oregon, 2014. Boxes range from the 25th to the 75th percentiles with a line indicating the median, and the whiskers representing the 10th and 90th percentiles.

Timing of Detection

The timing of fish detections inside and immediately upstream of the PFFC was similar among fish sizes and time of day. Data from the acoustic cameras located inside the PFFC showed an increase in the detections of fish from all size groups during the crepuscular periods (fig. 45). The percentage of non-predator fish detections in the morning peaked at about 7:00 a.m. for all three juvenile fish size categories, and then generally was low throughout the day until approximately 5:00 p.m. when fish detections began to increase again. Detections of predator-size fish (>300 mm) closely followed peak detections of the non-predator fish, with peak observations occurring at approximately 7:00 a.m. and 6:00 p.m. Detections of all fish size categories generally were low at night.

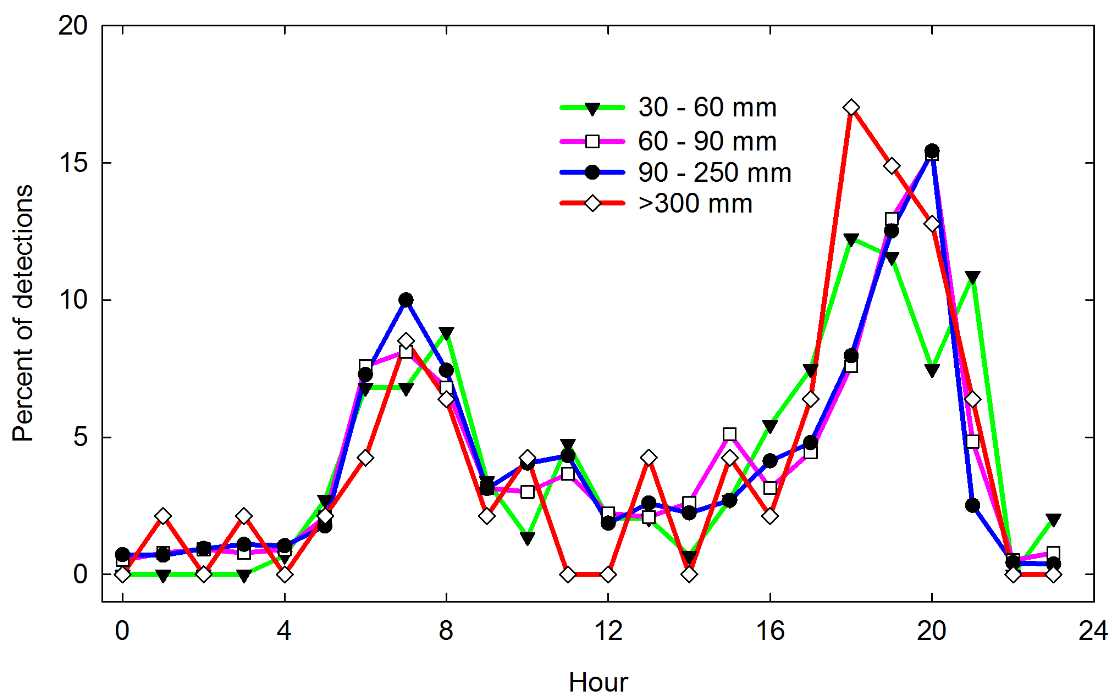

Figure 45. Graph showing hour of detection of fish by size category (in millimeters [mm]) of fish observed with the acoustic cameras inside the portable floating fish collector at Cougar Reservoir, Oregon, 2014.

Spatial Fish Distribution

The spatial distributions of fish tracks at the entrance of the PFFC were similar across all fish sizes, but varied slightly by treatment and photoperiod. The fish density data includes 15,724 individual tracks that were recorded by the cameras mounted inside the PFFC and directed outward. Based on these data, during the Low treatment there were large proportions of fish tracks observed inside and just outside the entrance of the PFFC (figs. 46–49). During the High treatment the largest proportion of fish tracks were just outside the PFFC flume entrance, with a relatively small proportion of fish observed in the entrance to the PFFC. The comparative spatial density of fish that were <90 mm in length, inside or outside the flume, was difficult to determine as few fish of this size were observed outside the flume. The lack of observations for these groups may be attributable to two factors: (1) The number of individuals present in the area when sampling occurred could be low, and (2) the acoustic cameras may have been unable to distinguish fish of this size because of sampling resolution in these areas. However, there appears to be a slightly greater concentration of fish tracks inside the entrance of the PFFC during the Low treatment compared to the High treatment for fish in both the 60–90 mm and 90–250 mm size classes, especially during the day.

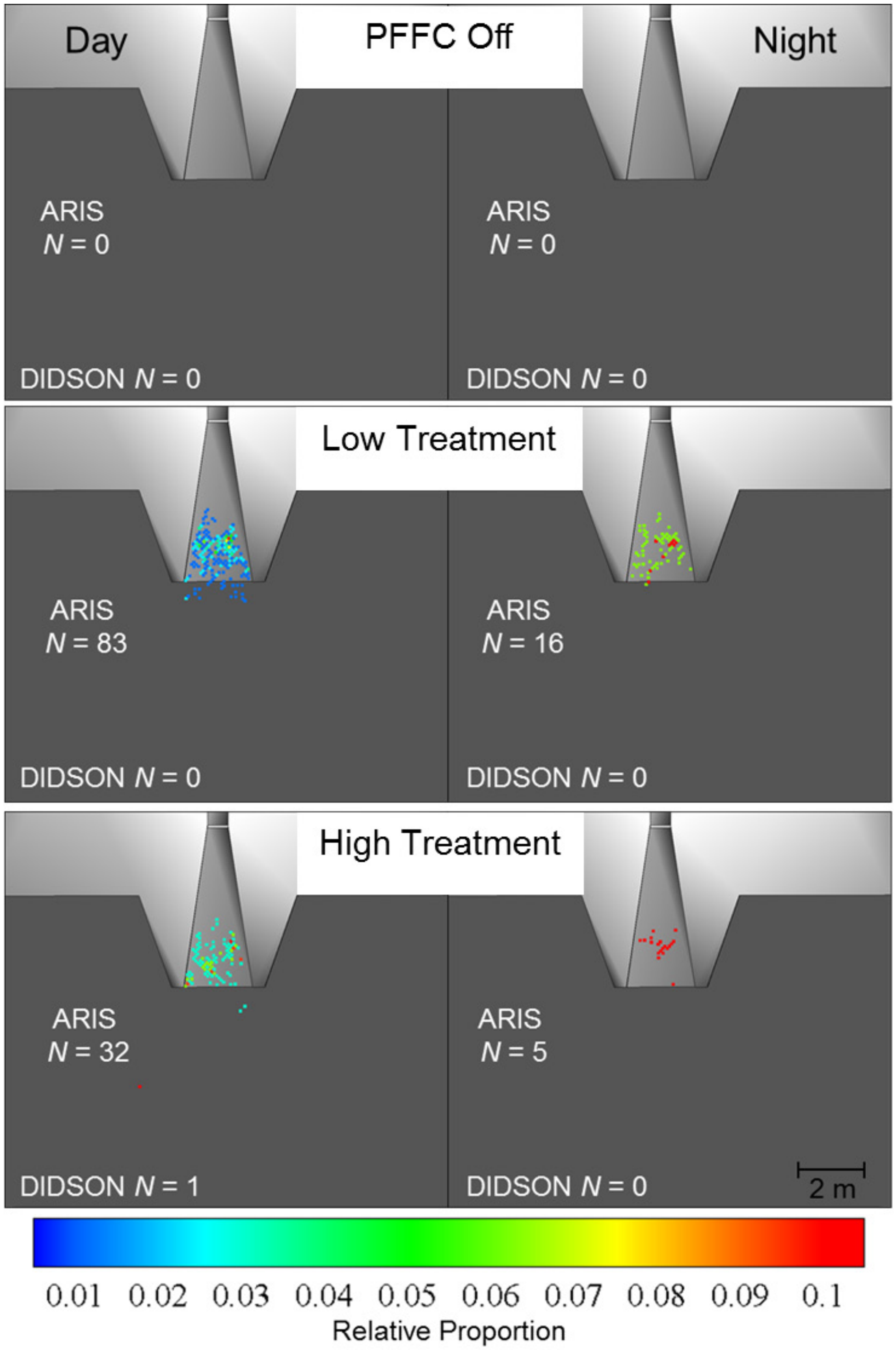

Figure 46. Graphs of the relative proportional density of fish by condition of portable floating fish collector (PFFC; PFFC Off, Low Treatment, or High Treatment) and diel period (Day, Night) for 30–60 millimeter long fish observed using acoustic cameras at the PFFC at Cougar Reservoir, Oregon, 2014.

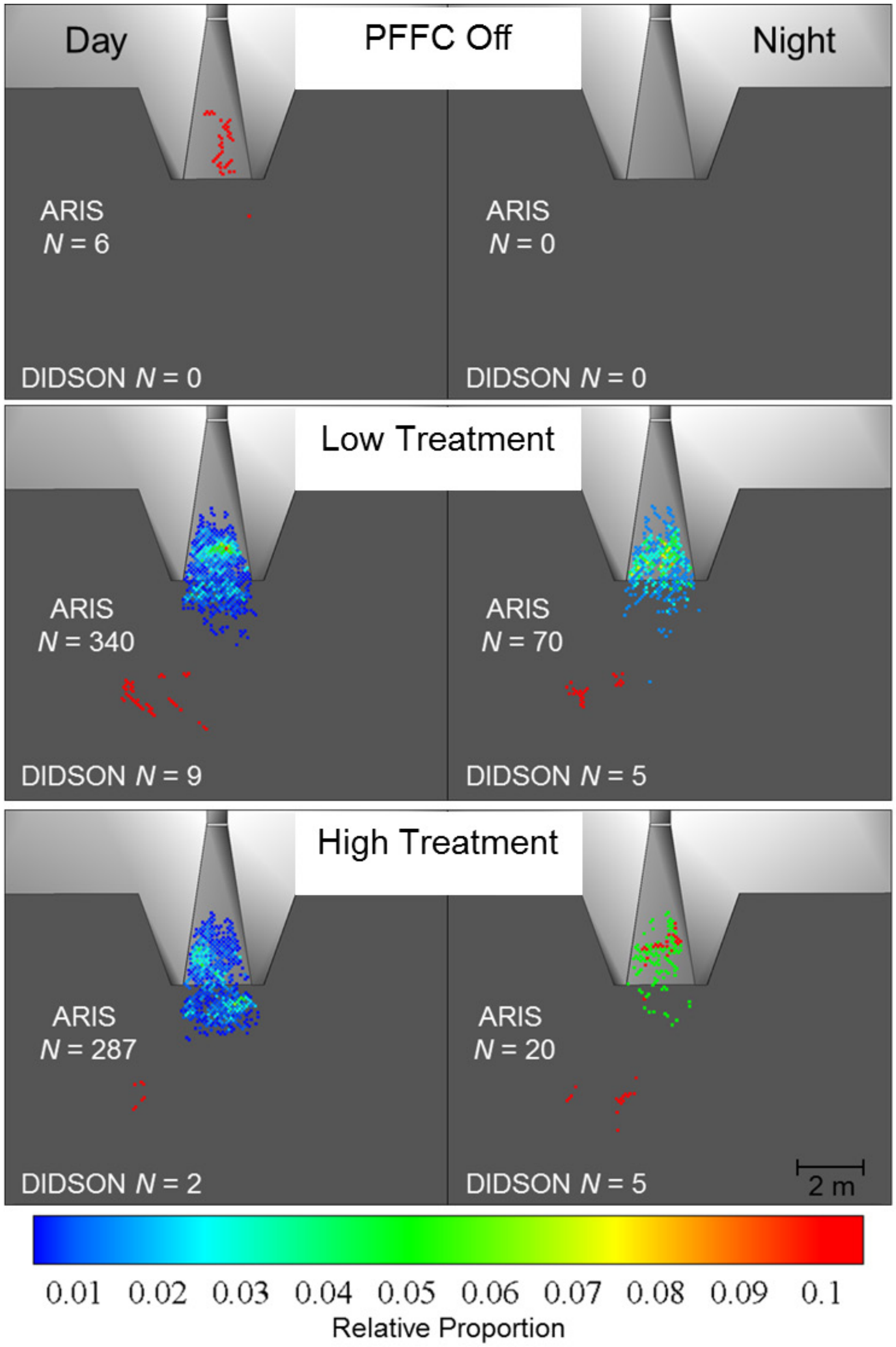

Figure 47. Graphs of the relative proportional density of fish by condition of portable floating fish collector (PFFC; PFFC Off, Low Treatment, or High Treatment) and diel period (Day, Night) for 60–90 millimeter long fish observed using acoustic cameras at the PFFC at Cougar Reservoir, Oregon, 2014.

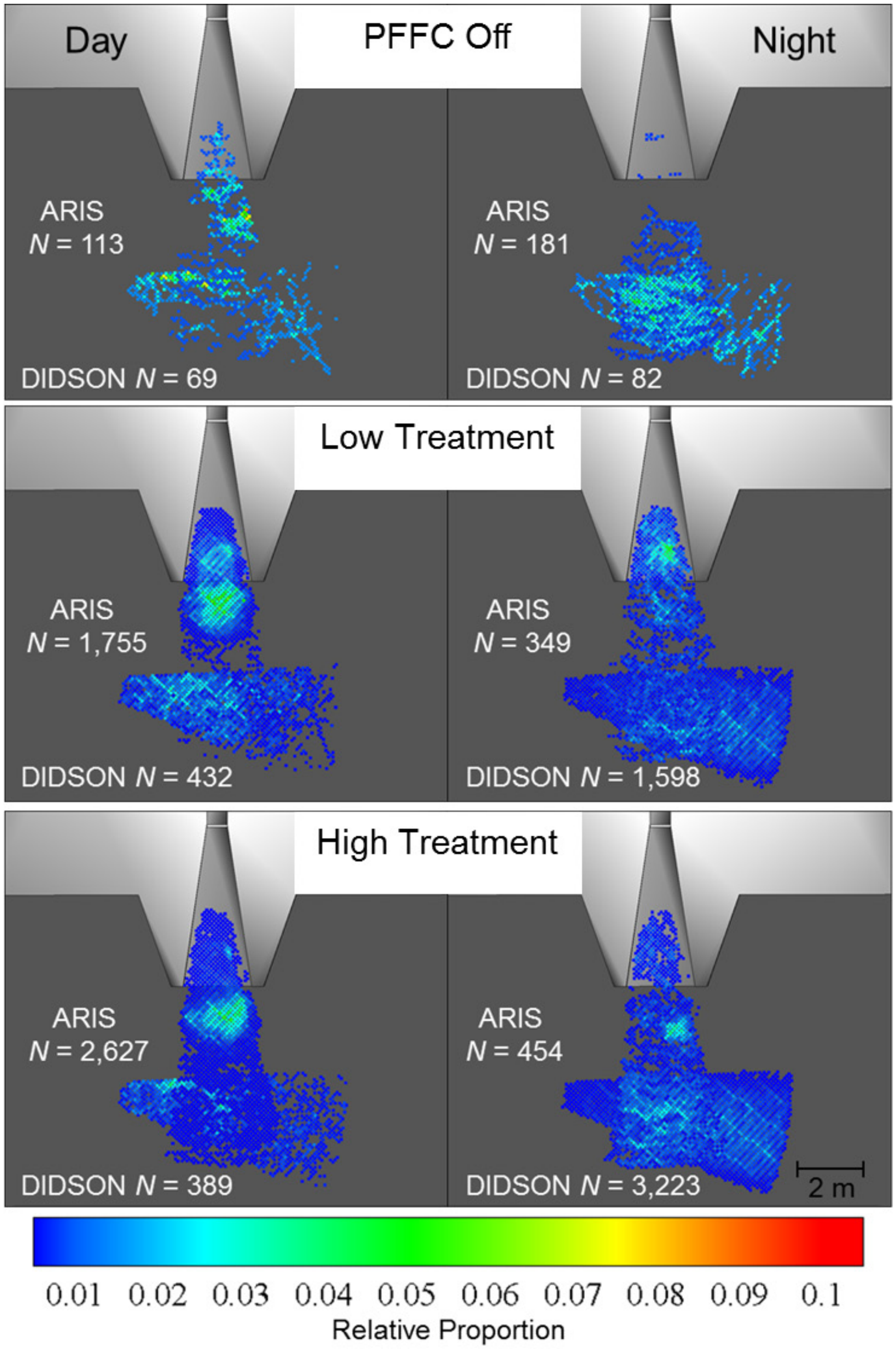

Figure 48. Graphs of the relative proportional density of fish by condition of portable floating fish collector (PFFC; PFFC Off, Low Treatment, or High Treatment) and diel period (Day, Night) for 90–250 millimeter long fish observed using acoustic cameras at the PFFC at Cougar Reservoir, Oregon, 2014.

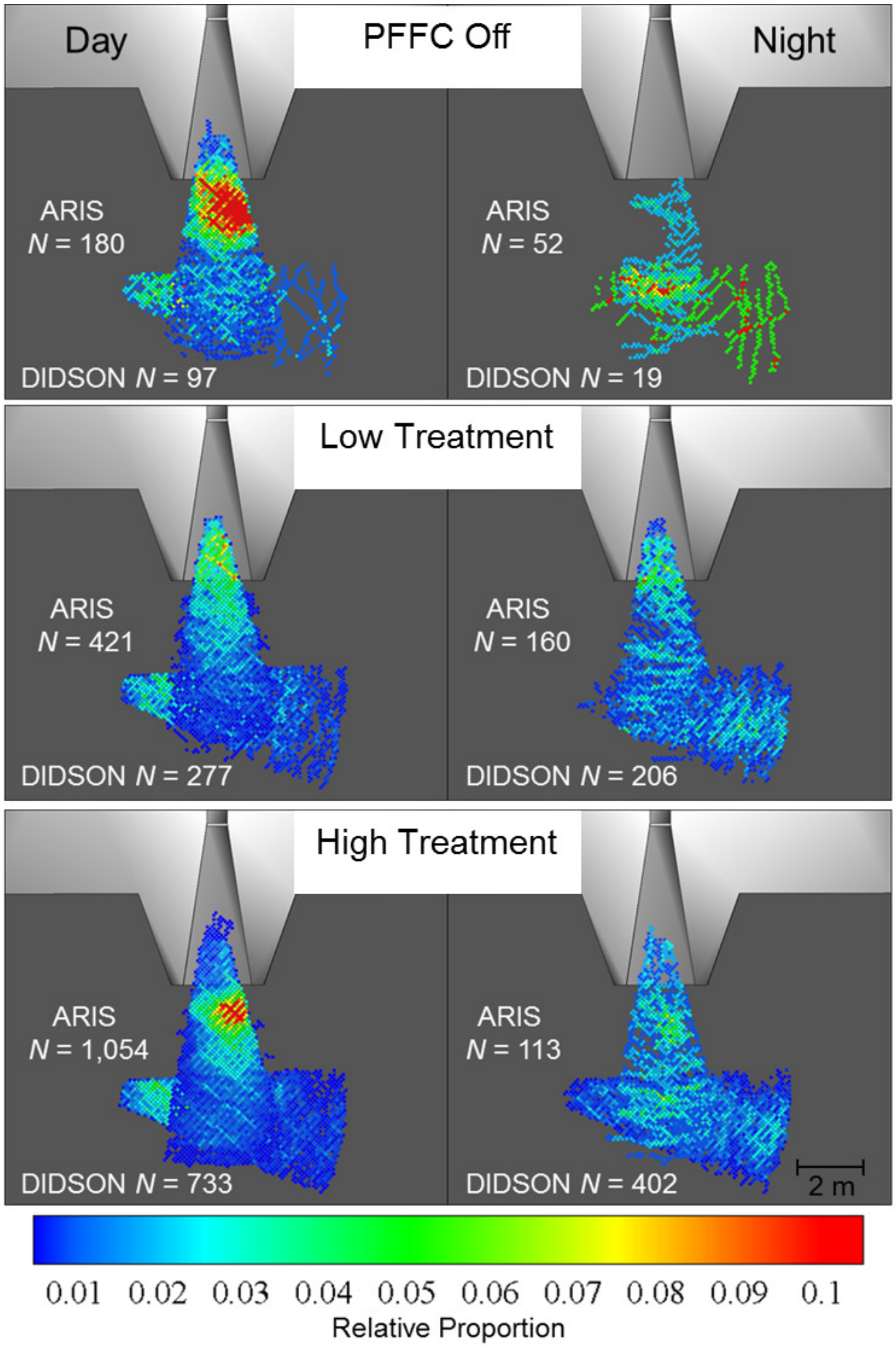

Figure 49. Graphs of the relative proportional density of fish by condition of portable floating fish collector (PFFC; PFFC Off, Low Treatment, or High Treatment) and diel period (Day, Night) for fish greater than (>) 300 millimeters long observed using acoustic cameras at the PFFC at Cougar Reservoir, Oregon, 2014.

Entrance and Rejection at the PFFC

Fish entrance and rejection at the opening of the PFFC varied by treatment and fish size category (figs. 50–52). Because of a small sample size for the 30–60 mm fish size category, few inferences can be made other than that the direction of movement generally was toward the PFFC during both Low and High treatments. In the 60–90 mm fish size category, the percentage of fish moving toward the PFFC was similar regardless of treatment or fish location, except that there was a greater rejection within 2.5 ft of the entrance during the High treatment. Fish from the 90–250 mm size category had a lower travel orientation toward the PFFC than the smaller sized groups. Fish outside the PFFC entrance were moving toward the PFFC more during the Low treatment than during the High treatment.

Regardless of fish size category, fish had an increased incidence of movement away from the PFFC (rejection) in the segment from the collector opening to 2.5 ft upstream of the PFFC, and from 2.5 to 5.0 ft inside the PFFC. During the Low treatment, fish generally were moving through the entrance, but were rejecting (or moving away) following entry. Conversely, during the High treatment the initial point of rejection for both fish size categories occurred at the entrance. This location corresponds with the site of a rapid increase in water velocity that was not present during the Low treatment.

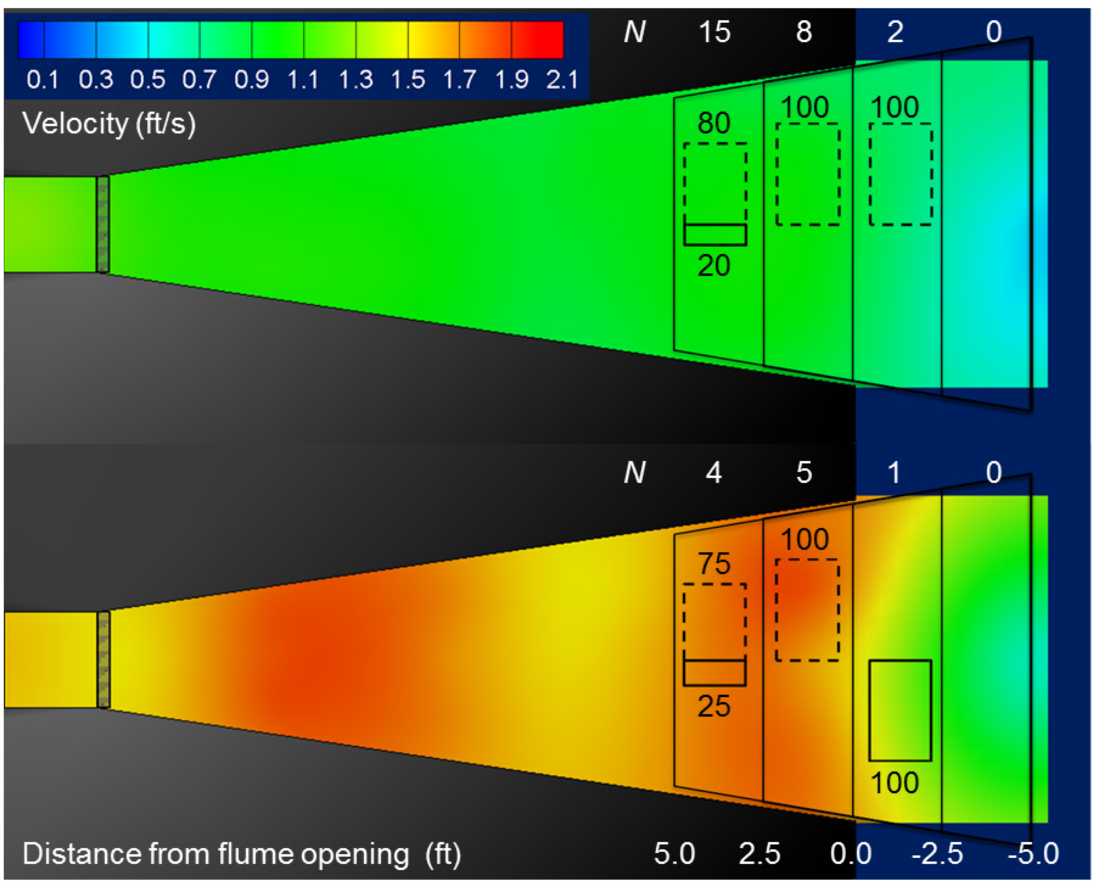

Figure 50. Percent directional movement of fish 30–60 millimeter target length observed with the acoustic cameras inside the portable floating fish collector (PFFC) during Low (top panel) and High (bottom panel) PFFC treatments overlaid on interpolated water velocities at the PFFC at Cougar Reservoir, Oregon, 2014. Sample sizes represent the number of fish (*N*) observed within each range. Boxes with dashed lines represent inward movement, and boxes with solid lines represent outward movement.

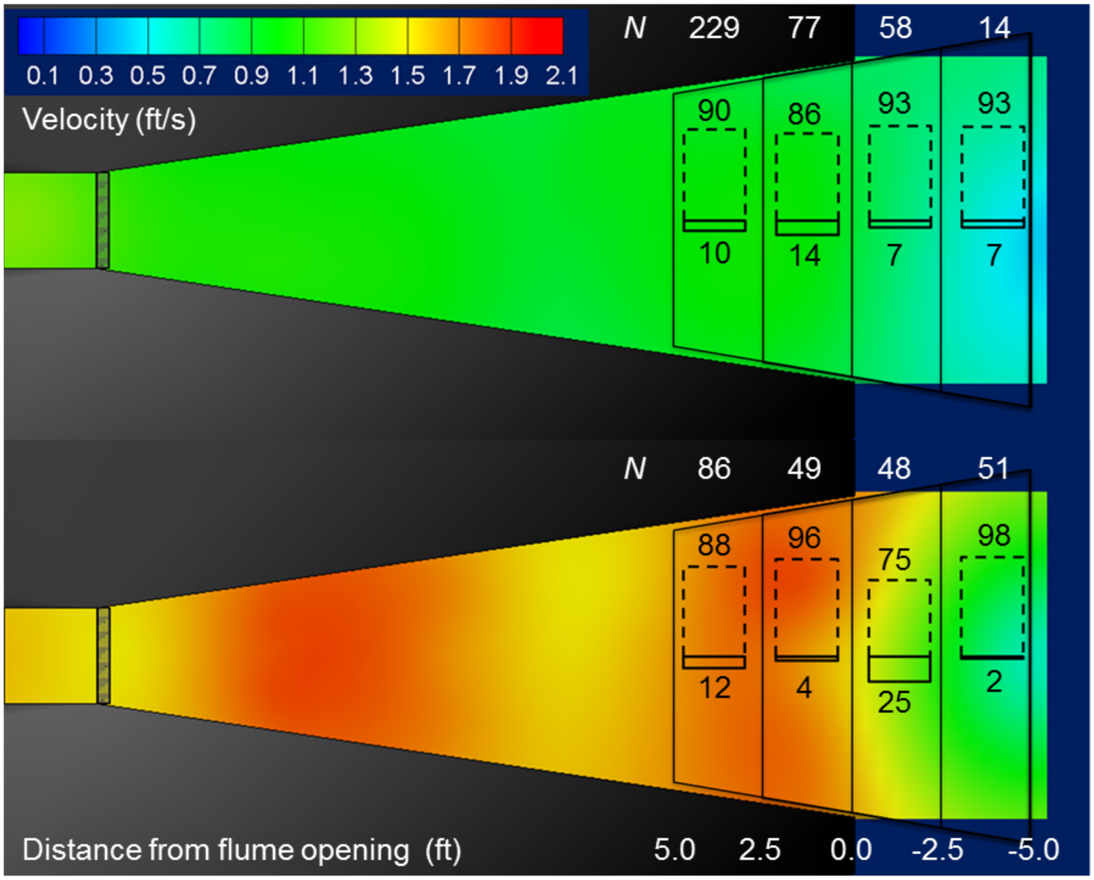

Figure 51. Percent directional movement of fish 60–90 millimeter target length observed with the acoustic cameras inside the portable floating fish collector (PFFC) during Low (top panel) and High (bottom panel) PFFC treatments overlaid on interpolated water velocities at the PFFC at Cougar Reservoir, Oregon, 2014. Sample sizes represent the number of fish (*N*) observed within each range. Boxes with dashed lines represent inward movement, and boxes with solid lines represent outward movement.

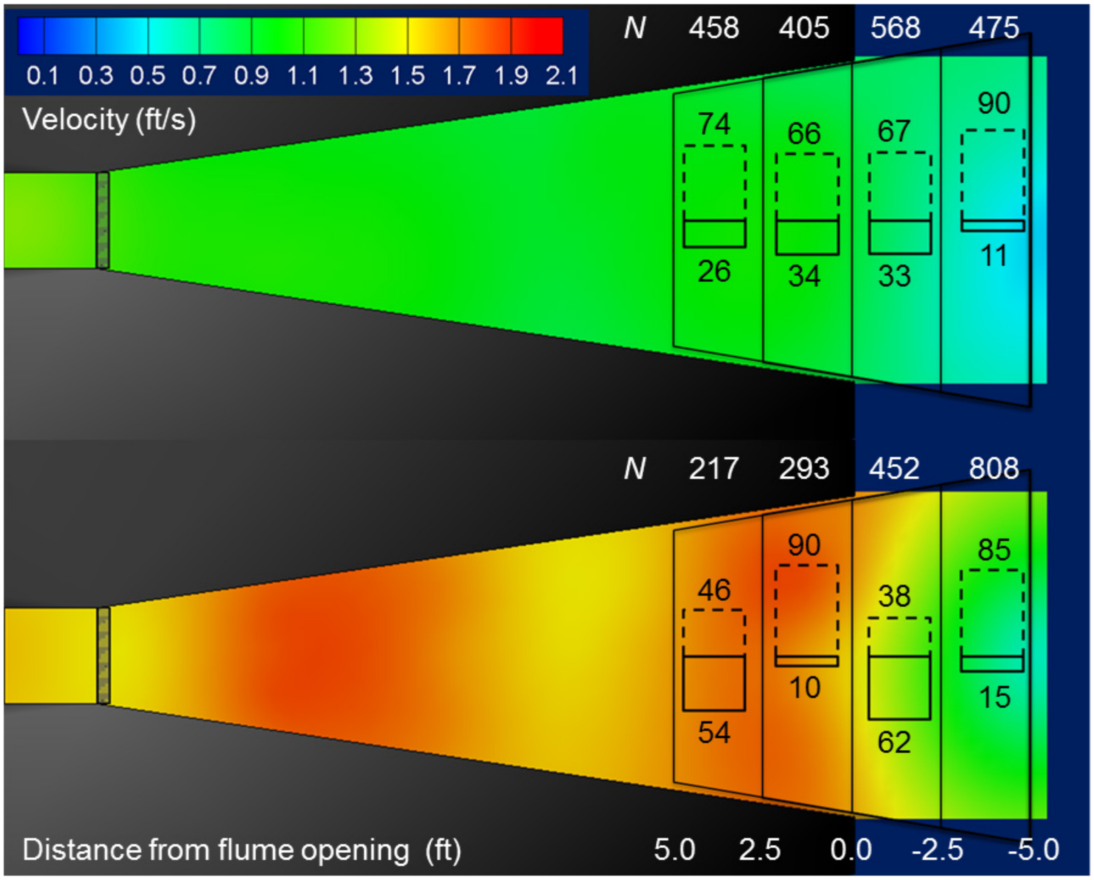

Figure 52. Percent directional movement of fish 90–250 millimeter target length observed with the acoustic cameras inside the portable floating fish collector (PFFC) during Low (top panel) and High (bottom panel) PFFC treatments overlaid on interpolated water velocities at the PFFC at Cougar Reservoir, Oregon, 2014. Sample sizes represent the number of fish (*N*) observed within each range. Boxes with dashed lines represent inward movement, and boxes with solid lines represent outward movement.

PFFC Collection Metrics

Collection metrics based on the acoustic camera data from the entrance of the PFFC indicated that fish were most likely to enter the PFFC during the Low treatment, but were most likely to be collected during the High treatment (table 19). During the Low treatment, 3,402 fish were observed within the entrance of the PFFC, whereas 4,940 fish were observed immediately outside the entrance (Discovery Zone), yielding an entrance efficiency (EE) of 0.689. Fewer fish were observed within the entrance (N = 2,050) during the High treatment, but the number of fish observed in the Discovery Zone was more than doubled (N = 10,744), resulting in an EE of 0.191. Although a greater number of fish were observed inside the entrance to the PFFC during the Low treatment, fish flux (the number of fish observed exiting the entrance, FF) also was greater during the Low treatment (N = 2,920) than during the High treatment (N = 1,944). When the fish count from the acoustic camera data were compared to the trap count data, both the collection efficiency (FCE) and the collection effectiveness (FCF) during the Low treatment (0.032 and 0.050, respectively) were lower than during the High treatment (0.064 and 0.059, respectively).

Table 19. Collection metrics of fish that were observed using the acoustic cameras inside the portable floating fish collector (PFFC) at Cougar Reservoir, Oregon, 2014.

[*N*, sample size. Sample size is the number of fish observation events with the acoustic camera, not necessarily the number of individual fish, because a given fish could be observed more than once]

Treatment	Fish in discovery zone (*N*)	Fish in PFFC entrance (*N*)	Entrance efficiency	Fish flux	Collection efficiency	Collection effectiveness
Low	4,940	3,402	0.689	2,920	0.032	0.050
High	10,744	2,050	0.191	1,944	0.064	0.059

Discussion

Results of this study indicate the biological performance of the PFFC in 2014, as measured by the FCE, was low because of several factors. These include the location of the PFFC relative to the tower, hydraulic conditions produced by the PFFC, flow fields in the cul-de-sac, and water temperatures. For example, the PFFC catch likely would have been higher if it were anchored closer to the tower (as planned) and in accordance with the bulk flow field and known areas of high fish densities. The USACE planned to locate the PFFC about 23 m from the tower entrance to coincide with the flow net of water entering the tower and areas of known concentrations of juvenile Chinook salmon (Beeman and others 2013, 2014b), but difficulties with anchoring the PFFC prevented the planned location from being used. As a result, the PFFC was an average of 44 m from the tower, placing it upstream of the areas used most intensely by the target fish and out of the prevailing flow field produced by water entering the tower. Additionally, the PFFC created a very small flow field near its entrance, increasing the importance of placing the PFFC in the flow field of the tower, and the changing velocity gradients and low water velocities within the PFFC were not conducive to entraining juvenile salmonids, as indicated by fish rejection and avoidance. Finally, water temperatures at the depth of the PFFC entrance often were higher than the preferred temperature of juvenile Chinook salmon, further diminishing the biological performance.

Rejection and avoidance are known to be affected by low water velocities, high velocity gradients, visual and mechanosensory cues, and light levels (Haro and others, 1998; Enders and others, 2012; Vowles and Kemp, 2012; Vowles and others, 2014). The low water velocities during both treatments and varying velocity gradients during the High treatment (both positive and negative) were not conducive to attracting and retaining fish. Enders and others (2012) found that a velocity gradient of 1 ft/s/ft caused avoidance by juvenile Chinook salmon in both accelerating and decelerating velocities, indicating that the magnitude rather than the sign of the gradient is the important factor. Haro and others (1998) found juvenile salmonid rejection at the same gradient, suggesting that 1 ft/s/ft may be a rejection threshold. We found that the areas of greatest fish rejection were associated with abrupt changes in velocities, but rejection occurred at much lower velocity gradients than 1 ft/s/ft. Rejection at relatively low velocity gradients may have been enhanced by the low water velocities, which were much less than the generally accepted juvenile salmonid capture velocity of 6–7 ft/s. Federal fish passage criteria state that bypass channel velocities should increase with distance and not exceed a gradient of 0.2 ft/s/ft “so fish move quickly through the bypass channel” (National Marine Fisheries Service, 2011). The criterion of the National Marine Fisheries Service (2011) is similar to gradients shown to elicit changes in rheotaxis of brown trout (*Salmo trutta*) (Vowles and Kemp, 2012). The hydraulic conditions during the Low treatment best met the National Marine Fisheries Service criteria, but also had the highest rejection rate. Mechanosensory factors such as vibration of the dewatering screens also are a possible source, given the low EE relative to the DE. The PFFC inflow was reduced after the first block because of excessive vibration, but vibration may still have affected fish responses. This premise is supported by data from acoustic+PIT-tagged fish indicating significantly lower DE during the High treatment. Data from acoustic cameras indicated that the numbers of fish near the PFFC entrance were greatest during the High treatment, but that could have been from recounting fish. Visual cues such as those from entering the bright white color inside the PFFC may also have caused rejection. Vowles and others (2014) found that avoidance responses of juvenile Chinook salmon were greater when visual cues were present, suggesting that the bright color of the PFFC could be contributing to the low biological performance by enhancing visual cues.

The PFFC collection decreased over the study period and likely was affected by water temperatures. The collection of juvenile Chinook salmon decreased over the 4 days of operation in May, was zero during much of the July–September period, and then remained low until the end of the study. In contrast, collection of warm-water species occurred primarily during the July–September period when water temperatures were at their warmest of the season, generally greater than 16 °C in the upper 3 m of the water column. The low collection of juvenile Chinook salmon at temperatures greater than about 16 °C fits well with the 13–15 °C preferred temperature we noted in data from the acoustic+PIT-tagged fish in this study, because those temperatures often occurred at depths greater than the entrance to the PFFC. Our temperature preference results are similar to the long-standing results of Brett (1952), who found 12–13 °C to be the preferred temperature of juvenile Chinook salmon during laboratory studies. Few of the acoustic+PIT-tagged fish were detected at depths with temperatures warmer than 14 °C during June (29 percent), July (9 percent), or August (5 percent), and only 3 percent were at temperatures greater than 16 °C. These results suggest that the collection of juvenile Chinook salmon of the size we tested will decrease as water temperatures at the collection depth increase. The data from the temperature string at the southeastern corner of the tower may better represent the vertical temperature profile near the tower than near the PFFC, so we suggest that future studies measure water temperatures at various depths near the entrance to the PFFC. Factors other than temperature, such as food availability, competition, and aggression, also may affect fish habitat use.

Dividing the fish migration and collection processes into their component parts showed that the low FCE was owing to processes near the PFFC entrance. Generalizing from Johnson and Dauble (2006), FCE is the product of all processes between fish entering a waterbody and collection in a passage route—in the context of this study, FCE = RPE*FBE*DE*EE. The acoustic+PIT-tagged fish in this study had high RPE and FBE, moderate DE, and very low EE. Despite the location of the PFFC, the DE was moderately high (Low treatment 0.729, High treatment 0.632); this likely was a result of the repeated migrations and wide dispersal of fish in the cul-de-sac noted in this and previous studies, which are in turn likely a result of the directed migrations through the reservoir and low passage rates into the tower (Beeman and others 2013, 2014b). The DE likely would be improved if the PFFC were moved closer to the tower entrance, where we noted the greatest intensity of use by acoustic+PIT-tagged fish; however, the effects of the PFFC outflow on fish distributions near the tower is unknown and fish distributions may vary with location of the PFFC and its flow fields. Increasing the flow net of the PFFC also could increase DE by providing a better cue to fish in the Discovery Zone (Johnson and Dauble, 2006; Sweeney and others, 2007). Given the low water velocities created by the PFFC inflow and the evidence of fish rejection within it, we presume that the Decision Zone, where fish sense a passage route’s flow net and decide to enter or reject it, was at or very near the entrance of the PFFC and likely extended well inside it. Increasing the water velocities and smoothing the velocity gradients within the PFFC can be expected to increase FCE by reducing rejection and thereby increasing EE.

The percent mortality of the collected subyearling Chinook salmon was high, totaling 32.2 percent over the study period. About 80 percent of the mortality was attributed to trap mortality; that is, dead fish noted during examination of the collection. High trap mortality suggests poor holding conditions, fish of a compromised health status, or both. Infection by the parasitic copepod *Salmincola californiensis*, known to have a high prevalence in Cougar Reservoir (Beeman and others, 2015; Monzyk and others, 2015), does not appear to have been a major factor in mortality of subyearling Chinook salmon because the few fish that were examined for the parasite had zero or very low numbers in their gills, but this could be further investigated. Eight yearling Chinook salmon were collected and one was dead when examined.

We used several methods to evaluate the biological performance of the PFFC because of the unique information each method could provide. Collection of untagged fish was the least informative tool we used. The collection of the PFFC provided information about the timing, size, and species composition of collected fish, but provided no diagnostic information about the processes affecting collection, such as the abundance of fish near the PFFC or the numbers entering or rejecting it. The primary information gained from the collection was that few juvenile Chinook salmon were collected and none were collected during the warmest months of the study, the only time warm-water fish were collected.

Collection of PIT-tagged fish released near the head of the reservoir provided an incremental increase of information over the collection of untagged fish. Releasing PIT-tagged fish enabled FCE to be estimated from a known population of juvenile Chinook salmon of a size commensurate with wild fish at the time of release. This method may have been suitable for evaluating the biological performance of a passage route, but it provides little information to diagnose the causes of low FCE. In this study, 3 of the 1,505 PIT-tagged fish were collected, and this method indicated little except that the joint processes of survival and migration from release to collection in the PFFC were low. However, several PIT-tagged fish detected at the PIT detector in the PFFC were not collected, providing limited evidence of fish entry and rejection prior to collection. Release of PIT-tagged fish could be a useful management tool to assess compliance with a collection standard, but the lack of detection capability between release and the PFFC limits its value as a research tool. The use of 12-mm long full-duplex PIT tags, for years the standard size used in juvenile salmonids, continues to prevent inferences from fish less than about 65 mm long (PIT Tag Steering Committee, 2014). Recent size reductions of full-duplex PIT tags to as small as 8 mm long show promise for use in smaller juvenile salmonids. Tiffan and others (2015) reported no biologically relevant effects of implanting 8- or 9-mm PIT tags in juvenile Chinook salmon as small as 40 mm under laboratory conditions, suggesting further research into their use in field studies was warranted. We found that detection probability within the PFFC was low for the 8 mm PIT tag tested by Tiffan and others (2015), suggesting expansion factors would be needed to estimate collection numbers, or data should be gathered from collected fish scanned by hand (the practice for all fish collected in the PFFC in 2014). The use of 8- or 9-mm PIT tags could greatly increase the proportion of the population represented by PIT-tagged fish in Cougar Reservoir and, if coupled with in-reservoir detection, could provide an economical means to conduct research on FCE.

Data from acoustic telemetry and acoustic cameras provided most of the information about the biological performance of the PFFC and were excellent research tools. Data from acoustic telemetry indicated:

- The proportions of tagged fish (115–180 mm in fork length) released near the head of the reservoir migrating to the forebay, cul-de-sac, and then nearby the PFFC or tower;
- Areas of fish use in the cul-de-sac and near the PFFC; and
- Fish behaviors near the PFFC and tower, including how their depths were related to water temperature.

These data formed the basis for estimating many of the migration and passage metrics (RPE, FBE, FPE, DE, EE) as well as determining that the PFFC was located in an area of low fish use, which likely reduced the DE. The primary drawbacks to the acoustic telemetry method were the minimum fish size limit owing to the implantation procedure and transmitter mass as well as the cost of receiving equipment and tags. A smaller transmitter has been developed (Deng and others, 2015), but information about how the smaller size will affect minimum taggable fish size was not available at the time of this report.

Data from acoustic cameras were the primary indicator of fish entrance to the PFFC and rejection prior to collection. The data from the camera inside the PFFC paired with the water velocity data collected using an Acoustic Doppler Velocimeter indicated that much of the rejection occurred in areas of low velocity magnitude and changing velocity gradient, consistent with literature on fish behavior (Haro and others, 1998; Sweeney and others, 2007; Enders and others, 2012). A distinct advantage in using acoustic cameras is the ability to detect untagged fish over a large range of sizes without affecting fish behavior. The limitations of acoustic cameras include:

- The lack of species specificity,
- Difficulty in identifying small targets (less than about 30–50 mm depending on the camera and fish location),
- The possibility of counting individuals more than once, and
- The acoustic noise produced by some environments.

The time required to process the vast amounts of data into meaningful results also can be burdensome, but we automated much of the process to reduce the time required and to increase the quantity of data used for analysis (Adams and others, 2015). Overall, using a combination of monitoring methods enabled us to describe many facets of the processes contributing to the low FCE.

The PFFC is one of several surface collectors in use at storage dams in the Pacific Northwest, and the only one serving an experimental function. The other collectors are at Upper and Lower Baker Lake on the Baker River, Washington (Puget Sound Energy); Swift Reservoir on the Lewis River, Washington (PacifiCorp); Round Butte Dam at Billy Chinook Reservoir, Oregon (Portland General Electric); North Fork Dam on the Clackamas River, Oregon (Portland General Electric); and Cushman Dam No.1 on the North Fork of the Skykomish River, Washington (Tacoma Power). Of these collectors, the facility at Upper Baker Lake appears to be the most successful, although some of the other facilities were relatively new at the time of this report and we were unable to find in-depth analyses using comparable methods between projects. The success of the collector at Upper Baker Lake is apparent from an average annual collection of nearly 450,000 juvenile salmonids and returns of about 25,000 adult fish per year since the current trap configuration began operating in 2008 (Nick Veretto, Puget Sound Energy, written commun., July 17, 2015). The inflows vary between 250 ft^3/s at Cushman to about 5,000 ft^3/s at Round Butte. Additionally, all facilities except the PFFC use some form of nets to help guide fish to the entrance.

Modifications to the PFFC during the winter of 2014–2015 addressed many of the factors we attribute to the low biological and hydraulic performance of the PFFC in 2014. These include modifying anchor placement so the PFFC can be moved closer to the tower and turned to face the prevailing water current, raising the water-control structure to improve the internal hydraulic conditions, and reducing vibration of the dewatering screens. The modifications are expected to result in hydraulic conditions generally recommended for fish collectors (Haro and others, 1998; Sweeney and others, 2007), including better fish holding conditions in the collector box, as well as placing the PFFC nearer to the known fish aggregation areas (Beeman and others 2013, 2014b). In addition to these improvements, a deeper entrance likely would increase collection of juvenile Chinook salmon during late spring and summer when they appear to avoid the warm surface waters.

References Cited

Adams, N.S., Smith, C.D., Plumb, J.M., Hansen, G.S., and Beeman, J.W., 2015, An evaluation of fish behavior upstream of the water temperature control tower at Cougar Dam, Oregon, using acoustic cameras, 2013: U.S. Geological Survey Open-File Report 2015-1124, 62 p, accessed July 6, 2015, at http://dx.doi.org/10.3133/ofr20151124/.

Bainbridge, R., 1960, Speed and stamina of three fish: Journal of Experimental Biology, v.37, p. 129–153.

Batschelet, E., 1981, Circular statistics in biology: New York, Academic Press, 371 p.

Beeman, J.W., Evans, S.D., Haner, P.V., Hansen, A.C., Hansel, H.C., Smith, C.D., and Sprando, J.M., 2014a, Passage and survival probabilities of juvenile Chinook salmon at Cougar Dam, Oregon, 2012: U.S. Geological Survey Open-File Report 2014-1038, 64 p., accessed May 2015 at http://dx.doi.org/10.3133/ofr20141038/.

Beeman, J.W., Hansel, H.C., Hansen, A.C., Evans, S.D., Haner, P.V., Hatton, T.W., Kofoot, E.E., Sprando, J.M., and Smith, C.D., 2014b, Behavior and dam passage of juvenile Chinook salmon at Cougar Reservoir and Dam, Oregon, March 2012–February 2013: U.S. Geological Survey Open-File Report 2014-1177, 52 p., accessed May 2015 at http://dx.doi.org/10.3133/ofr20141177/.

Beeman, J.W., Hansel, H.C., Hansen, A.C., Haner, P.V., Sprando, J.M., Smith, C.D., Evans, S.D., and Hatton, T.W., 2013, Behavior and dam passage of juvenile Chinook salmon at Cougar Reservoir and Dam, Oregon, March 2011–February 2012: U.S. Geological Survey Open-File Report 2013-1079, 48 p., accessed May 2015 at http://pubs.usgs.gov/of/2013/1079/.

Beeman, J.W., Hansen, A.C., Evans, S.D., Haner, P.V., Hansel, H.C., and Smith, C.D., 2012, Passage probabilities of juvenile Chinook salmon through the powerhouse and regulating outlet at Cougar Dam, Oregon, 2011: U.S. Geological Survey Open-File Report 2012-1250, 26 p., accessed May 2015 at http://pubs.usgs.gov/of/2012/1250/.

Beeman, J.W., Hansen, A.C., and Sprando, J.M., 2015, Observational data on the effects of infection by the copepod Salmincola californiensis on the short- and long-term viability of juvenile Chinook salmon (Oncorhynchus tshawytscha) implanted with telemetry tags: Animal Biotelemetry 3:20, doi:10.1186/s40317-015-0056-5, accessed July 16, 2015, at http://www.animalbiotelemetry.com/content/3/1/20.

Beeman, J.W., and Perry, R.W., 2012, Bias from false-positive detections and strategies for their removal in studies using telemetry, *in* Adams, N.S., Beeman, J.W., and Eiler, J.H., eds., Telemetry techniques—A user guide for fisheries research: Bethesda, Maryland, American Fisheries Society, p. 505–518.

Boswell, K.M., Wilson, M.P., and Cowan, J.H., Jr., 2008, A semiautomated approach to estimating fish size, abundance, and behavior from dual-frequency identification sonar (DIDSON) data: North American Journal of Fisheries Management, v. 28, p. 799–807.

Brett, J.R., 1952, Temperature tolerance in young Pacific salmon, genus Oncorhynchus: Journal of the Canadian Research Board of Canada, v.9, p. 265–323.

Burnham, K.P., and Anderson, D.R., 2002, Model selection and multimodel inference—A practical information-theoretic approach: New York, Springer-Verlag, 488 p.

Cormack, R.M., 1964, Estimates of survival from the sighting of marked animals: Biometrika, v.51, nos. 3–4, p. 429–438.

Deng, Z.D., Carlson, T.J., Li, H., Xiao, J., Myjak, M.J., Lu, J., Martinez, J.J., Woodley, C.M., Weiland, M.A., and Eppard, M.B., 2015, An injectable acoustic transmitter for juvenile salmon: Scientific Reports 5:8111, accessed October 15, 2015, at http://www.nature.com/articles/srep08111.

Enders, E.C., Gessel, M.H., Anderson, J.J., and Williams, J.G., 2012, Effects of decelerating and accelerating flows on juvenile salmonid behavior: Transactions of the American Fisheries Society, v. 141, p. 357–364.

Haro, A., Odeh, M., Noreika, J., and Castro-Santos, T., 1998, Effect of water acceleration on downstream migratory behavior of Atlantic salmon smolts and juvenile American shad at surface bypasses: Transactions of the American Fisheries Society, v. 127, p. 118–127.

HDR, 2012, Design criteria manual—Portable floating fish collector plans Cougar Dam, Oregon: Report of HDR, Portland, Oregon, for U.S. Army Corps of Engineers, Portland, Oregon, contract W9127N-11-D-0011, task order 0003, mod 3, 48 p.

Hosmer, D.W., and Lemeshow, S., 1999, Applied survival analysis—Regression modeling of time to event data: New York, Wiley, 386 p.

Johnson, G.A., and Dauble, D.D., 2006, Surface flow outlets to protect juvenile salmonids passing through hydropower plants: Reviews in Fishery Science, v. 14, p. 213–244.

Johnson, R.L., and Moursund, R.A., 2000, Evaluation of juvenile salmon behavior at Bonneville Dam, Columbia River, using a multibeam technique: Aquatic Living Resources, v. 13, no. 5, p. 313–318.

Jolly, G.M., 1965, Explicit estimates from capture-recapture data with both death and immigration-stochastic model: Biometrika, v. 52, nos. 1–2, p. 225–247.

Kang, M., 2011, Semiautomated analysis of data from an imaging sonar for fish counting, sizing, and tracking in a post-processing application: Fisheries and Aquatic Sciences, v. 14, no. 3, p. 218–225.

Khan, F., Johnson, G.E., Royer, I.M., Phillips, N.R., Hughes, J.S., Fischer, E.S., Ham, K.D., and Ploskey, G.R., 2012, Acoustic imaging evaluation of juvenile salmonid behavior in the immediate forebay of the water temperature control tower at Cougar Dam, 2010: Pacific Northwest National Laboratory report PNNL-20625, 50 p.

Klein, F.W., 1978, Hypocenter location program HYPOINVERSE, 1, User's guide to versions 1, 2, 3, 4: U.S. Geological Survey Open-File Report 78-694, 103 p.

Kranstauber, B., Kays, R., LaPoint, S.D., Wikelski, M., and Safi, M., 2012, A dynamic Brownian bridge movement model to estimate utilization distributions for heterogeneous animal movement: Journal of Animal Ecology, v. 81, p. 738–746.

Lee, W.H.K., and Stewart, S.W., 1981, Principles and applications of microearthquake networks: New York, Academic Press, 293 p.

Manley, B.F.J., McDonald, L.L., and Thomas, D.L., 1993, Resource selection by animals—Statistical design and analysis for field studies: London, Chapman and Hall, 177 p.

Mardia, K.V., and Jupp, P.E., 2000, Directional statistics: Chichester, United Kingdom, John Wiley & Sons Ltd., 492 p.

McMichael, G.A., Eppard, M.B., Carlson, T.J., Carter, J.A., Ebberts, B.D., Brown, R.S., Weiland, M., Ploskey, G.R., Harnish, R.A., and Deng, Z.D., 2010, The juvenile salmon acoustic telemetry system—A new tool: Fisheries, v. 35, no. 1, p. 9–22.

Menke, W., 1989, Geophysical data analysis—Discrete inverse theory: San Diego, Academic Press, 291 p.

Mesa, M., Phelps, J., and Weiland, L.K., 2008, Spring swimming performance of wild bull trout (*Salvelinus confluentus*): Northwest Science, v. 82, p. 1–6.

Monzyk, F.R., 2012, Cougar Dam route passage survival indices based on release-recapture of PIT-tagged hatchery fish: Report of Oregon Department of Fish and Wildlife, Corvallis, for U.S. Army Corps of Engineers, Portland, Oregon, 18 p.

Monzyk, F.R., Emig, R., Romer, J.D., and Friesen, T.A., 2013, Life-history characteristics of juvenile spring Chinook salmon rearing in Willamette Valley reservoirs: Report of Oregon Department of Fish and Wildlife, Corvallis, for U.S. Army Corps of Engineers, Portland, Oregon, contract W9127N-10-2-0008, 72 p., accessed November 23, 2015, at http://oregonstate.edu/dept/ODFW/willamettesalmonidrme/sites/default/files/reservoir-research/life-history_characteristics_in_reservoirs_annual_report_2012_-final.pdf.

Monzyk, F.R., Friesen, T.A., and Romer, J.D., 2015, Infection of juvenile salmonids by *Salmincola californiensis* (Copepoda: Lernaeopodidae) in reservoirs and streams of the Willamette River Basin, Oregon: Transactions of the American Fisheries Society, v. 144, p. 891–902, doi:10.1080/00028487.2015.1052558.

Monzyk, F.R., Romer, J.D., Emig, R., and Friesen, T.A., 2011a, Life-history characteristics of juvenile spring Chinook salmon rearing in Willamette Valley reservoirs: Report of Oregon Department of Fish and Wildlife, Corvallis, for U.S. Army Corps of Engineers, Portland, Oregon, contract W9127N-10-2-0008, 38 p.

Monzyk, F.R., Romer, J.D., Emig, R., and Friesen, T.A., 2011b, Pilot head-of-reservoir juvenile salmonid monitoring: Report of Oregon Department of Fish and Wildlife, Corvallis, for U.S. Army Corps of Engineers, Portland, Oregon, contract W9127N-10-2-0008, 21 p.

Monzyk, F.R., Romer, J.D., Emig, R., and Friesen, T.A., 2012, Life-history characteristics of juvenile spring Chinook salmon rearing in Willamette Valley reservoirs: Report of Oregon Department of Fish and Wildlife, Corvallis, for Army Corps of Engineers, Portland, Oregon, contract W9127N-10-2-0008, 60 p., accessed November 23, 2015 at http://oregonstate.edu/dept/ODFW/willamettesalmonidrme/sites/default/files/reservoir-research/life-history_characteristics_in_reservoirs_annual_report_2012_-final.pdf.

Moser, T.J., 1991, Shortest path calculation of seismic rays: Geophysics, v. 56, p. 59–67.

National Marine Fisheries Service, 2011, Anadromous salmonid passage facility design: National Marine Fisheries Service, Northwest Region, Portland, Oregon. 138 p.

National Oceanic and Atmospheric Administration, 2008, Endangered Species Act section 7(a)(2) consultation biological opinion and Magnuson-Stevens Fishery Conservation and Management Act essential fish habitat consultation—Consultation on the Willamette River Basin Flood Control Project: National Oceanic and Atmospheric Administration Fisheries Log Number FINWRl2000/02117, June 11, 2008., accessed May 2015 at http://www.nwr.noaa.gov/Salmon-Hydropower/Willamette-Basin/Willamette-BO.cfm.

Normandeau and Associates, Inc., 2010, Estimates of direct survival and injury of juvenile Chinook salmon (*Oncorhynchus tshawytscha)*, passing a regulating outlet and turbine at Cougar Dam, Oregon: Normandeau Associates, Inc., prepared for U.S. Army Corps of Engineers, Portland District, Portland, Oregon, contract 912EF-08-D-0005 task order DT01, 160 p.

Pewsey, A., Neuhauser, M., and Ruxton, G.D., 2013, Circular statistics in R (1st ed.): Oxford, United Kingdom, Oxford University Press, 208 p.

Pincock, D.G., and Johnston, S.V., 2012, Acoustic telemetry overview, *in* Adams, N.S., Beeman, J.W., and Eiler, J.H., eds., Telemetry techniques—A user guide for fisheries research: Bethesda, Maryland, American Fisheries Society, p. 305–338.

PIT Tag Steering Committee, 2014, PIT tag marking procedures manual, version 3.0: PIT Tagging Steering Committee, 28 p., accessed October 30, 2015 at http://www.ptagis.org/resources/document-library/ptagis-program-documents.

R Core Team, 2014, R—A language and environment for statistical computing: Vienna, Austria, Foundation for Statistical Computing, accessed 2014, at http:// www.R-project.org/.

Rettie, W.J., and Messier, F., 2000, Hierarchical habitat selection by woodland caribou—Its relationship to limiting factors: Ecography, v. 23, p. 466–478.

Romer, J.D., Monzyk, F.R., Emig, R., and Friesen, T.A., 2012, Juvenile salmonid outmigration monitoring at Willamette Valley Project reservoirs: Report of Oregon Department of Fish and Wildlife, Corvallis, for U.S. Army Corps of Engineers, Portland, Oregon, contract W9127N-10-2-0008, 42 p., accessed October 25, 2013 at http://oregonstate.edu/dept/ODFW/willamettesalmonidrme/sites/default/files/reservoir-research/outmigration_monitoring_annual_2011.pdf

Romer, J.D., Monzyk, F.R., Emig, R., and Friesen, T.A., 2013, Juvenile salmonid outmigration monitoring at Willamette Valley Project reservoirs: Report of Oregon Department of Fish and Wildlife, Corvallis, for U.S. Army Corps of Engineers, Portland, Oregon, contract W9127N-10-2-0008, 52 p., accessed November 23, 2015 at http://oregonstate.edu/dept/ODFW/willamettesalmonidrme/sites/default/files/reservoir-research/outmigration_monitoring_annual_report_2012.pdf.

Seber, G.A.F., 1965, A note on the multiple-recapture census: Biometrika, v. 52, nos. 1–2, p. 249–259.

Simmonds, J. and MacLennan, D., 2005, Fisheries acoustics—Theory and practice (2d ed.): Oxford, United Kingdom, Blackwell Scientific Publications, 456 p.

Sokal, R.B., and Rohlf, F.J., 1969, Biometry: San Francisco, W.H. Freeman and Company, 859 p.

Speisberger, J.L., and Fristrup, K.M., 1990, Passive location of calling animals and sensing of their acoustic environment using acoustic tomography: American Naturalist, v. 135, p. 107–153.

Surgical Protocols Steering Committee, 2011, Surgical protocols for implanting JSATS transmitters into juvenile salmonids for studies conducted for the U.S. Army Corps of Engineers: Report prepared by Surgical Protocols Steering Committee for U.S. Army Corps of Engineers, Portland, Oregon, 18 p.

Sweeney, C.E., Giorgi, A.E., Johnson, G.E., Hall, R., and Miller, M., 2007, Surface bypass program comprehensive review report: ENSR Corporation document number 09000-399-0409, 494 p.

Taylor, E.B., and McPhail, J.D., 1985, Variation in burst and prolonged swimming performance among British Columbia populations of coho salmon, *Oncorhynchus kisutch*: Canadian Journal of Fisheries and Aquatic Sciences v. 42, p. 2,029–2,033.

Tiffan, K.F., Perry, R.W., Connor, W.P., Mullins, F.L., Rabe, C.D., and Nelson, D.D., 2015, Survival, growth, and tag retention in age-0 Chinook salmon implanted with 8-mm, 9-mm, and 12-mm PIT tags: North American Journal of Fisheries Management v. 134, p. 892–900.

Titzler, P.S., McMichael, G.A., and Carter, J.A., 2010, Autonomous acoustic receiver deployment and mooring techniques for use in large rivers and estuaries: North American Journal of Fisheries Management, v. 30, p. 853–859.

Vowles, A.S., and Kemp, P.S., 2012, Effects of light on the behaviour of brown trout (*Salmo* t*rutta*) encountering accelerating flow—Application to downstream passage: Ecological Engineering, v. 47, p. 247–263.

Vowles, A.S., Anderson, J.J., Gessel. M.H., Williams, J.G., and Kemp, P.S., 2014, Effects of avoidance behavior on downstream fish passage through accelerating flow when light and dark: Animal Behavior, v. 92, p. 101–109.

Webb, P.A., 1978, Temperature effects on acceleration of rainbow trout (*Salmo gairdneri*): Journal of the Fisheries Research Board of Canada, v. 35, p. 1,417–1,422.

Weiland, M.A, Ploskey, G.R., Hughes, J.S., Deng, Z., Fu, T., Monter, T.J., Johnson, G.E., Khan, F., Wilberding, M.C., Cushing, A.W., Zimmerman, S.A., Faber, D.M., Durham, R.E., Townsend, R.L., Skalski, J.R., Kim, J., Fischer, E.S., and Meyer, M.M., 2009, Acoustic telemetry evaluation of juvenile salmonid passage and survival at John Day Dam with emphasis on the prototype surface flow outlet, 2008: Pacific Northwest National Laboratory, Richland, Washington, Report PNNL-18890, 259 p.

Weiland, M.A., Deng, ZD., Seim, T., LaMarche, B.L., Choi, E.Y., Fu, T., Carlson, T.J., Thronas, A.I., and Eppard, M.B., 2011, A cabled acoustic telemetry system for detecting and tracking juvenile salmon—Part 1—Engineering design and instrumentation: Sensors, v. 11, p. 5,645–5,660, accessed August 12, 2015, at http://dx.doi.org/10.3390/s110605645.

White, G.C., and Burnham, K.P., 1999, Program MARK–Survival estimation from populations of marked animals: Bird Study, v. 46 (supp.), p. 120–138.

Zar, J. H., 1999, Biostatistical analysis (4th ed.): Upper Saddle River, New Jersey, Prentice Hall, 663 p.

Appendix A. Performance of the Portable Floating Fish Collector Passive Integrated Transponder Interrogator

Introduction

Detection probabilities of telemetry systems often are imperfect, so it is important to estimate and account for detection probability when estimating tag presence using this methodology. In the context of this study, it is important to use estimates of detection probability of the passive integrated transponder (PIT) interrogator within the portable floating fish collector (PFFC) when estimating the numbers of tagged fish present. We, therefore, estimated detection probability of the system using the full-duplex PIT tag model used to tag juvenile Chinook salmon in Cougar Reservoir. There also are bull trout (*Salvelinus confluentus*) implanted with half-duplex PIT tags within the reservoir, but detection probabilities of half-duplex interrogators generally are higher than full-duplex systems, so we did not use half-duplex tags in our evaluation. We did use a new generation of 8 mm long PIT tags that may be used in juvenile salmonids in the near future.

Methods

We released test PIT tags through the PFFC to estimate the detection probability of the PIT detection system. We first ran a simulation to determine the number of test tags required using Program MARK (White and Burnham, 1999) and determined that releases of greater than 150 tags would not substantially improve the 95-percent confidence intervals of detection probability (fig. A1). Test tags were attached to a 1-m section of 40 mm polyvinyl chloride (PVC) (to keep tag orientation constant and parallel to the inflow) with adjustable floatation on each end (to set the depth). Tests of the effect of tag size and type were conducted using 12-mm SST, 8-mm HPT, and 8-mm MiniHPT Biomark® PIT tags. Additionally, we tested the effect of tag collision on detection probability during two trials by attaching 12-mm SST tags at 12, 28, or 46 cm intervals to single sections of PVC pipe. Detection probabilities of physical and virtual tags were estimated using a three-occasion Cormack-Jolly-Seber mark-recapture model (Cormack, 1964; Jolly, 1965; Seber, 1965) in Program MARK.

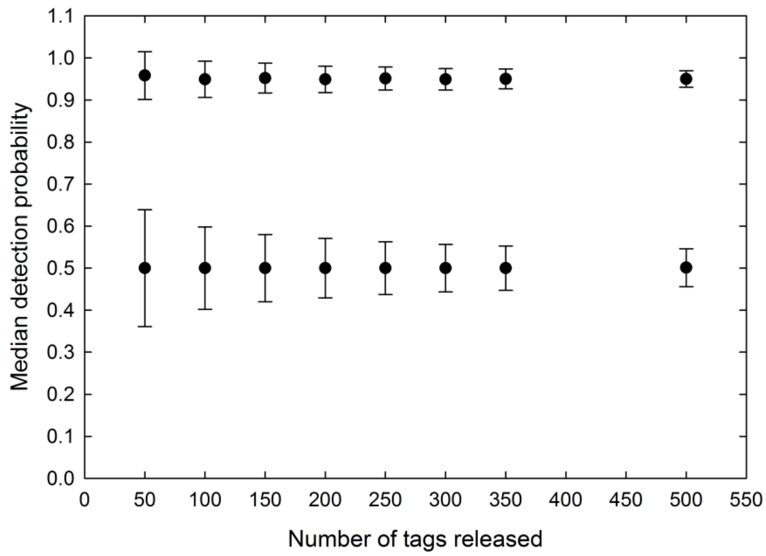

Figure A1. Graph showing results of simulations with 1,000 replicates of passive integrated transponder releases assuming 50- and 95-percent detection probabilities and no tag collisions. Error bars show 95-percent confidence intervals.

Estimating the continuous detection probabilities of the virtual tag was based on the evaluation of a suite of models representing varying assumptions thought to affect detection probability. Models evaluated ranged from an overall model assuming no effect of time or treatment, a model based on treatment independence with no effect of time, models based on varying time intervals with no treatment effect, and a model with the interaction of treatment and time based on the block design. The probabilities of detection were estimated from model-averaged coefficients (Burnham and Anderson, 2002).

Results

Detection probability of the PIT interrogator was influenced by tag number and tag size. Multiple tag collision greatly reduced the detection efficiency of the PIT-tag interrogator from about 0.9 for a single tag to less than 0.3 for 6 tags at a 12-cm separation (fig. A2A). The estimated detection probabilities for 8-mm HPT (0.16) and 8-mm MiniHPT (0.03) tags were much lower than for the 12-mm SST tags (0.89; fig. A2B). The 8-mm tags were tested because they were the smallest commercially available tags and can be used in smaller fish than the 12-mm long tags commonly used in juvenile salmonids (Tiffan and others, 2015); however, they were not being used in Cougar Reservoir in 2014.

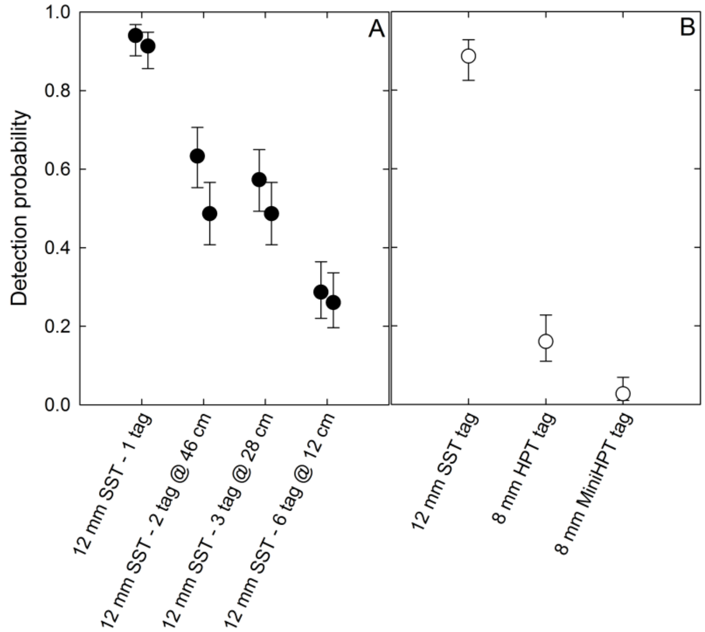

Figure A2. Graph showing estimated detection probabilities of the portable floating fish collector passive integrated transponder (PIT) interrogator during trials of (A) different numbers of PIT tags during the two trials at the High treatment, and (B) sizes of PIT tags during the single trial at the Low treatment at Cougar Reservoir, Oregon, 2014.

After initial testing, the 12-mm SST tag produced detection probabilities similar to those of the virtual tag reads (Mantel-Haenszel Statistic; 0.0507; df = 1; P = 0.8219). Based on those results, we used the virtual tag data to monitor detection efficiency throughout the study.

Data and models of detection probability based on the virtual tag data indicated almost no support for differences between treatments, as indicated by a delta AICc of more than 36 units. The most supported models included effects of block and time (month); there also was moderate support for a model based on a Treatment and Block interaction (table A1). The model-averaged point estimates indicated that the PIT-tag interrogator detection probability ranged from 0.922 to 1.000 among blocks, with a mean of 0.978 (fig. A3).

Table A1. Suite of three-occasion models for the analysis of detection probabilities of virtual tags from the passive integrated transponder interrogator on the PFFC at Cougar Reservoir, Oregon, 2014.

[AICc, Akaike Information Criterion with an adjustment for effects of sample size; Num par, number of parameters]

Model	AICc	Delta AICc	AICc weights	Model likelihood	Num par	Deviance
1 P(Block)	909.551	0.000	0.844	1.000	13	13.758
2 P(Month)	913.455	3.904	0.120	0.142	7	26.692
3 P(Treatment*Block)	915.882	6.331	0.036	0.042	23	0.000
4 P(Treatment)	946.492	36.941	0.000	0.000	2	72.741
5 P(Overall)	947.712	38.161	0.000	0.000	1	75.962

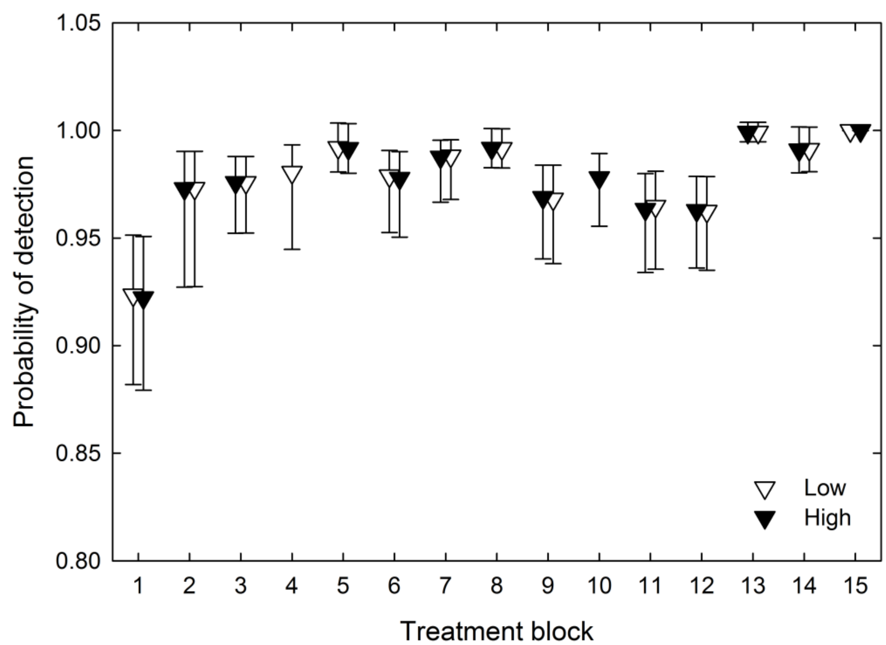

Figure A3. Estimated detection probabilities of virtual full-duplex passive integrated transponder (PIT) tags at the portable floating fish collector PIT interrogator, Cougar Reservoir, Oregon, 2014.

Appendix B. Transmitter Life Tests

Introduction

The operational life of a subset of the acoustic transmitters used in this study was empirically determined to define an appropriate follow-up time for analysis. The purpose of defining a follow-up time was to ensure a high probability of transmitter functionality during the period of analysis.

Methods

We selected 50 acoustic transmitters from the spring tags and empirically determined tag life. We activated the tags on March 13, 2014, sorted them into two 25 transmitters groups, placed each group in a 82.6 × 279.4 × 31.7 mm plastic box, and submerged the boxes in replicate 1.5-m diameter circular tanks at the U.S. Geological Survey Columbia River Research Laboratory in Cook, Washington. Water temperatures were adjusted periodically to reflect temperatures at Cougar Reservoir. Transmitter messages were recorded with an Advanced Telemetry Systems model Trident SR5000 receiver (ATS; Isanti, Minnesota) and processed as other autonomous receivers. Data were summarized using Kaplan-Meier survivorship analysis (Hosmer and Lemeshow, 1999).

Results

The estimated lives of the acoustic transmitters tested were as expected. The median life of the transmitters was 149.5 days, and the maximum life was 183.9 days (fig. B1). The first tag stopped working after 133.0 days and the 90th percentile of tag life was 144.0 days. The estimated 90th percentile of tag life was used as the follow-up period.

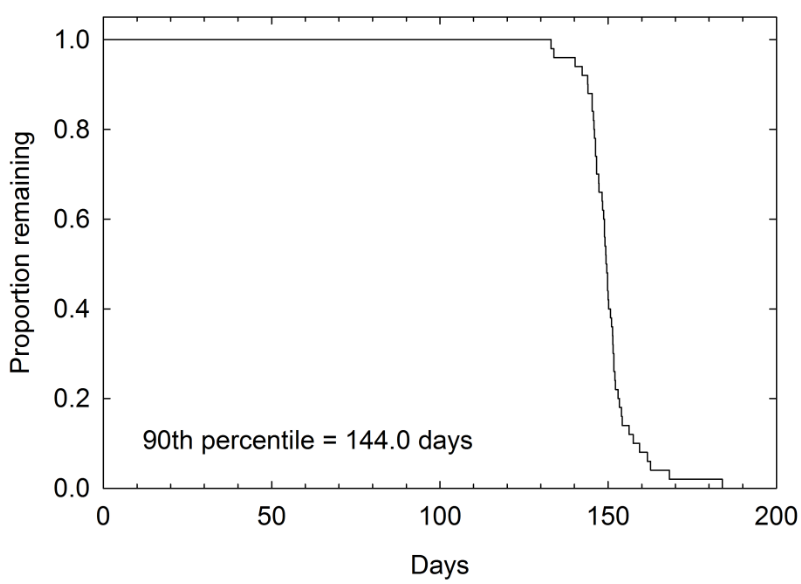

Figure B1. Graph of the survival distribution function of days from activation to expiration for acoustic transmitters tested as part of the study at Cougar Reservoir, Oregon, 2014.

This page left intentionally blank

Appendix C. Positioning System Accuracy

Introduction

It is important to estimate location estimation errors from positioning systems so the resulting data can be placed into proper context relative to the objectives of the study. For this study, our goal was to estimate positions of acoustic+PIT-tagged fish over a large area near the portable floating fish collector (PFFC) and temperature control tower at Cougar Dam (the cul-de-sac) and to have position accuracies within about 1 m of the true position near the entrance to the PFFC and within a few meters of the true position throughout the rest of the monitored area. This goal was determined by U.S. Geological Survey and U.S. Army Corps of Engineers staff to meet the study objectives. Location estimation errors also were used to estimate Utilization Distributions (see section, "Spatial Intensity of Use").

Methods

Accuracies of the fish positions determined from the juvenile salmon acoustic telemetry system (JSATS) cabled systems in the cul-de-sac were determined from empirical estimates of system accuracy based on test tags. Tag data came from tags with 5-second pulse rate intervals towed by a remote-controlled boat and stationary tags affixed to the PFFC or to floating platforms. Eleven tags towed by the boat were grouped in pairs or triplets and suspended below the surface of the water at approximately 1.83-m intervals 1.83–9.84 m deep while the boat moved throughout the monitored area at a rate of about 0.3 m/s. The boat path was restricted by the series of JSATS communication cables and PFFC anchor lines. Locations of the four stationary tags included carbon-fiber poles at each side of the PFFC entrance and at two floating platforms about 20 m upstream of the PFFC; each tag was mounted 10.5 m below the water surface. The x-y positions of test tags were determined with Javad GNSS® antennas collecting data directly over the tags every 5 seconds and were compared to data from the JSATS system at the nearest time. Spatially explicit system errors in the x-y (horizontal) plane were estimated as the absolute difference between the positions estimated using the acoustic telemetry system and the Global Positioning System. Errors in the z (vertical) plane were estimated as the absolute difference between the known depths and those estimated using the acoustic telemetry system. The spatially explicit position errors were assigned to the fish positions using the Kriging process and were used in estimates of the intensity of fish use within the area monitored in the cul-de-sac (see section, "Spatial Intensity of Use").

Results

The accuracy of the estimated fish positions varied spatially and ranged from less than 1 m to more than 10 m. Accuracy within the hydrophone array was consistently greater than outside the array, as expected based on hydrophone geometry (Pincock and Johnston, 2012; fig. C1). Estimated position accuracies within the hydrophone array in the x-y and z planes generally were about 1–2 m, except off the Port bow and Starboard stern of the PFFC. The estimated accuracies in those areas do not likely reflect the true accuracy because JSATS communication cables and PFFC anchor lines blocked the travel of the test tag vessel, preventing us from collecting data there. The estimated system accuracies within the bounds of the hydrophone array met the stated goal.

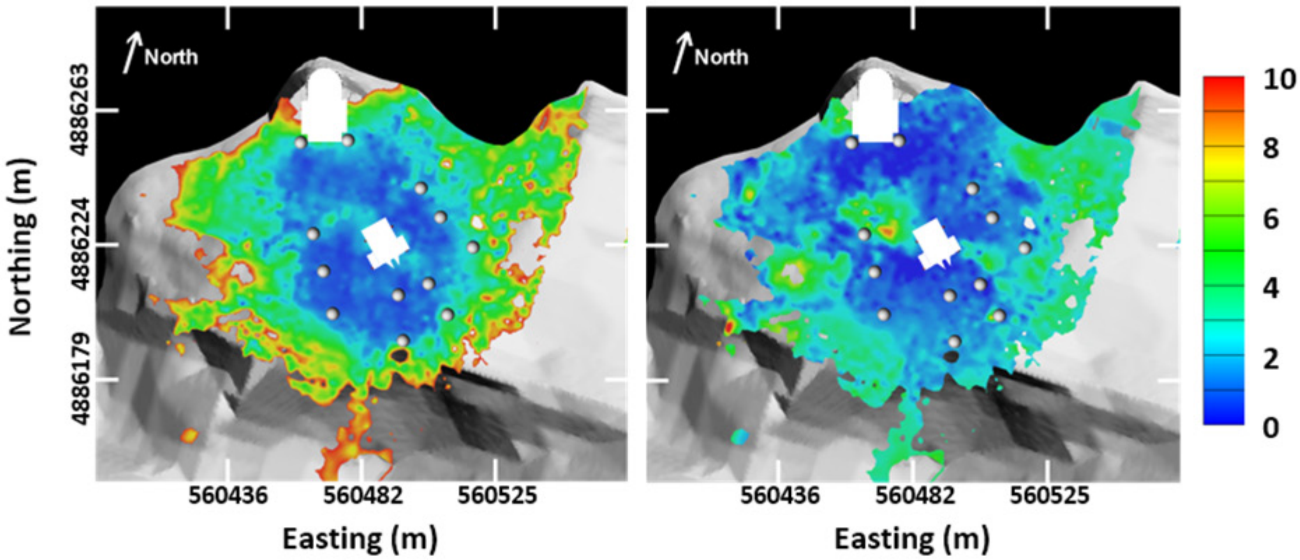

Figure C1. Graphs of the estimated position accuracies (in meters [m]) of the acoustic telemetry system in the horizontal (left graph) and vertical (right) planes in the cul-de-sac of Cougar Reservoir, Oregon, 2014. The portable floating fish collector is shown near the center of each graph and the water temperature control tower is at the top center of each graph. Gray circles indicate the positions of the hydrophones.

Appendix D. Utilization Distributions from Acoustic+Passive Integrated Transponder-Tagged Juvenile Chinook salmon in the Cul-de-Sac of Cougar Reservoir and Dam, Oregon, 2014

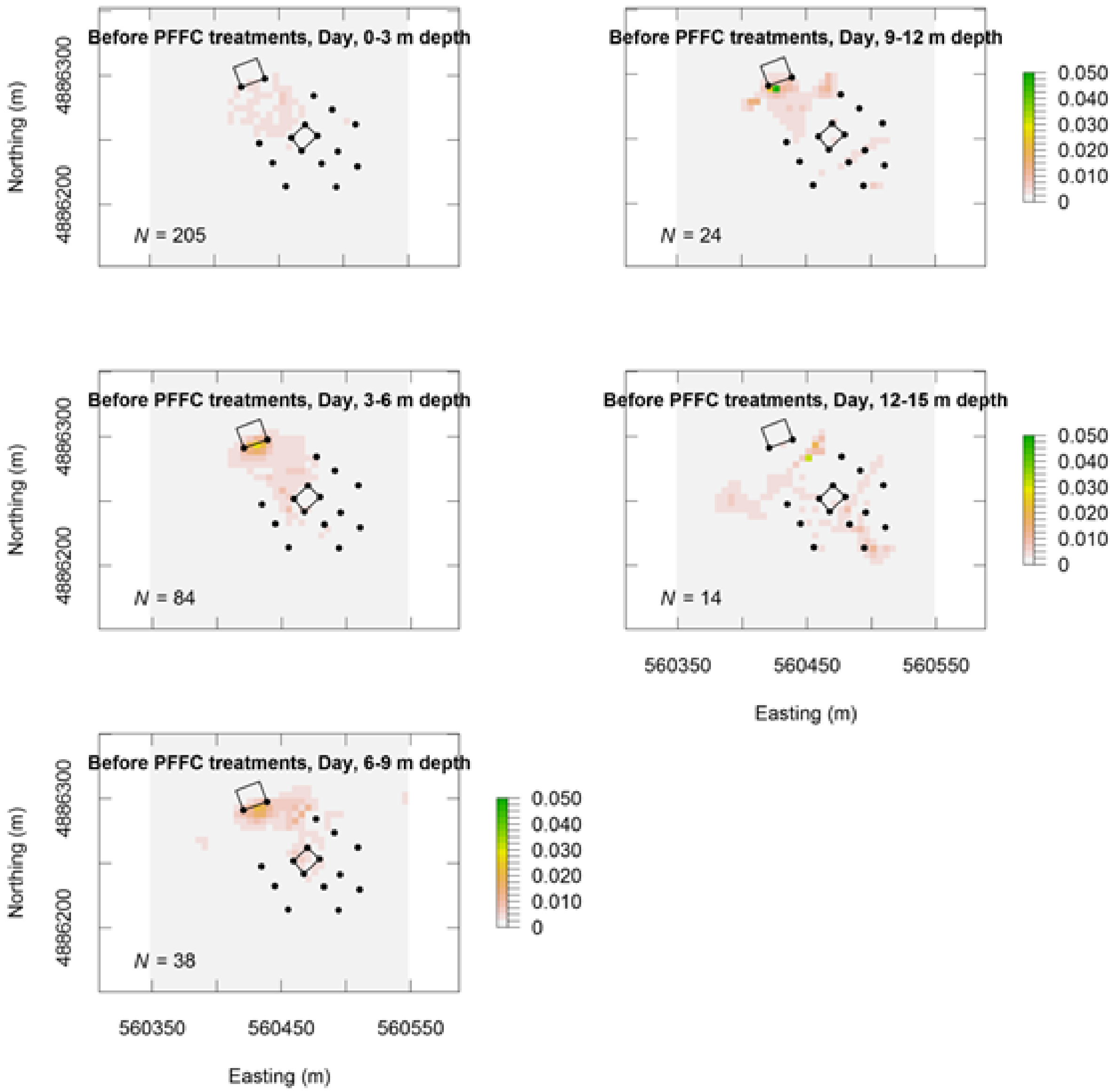

Figure D1. Utilization Distributions from acoustic+PIT-tagged juvenile Chinook salmon in the cul-de-sac of Cougar Reservoir and Dam, Oregon, 2014. Data are from the day during May 16–26, 2014, before the portable floating fish collector (PFFC) began operation on May 27, 2014.

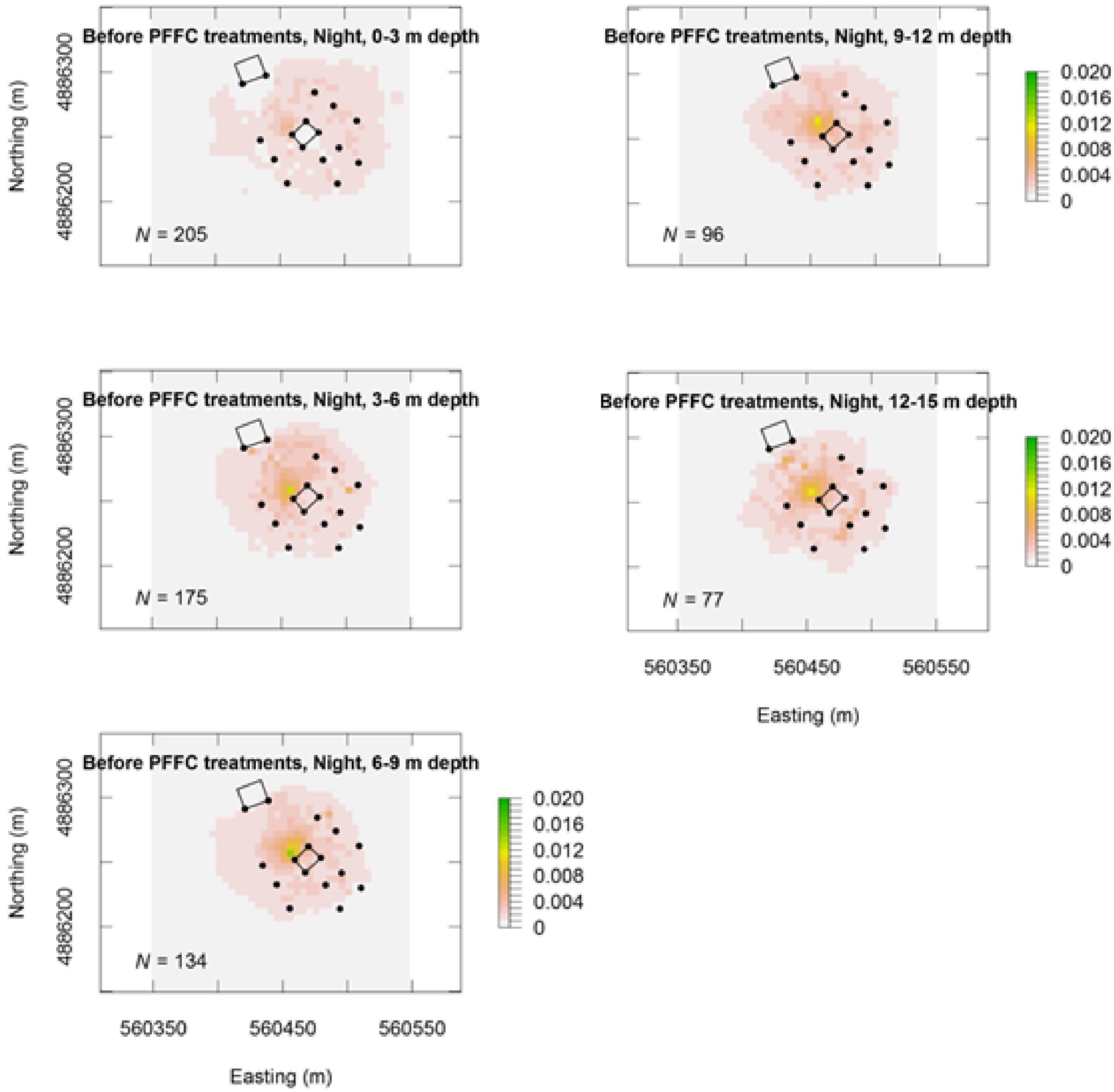

Figure D2. Utilization Distributions from acoustic+PIT-tagged juvenile Chinook salmon in the cul-de-sac of Cougar Reservoir and Dam, Oregon, 2014. Data are from the night during May 16–26, 2014, before the portable floating fish collector (PFFC) began operation on May 27, 2014.

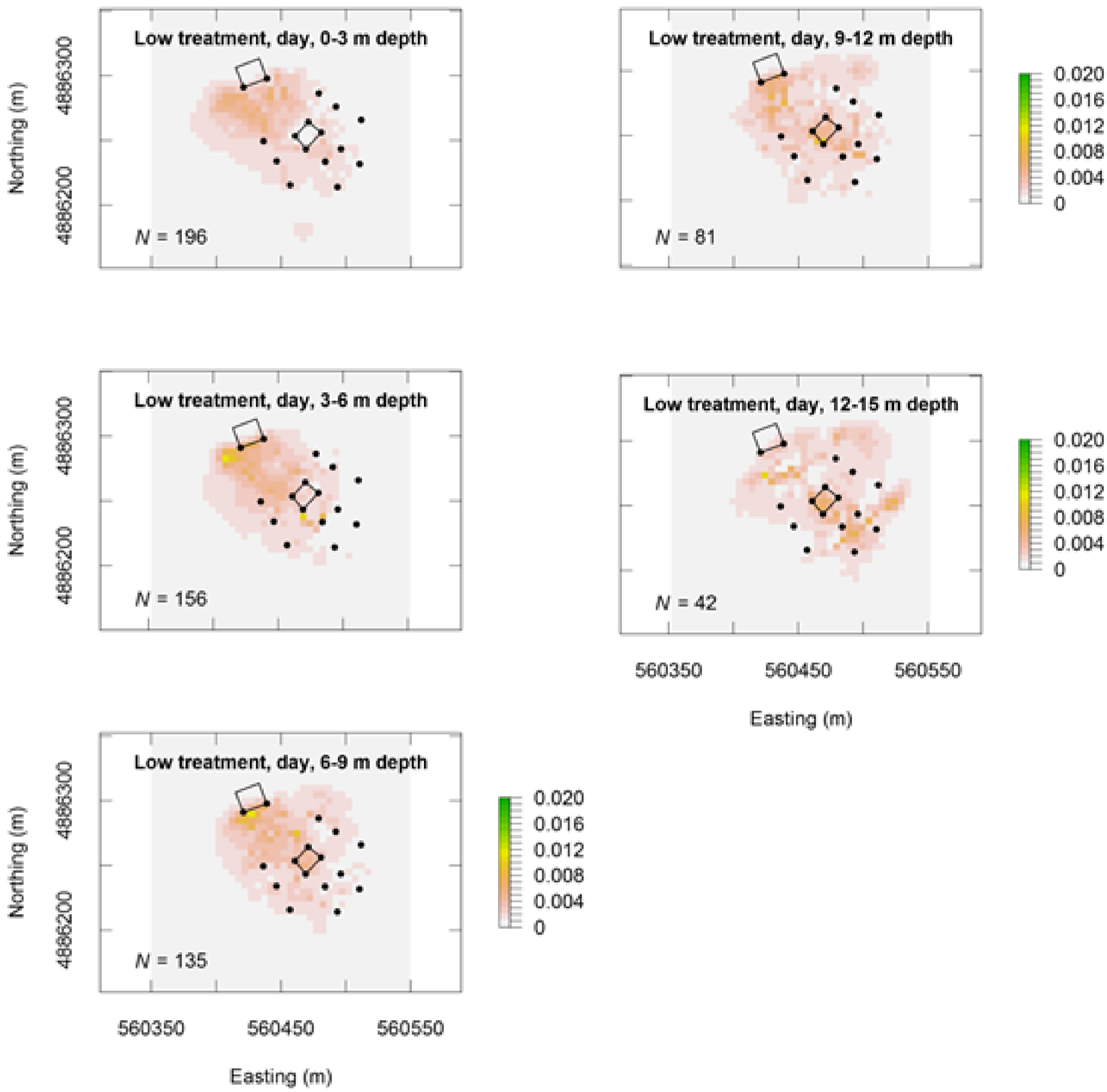

Figure D3. Utilization Distributions from acoustic+PIT-tagged juvenile Chinook salmon in the cul-de-sac of Cougar Reservoir and Dam, Oregon, 2014. Data are from the day during the Low treatment.

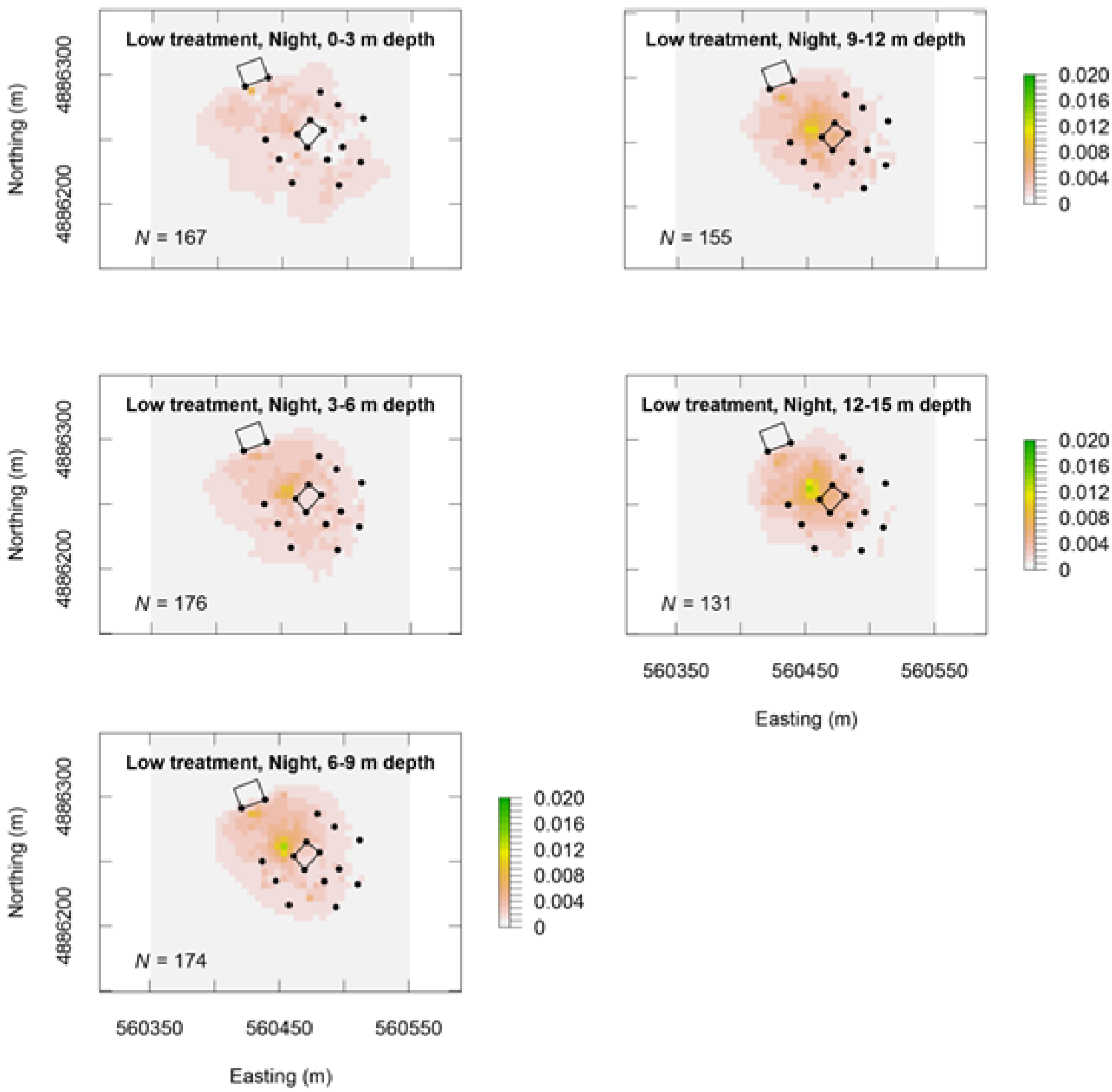

Figure D4. Utilization Distributions from acoustic+PIT-tagged juvenile Chinook salmon in the cul-de-sac of Cougar Reservoir and Dam, Oregon, 2014. Data are from the night during the Low treatment.

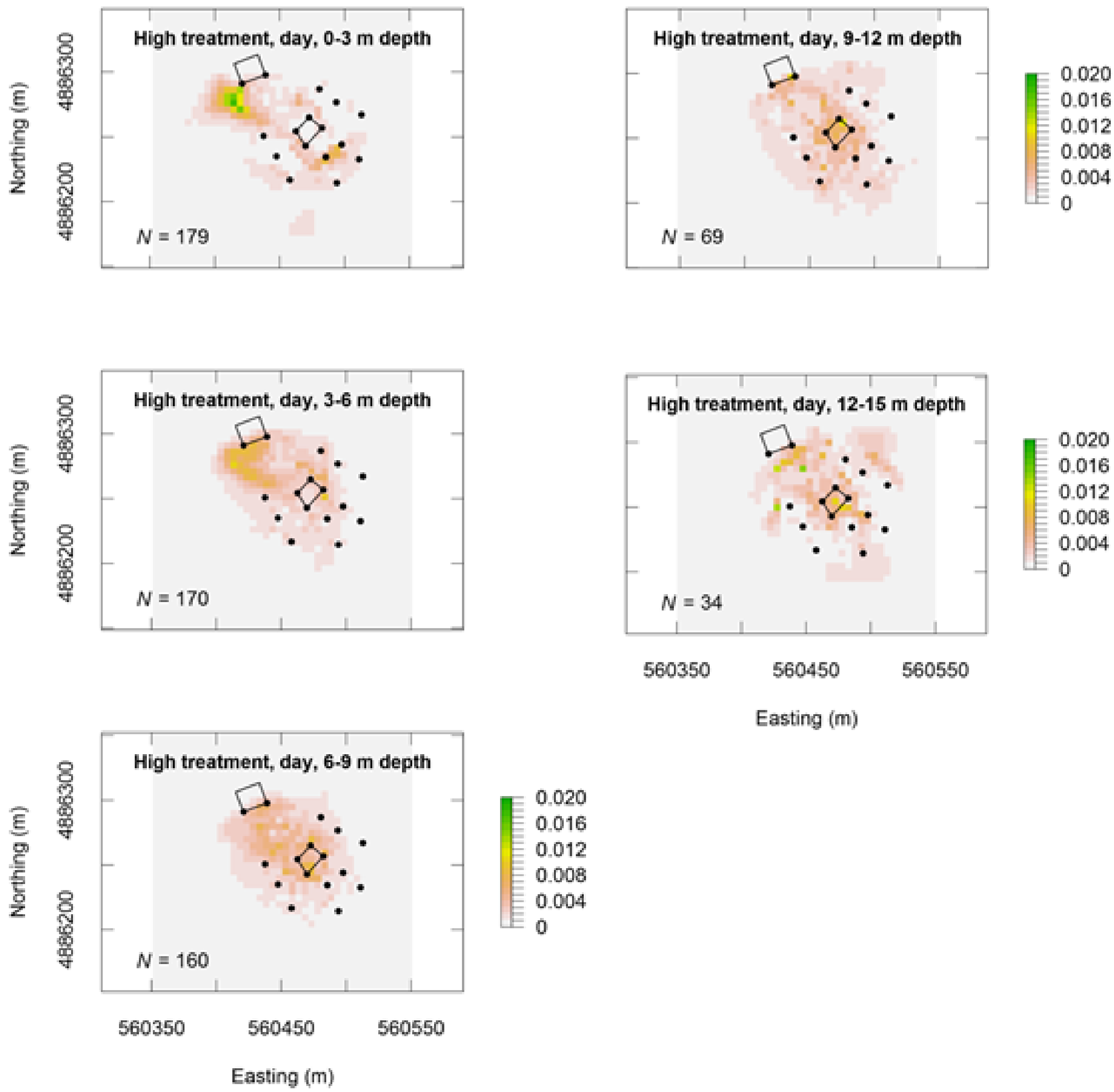

Figure D5. Utilization Distributions from acoustic+PIT-tagged juvenile Chinook salmon in the cul-de-sac of Cougar Reservoir and Dam, Oregon, 2014. Data are from the day during the High treatment.

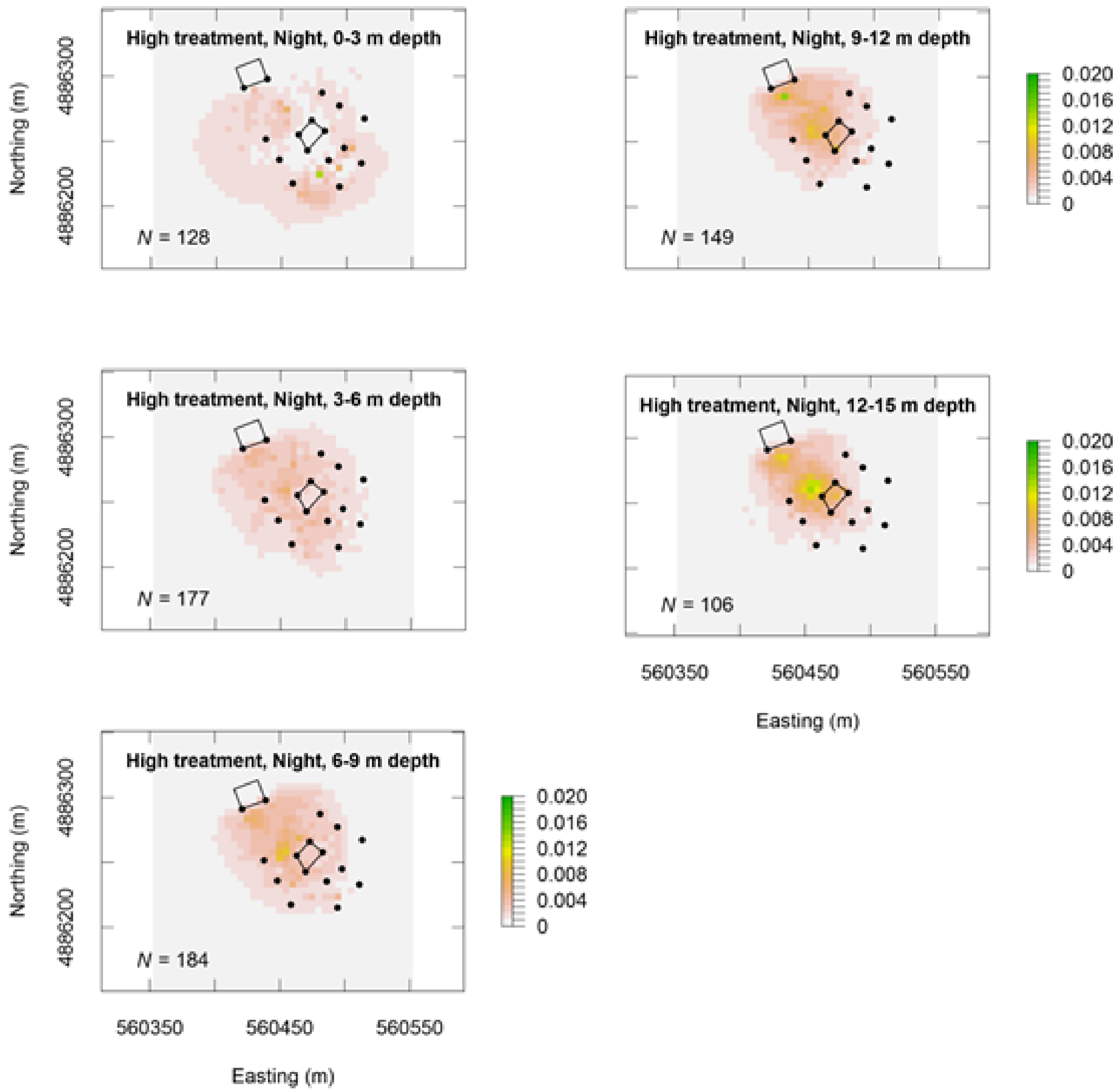

Figure D6. Utilization Distributions from acoustic+PIT-tagged juvenile Chinook salmon in the cul-de-sac of Cougar Reservoir and Dam, Oregon, 2014. Data are from the night during the High treatment.

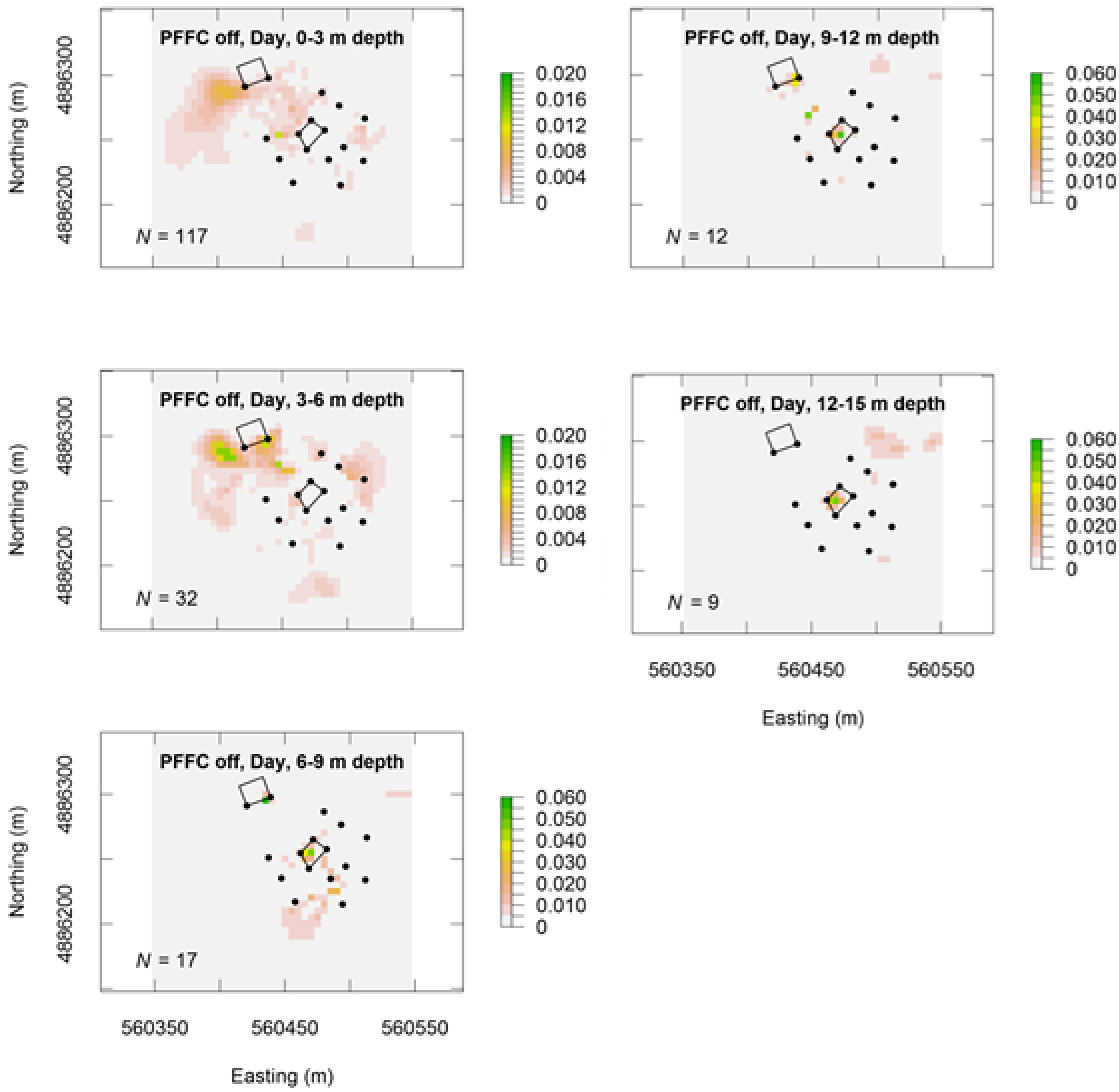

Figure D7. Utilization Distributions from acoustic+PIT-tagged juvenile Chinook salmon in the cul-de-sac of Cougar Reservoir and Dam, Oregon, 2014. Data are from the day during the times that the portable floating fish collector (PFFC) was off.

This page left intentionally blank

Appendix E. Summary of Dam Operating Conditions Calculated from Hourly Data at Cougar Dam, Oregon, 2014

Table E1. Summary statistics of dam operations and environmental conditions at Cougar Reservoir, Oregon, April 9–December 16, 2014.

[SD, standard deviation; RO, regulating outlet; ft^3/s, cubic foot per second]

Dam operating conditions	Period	Mean	Median	Range	SD
Total project (ft^3/s)	Overall	918.8	670.0	380.0–2,990.0	627.7
	Day	873.2	670.0	380.0–2,990.0	586.2
	Night	984.1	685.0	390.0–2,990.0	677.4
Powerhouse (ft^3/s)	Overall	652.0	460.0	0.0–1,630.0	293.5
	Day	639.9	460.0	0.0–1,630.0	279.2
	Night	669.4	470.0	0.0–1,210.0	312.0
Regulating outlet (ft^3/s)	Overall	266.7	0.0	0.0–2,600.0	476.6
	Day	233.3	0.0	0.0–2,560.0	445.4
	Night	314.7	0.0	0.0–2,600.0	514.3
Forebay elevation (feet)	Overall	1,641.8	1,656.5	1,528.5–1,691.1	41.7
	Day	1,647.7	1,662.4	1,528.6–1,691.1	38.9
	Night	1,633.4	1,642.4	1,528.5–1,691.1	44.1
Head over the weir gates	Overall	10.2	9.6	1.6–31.1	5.9
	Day	10.2	9.7	1.9–31.0	5.6
	Night	10.2	9.5	1.6–31.1	6.0
Water temperature (degrees Celsius)	Overall	13.4	14.1	6.0–21.3	3.8
.	Day	13.5	14.2	6.0–21.1	3.7
	Night	13.2	13.9	6.1–21.3	3.9
Percent RO of total	Overall	16.1	0.0	0.0–100.0	26.4
	Day	14.6	0.0	0.0–100.0	25.4
	Night	18.2	0.0	0.0–100.0	27.7

This page left intentionally blank

Appendix F. Summary of Portable Floating Fish Collector Operating Conditions Collected by U.S. Army Corps of Engineers Staff at Cougar Reservoir and Dam, Oregon, 2014

Table F1. Means of observed portable floating fish collector operation and environmental data collected by U.S. Army Corps of Engineers staff at Cougar Reservoir and Dam, Oregon, 2014.

[Tower, water temperature control tower. Leveling pump, weir width, weir height are measured in inches. Distance from the water temperature control tower and reservoir elevation are measured in feet. Water temperatures are recorded in degrees Celsius. Number of observations is the number of times U.S. Army Corps of Engineers staff recorded data during each treatment and block. ND, no data]

Block	Treat-ment	Percent attraction pump	Leveling pump	Weir width	Weir height	Distance from tower	Mean observed reservoir elevation	Water temperature			Number of observations
								Submersible pump	Hopper	Reservoir	
1	Low	60	100.0	15.0	17.5	148.0	1,689.6	ND	18.8	ND	5
	High	90	100.0	15.0	15.0	144.0	1,687.7	ND	16.9	ND	5
2	High	85	100.0	15.0	15.0	148.5	1,683.5	15.2	16.0	17.2	4
	Low	50	100.0	15.0	17.5	151.5	1,680.2	13.9	15.7	16.5	2
	High	85	100.0	15.0	15.0	150.0	1,678.9	14.4	16.0	ND	1
	Low	50	100.0	15.0	17.5	154.5	1,677.1	12.7	15.6	18.0	2
3	High	85	102.0	15.0	15.0	159.0	1,670.5	14.0	16.5	19.0	4
	Low	50	102.0	15.0	17.5	162.0	1,667.4	14.6	17.2	20.1	3
4	High	85	102.0	15.0	15.0	162.0	1,666.0	17.3	19.2	22.3	3
	Low	50	102.0	15.0	17.5	159.0	1,663.7	16.6	18.0	22.5	4
5	Low	50	102.0	15.0	17.5	155.0	1,661.7	18.1	19.2	21.5	2
	High	85	102.0	15.0	15.0	158.0	1,659.6	17.9	21.2	23.7	3
6	Low	50	102.0	15.0	17.5	156.0	1,655.5	19.2	21.1	21.9	2
	High	85	102.0	15.0	15.0	154.5	1,651.0	17.9	19.9	21.6	2
7	High	85	102.0	15.0	15.0	154.5	1,647.0	18.5	19.6	20.1	2
	Low	50	106.0	15.0	17.5	150.0	1,643.0	18.5	19.2	19.8	2
8	High	85	102.0	15.0	15.0	156.0	1,639.7	17.5	18.1	18.8	3
	Low	50	102.0	15.0	17.5	154.0	1,635.7	17.3	17.6	17.9	6
9	High	85	102.0	15.0	15.0	159.0	1,631.1	16.3	17.0	17.6	3

Block	Treat-ment	Percent attraction pump	Leveling pump	Weir width	Weir height	Distance from tower	Mean observed reservoir elevation	Water temperature			Number of observations
								Submersible pump	Hopper	Reservoir	
	Low	50	102.0	15.0	17.5	151.5	1,628.3	16.4	16.6	16.7	2
10	High	85	89.3	15.0	15.0	151.2	1,623.7	12.9	15.6	16.1	6
11	High	85	85.3	15.0	15.0	137.3	1,616.5	9.9	14.4	14.3	4
	Low	50	76.0	15.0	17.5	145.5	1,610.0	ND	13.3	13.2	2
12	High	85	99.0	15.0	15.0	147.0	1,596.4	ND	13.3	12.4	4
	Low	50	90.0	15.0	17.5	165.0	1,579.6	ND	ND	10.3	3
13	High	85	92.0	15.0	15.0	180.0	1,575.3	ND	ND	8.7	1
	Low	50	78.4	15.0	17.5	68.7	1,563.3	ND	ND	8.6	5
14	High	85	96.0	15.0	15.0	171.5	1,560.1	ND	ND	7.7	3
	Low	50	97.3	15.0	17.5	78.0	1,551.7	ND	ND	7.3	3
15	Low	50	100.0	15.0	17.5	81.0	1,540.9	ND	ND	7.3	1
	High	75–90	96.0	10.0	0.0	152.0	1,528.6	ND	ND	6.9	1

Appendix G. Rose Diagrams of Mean Fish Travel Directions Collected Using Acoustic Cameras at the Portable Floating Fish Collector at Cougar Dam, Oregon, 2014.

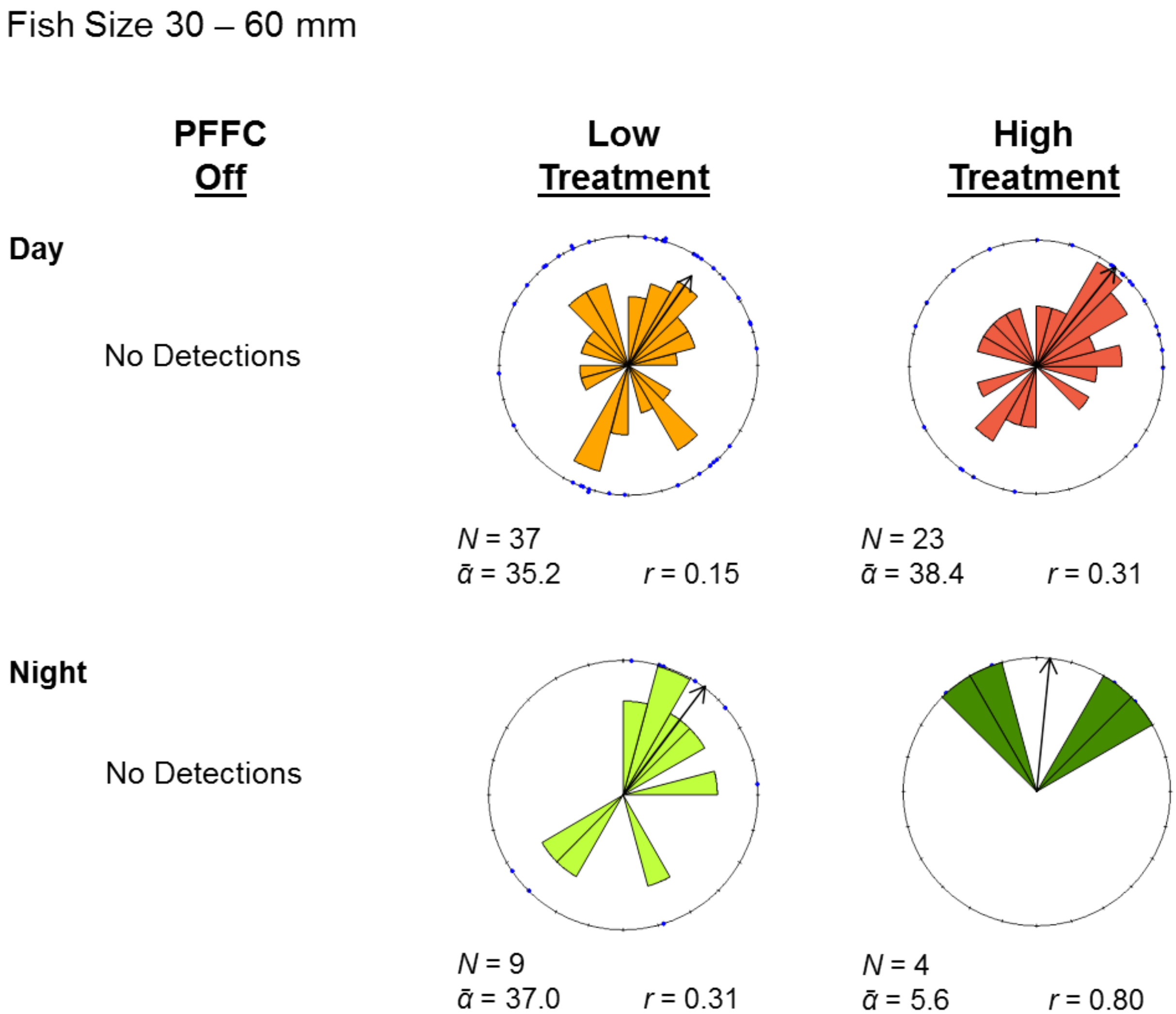

Figure G1. Rose diagrams of mean travel directions (in degrees) by diel period (Day or Night) and portable floating fish collector (PFFC) condition (PFFC Off, Low Treatment, or High Treatment) for the 30–60 millimeter (mm) size category of fish detected inside the entrance of the PFFC using an ARIS® acoustic camera inside the PFFC at Cougar Reservoir, Oregon, 2014. The heading to the entrance of the PFFC is normalized to 0° (top). Sample sizes represent the number of fish (*N*) observed during each period. The mean vector ($\bar{\alpha}$) and mean vector resultant length (*r*) are described by the arrows.

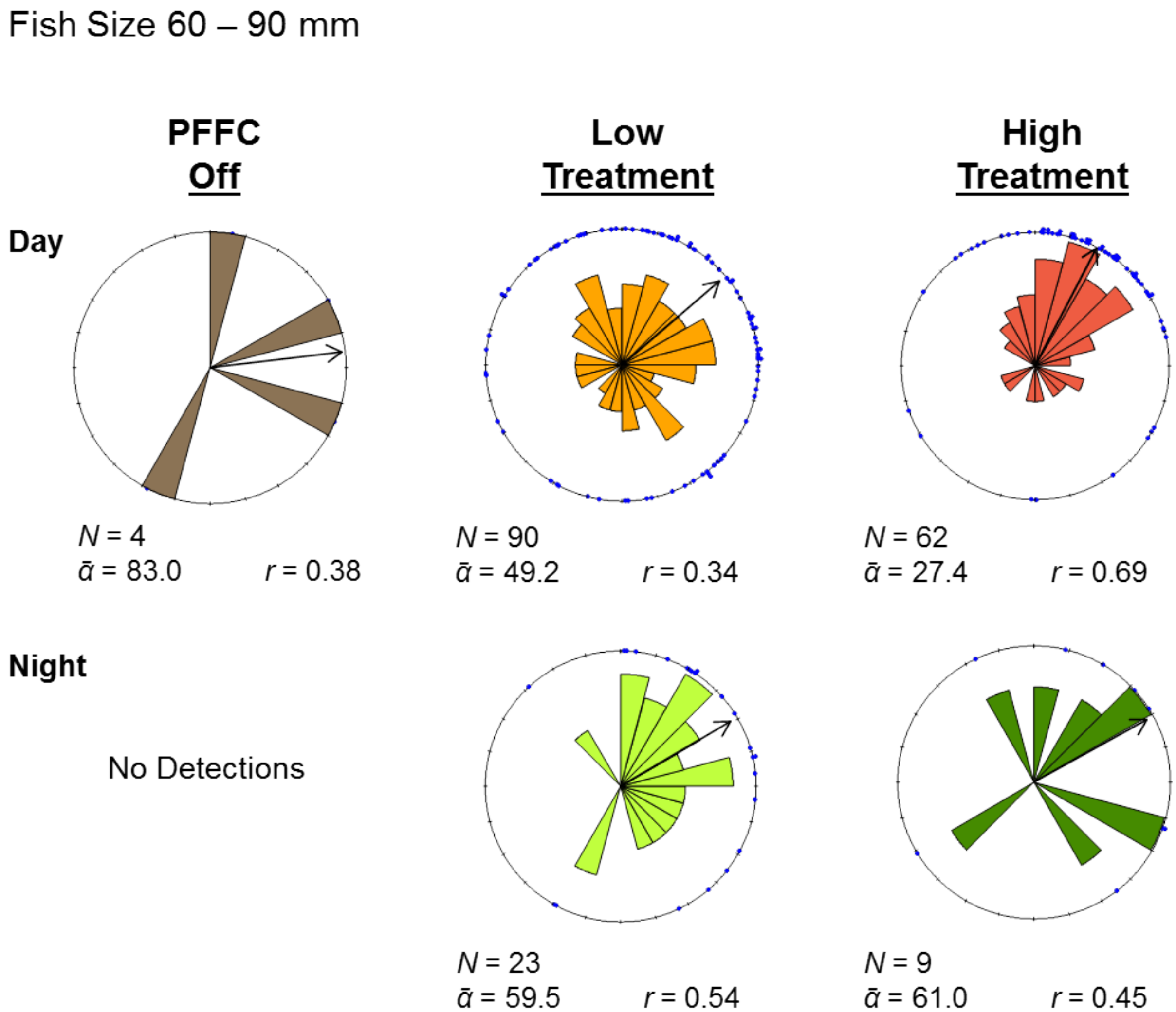

Figure G2. Rose diagrams of mean travel directions (in degrees) by diel period (Day or Night) and portable floating fish collector (PFFC) condition (PFFC Off, Low Treatment, or High Treatment) for the 60–90 millimeter (mm) size category of fish detected inside the entrance of the PFFC using an ARIS® acoustic camera inside the PFFC at Cougar Reservoir, Oregon, 2014. The heading to the entrance of the PFFC is normalized to 0° (top). Sample sizes represent the number of fish (*N*) observed during each period. The mean vector ($\bar{\alpha}$) and mean vector resultant length (*r*) are described by the arrows.

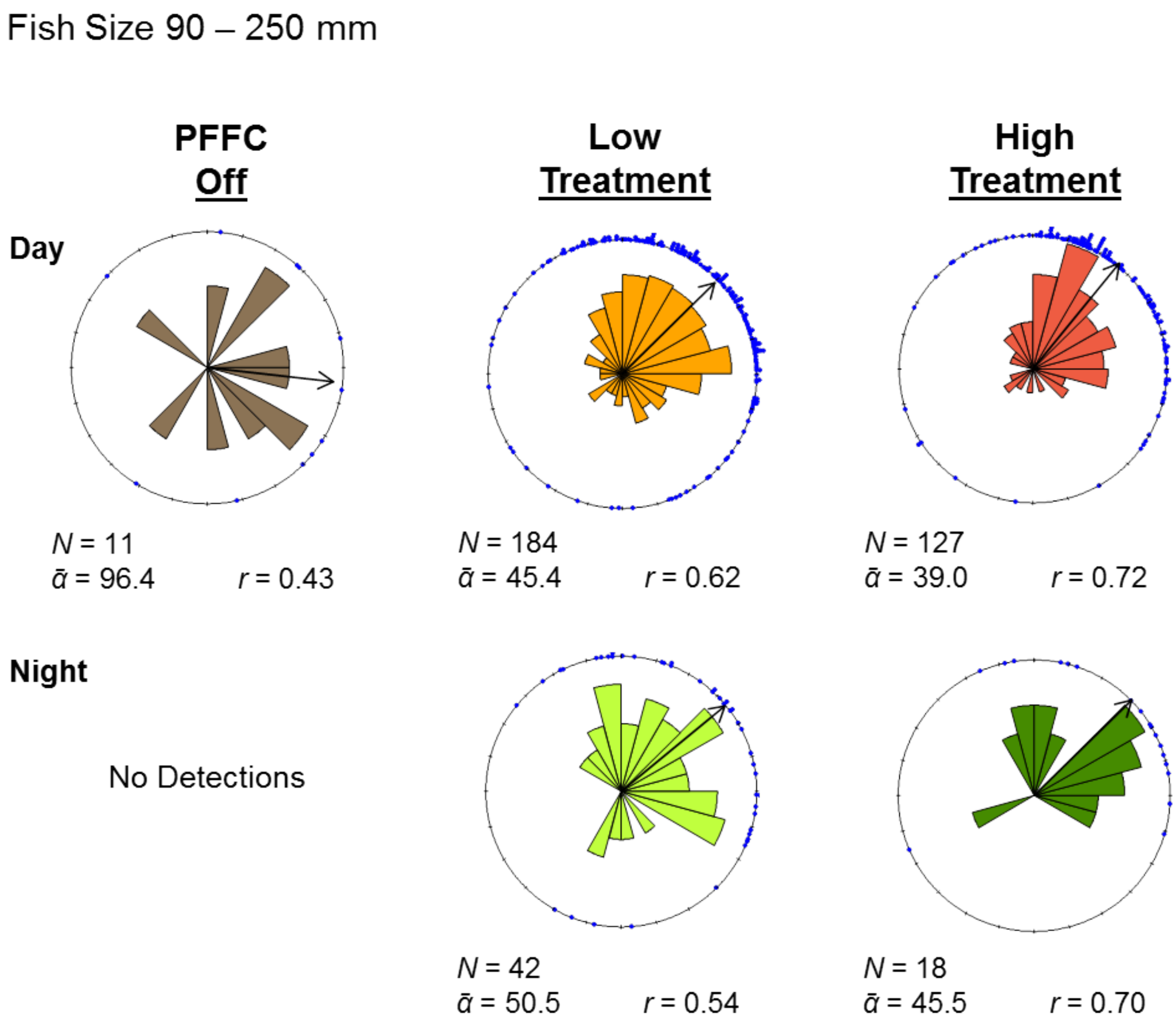

Figure G3. Rose diagrams of mean travel directions (in degrees) by diel period (Day or Night) and portable floating fish collector (PFFC) condition (PFFC Off, Low Treatment, or High Treatment) for the 90–250 millimeter (mm) size category of fish detected inside the entrance of the PFFC using an ARIS® acoustic camera inside the PFFC at Cougar Reservoir, Oregon, 2014. The heading to the entrance of the PFFC is normalized to 0° (top). Sample sizes represent the number of fish (*N*) observed during each period. The mean vector ($\bar{\alpha}$) and mean vector resultant length (*r*) are described by the arrows.

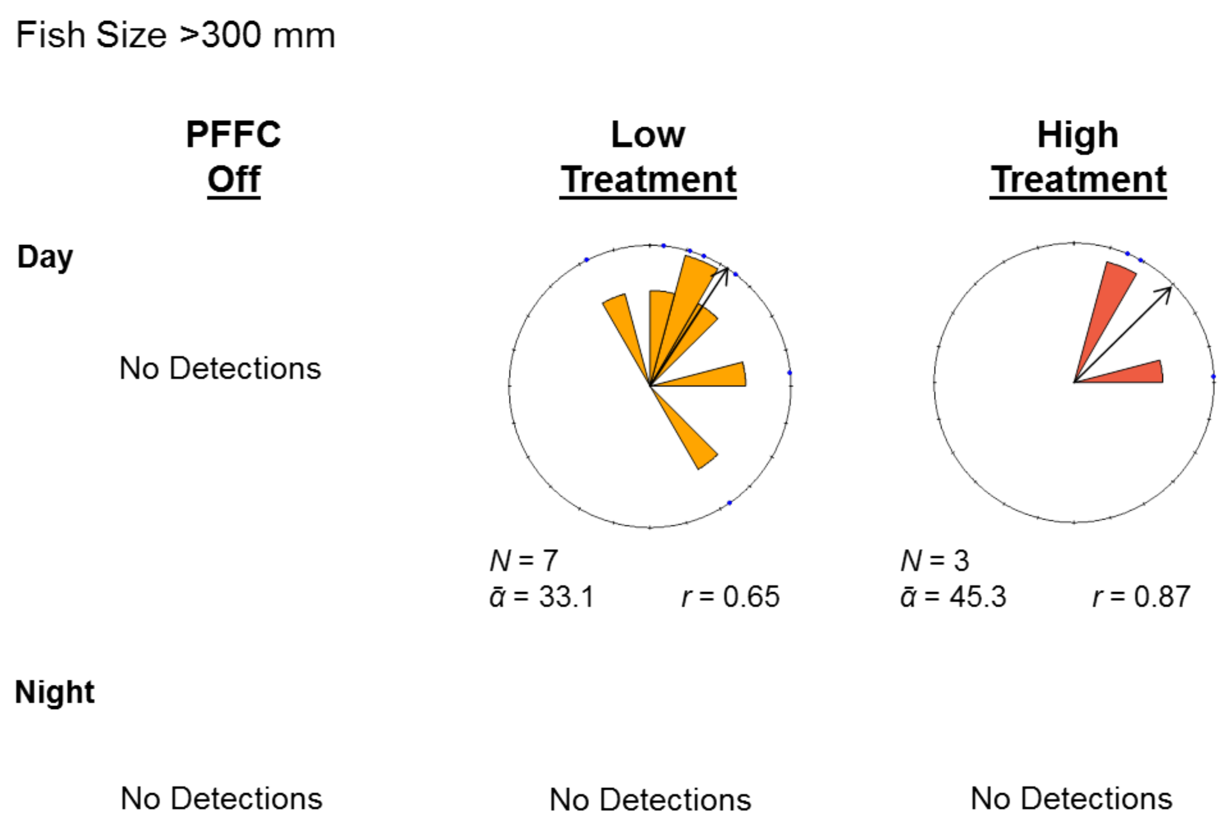

Figure G4. Rose diagrams of mean travel directions (in degrees) by diel period (Day or Night) and portable floating fish collector (PFFC) condition (PFFC Off, Low Treatment, or High Treatment) for the greater than (>) 300 millimeter (mm) size category of fish detected inside the entrance of the PFFC using an ARIS® acoustic camera inside the PFFC at Cougar Reservoir, Oregon, 2014. The heading to the entrance of the PFFC is normalized to 0° (top). Sample sizes represent the number of fish (*N*) observed during each period. The mean vector (ᾱ) and mean vector resultant length (*r*) are described by the arrows.

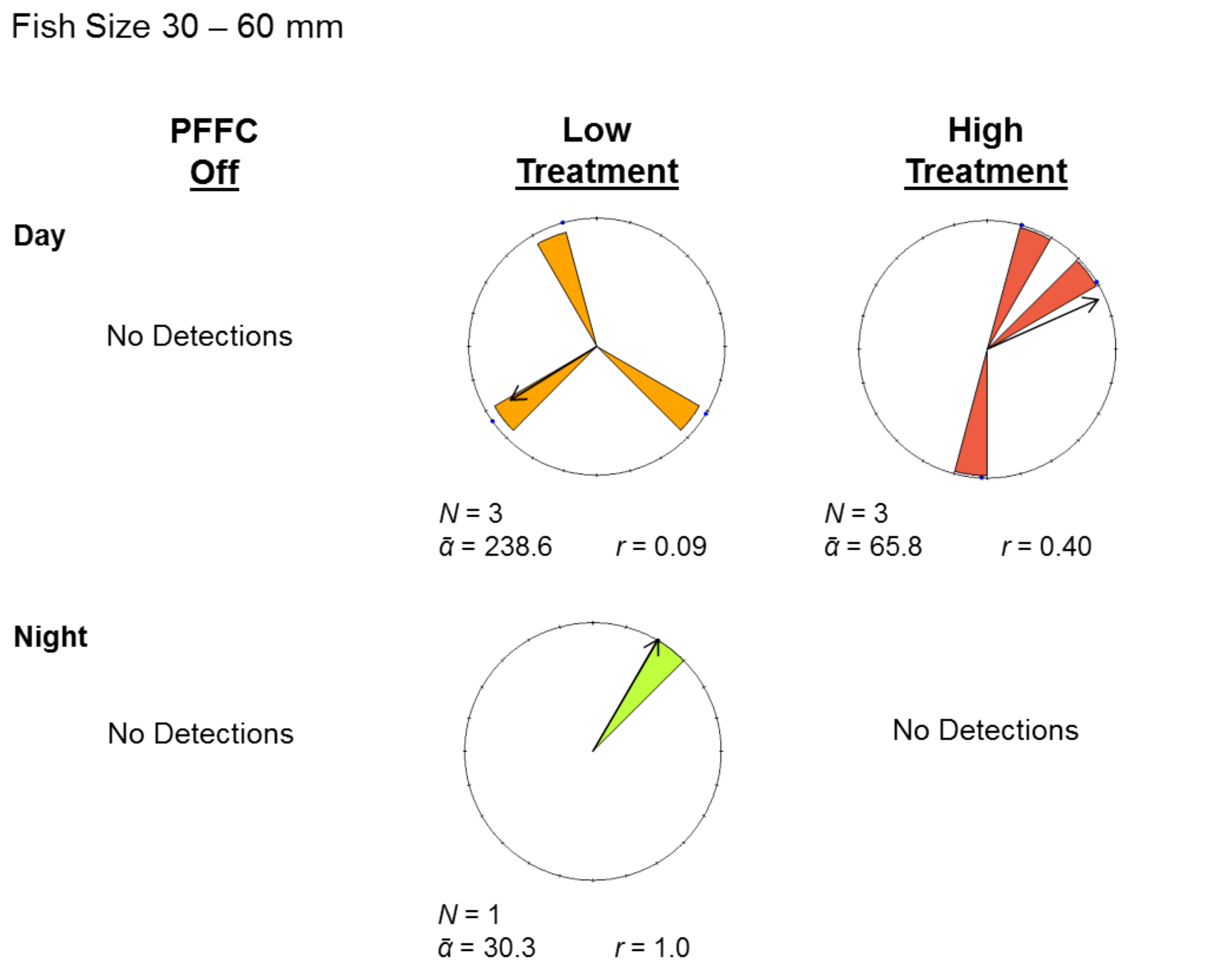

Figure G5. Rose diagrams of mean travel directions (in degrees) by diel period (Day or Night) and portable floating fish collector (PFFC) condition (PFFC Off, Low Treatment, or High Treatment) for the 30–60 millimeter (mm) size category of fish detected outside the entrance of the PFFC using an ARIS® acoustic camera inside the PFFC at Cougar Reservoir, Oregon, 2014. The heading to the entrance of the PFFC is normalized to 0° (top). Sample sizes represent the number of fish (*N*) observed during each period. The mean vector (ᾱ) and mean vector resultant length (*r*) are described by the arrows.

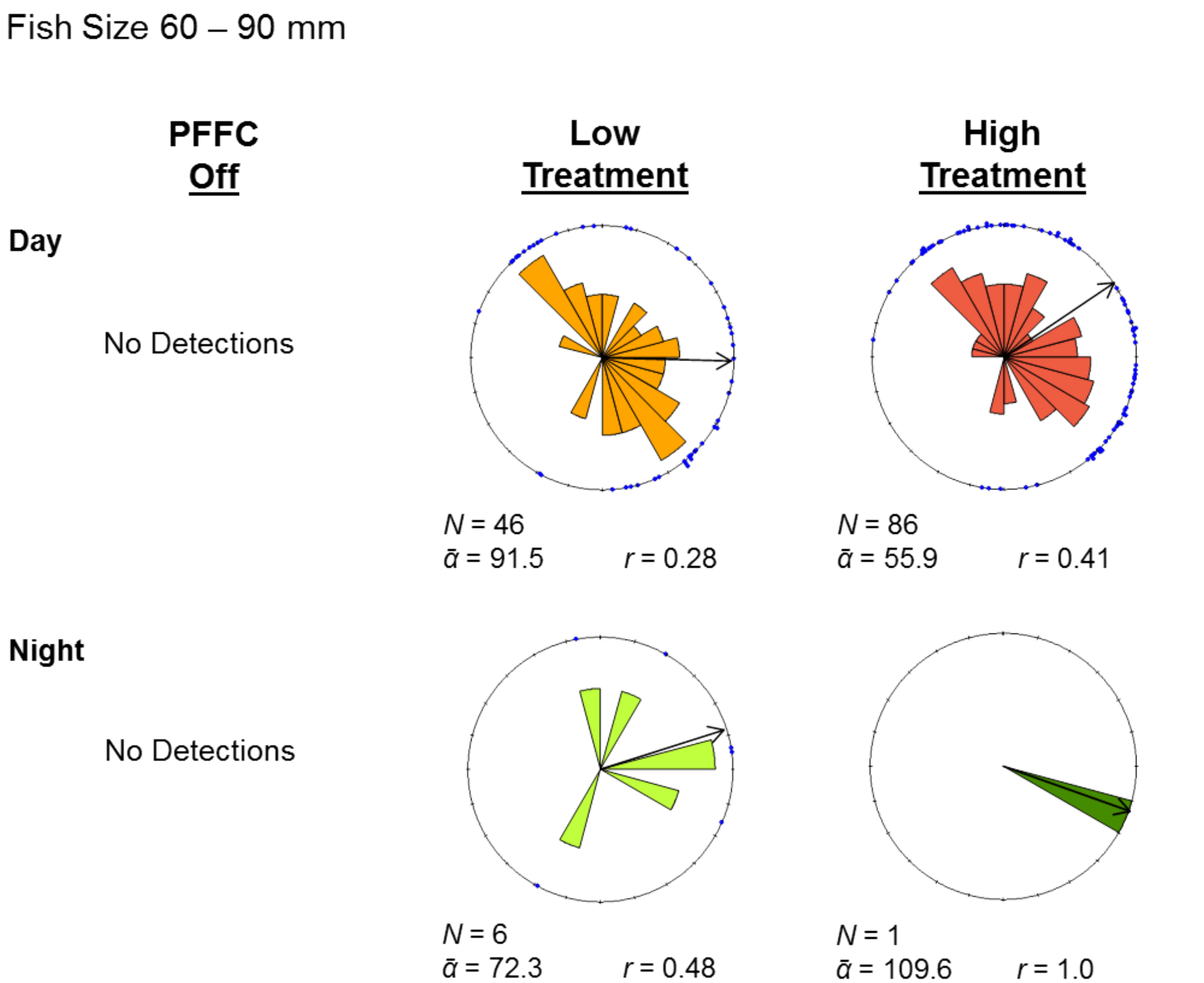

Figure G6. Rose diagrams of mean travel directions (in degrees) by diel period (Day or Night) and portable floating fish collector (PFFC) condition (PFFC Off, Low Treatment, or High Treatment) for the 60–90 millimeter (mm) size category of fish detected outside the entrance of the PFFC using an ARIS® acoustic camera inside the PFFC at Cougar Reservoir, Oregon, 2014. The heading to the entrance of the PFFC is normalized to 0° (top). Sample sizes represent the number of fish (*N*) observed during each period. The mean vector ($\bar{\alpha}$) and mean vector resultant length (*r*) are described by the arrows.

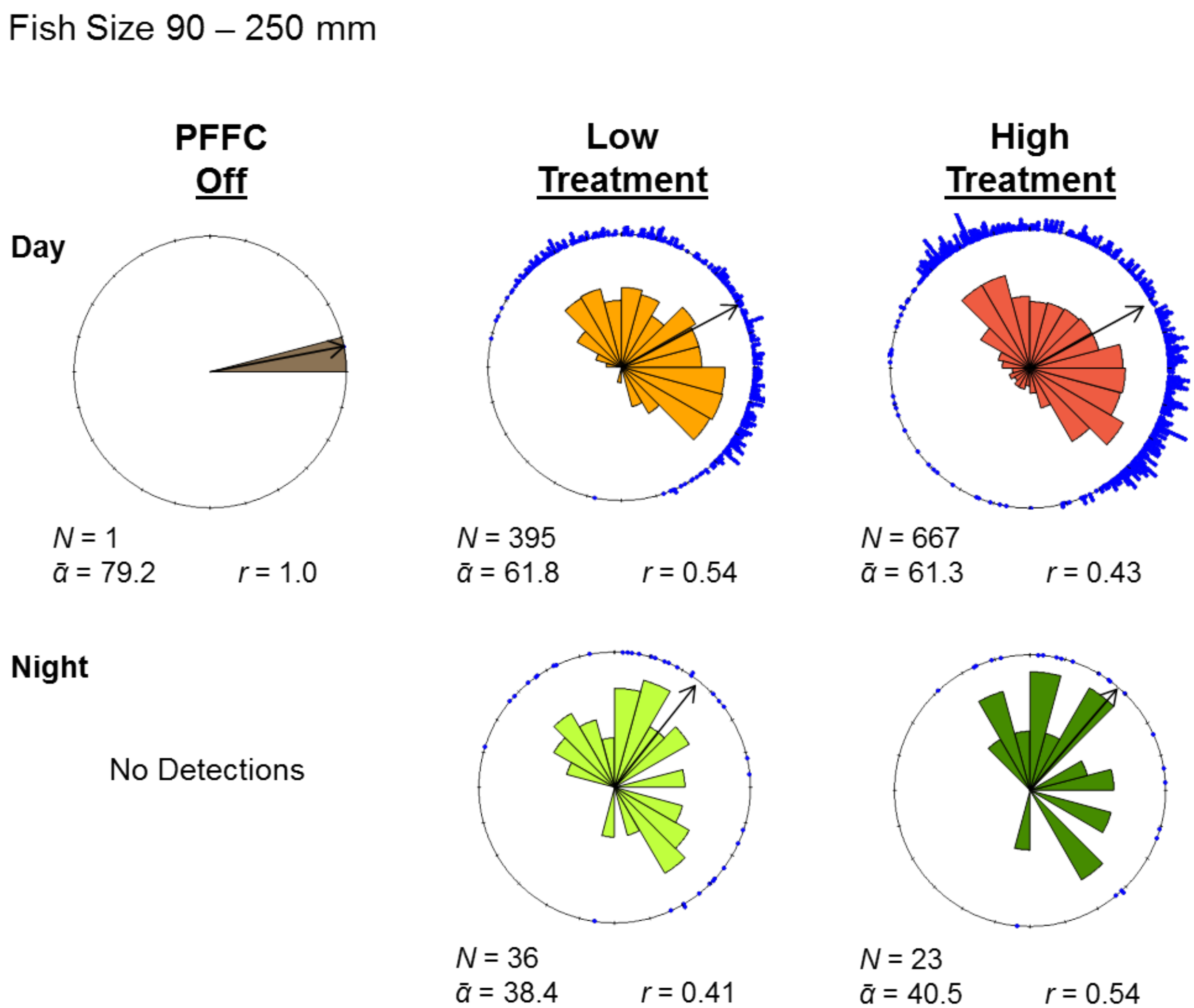

Figure G7. Rose diagrams of mean travel directions (in degrees) by diel period (Day or Night) and portable floating fish collector (PFFC) condition (PFFC Off, Low Treatment, or High Treatment) for the 90–250 millimeter (mm) size category of fish detected outside the entrance of the PFFC using an ARIS® acoustic camera inside the PFFC at Cougar Reservoir, Oregon, 2014. The heading to the entrance of the PFFC is normalized to 0° (top). Sample sizes represent the number of fish (*N*) observed during each period. The mean vector ($\bar{\alpha}$) and mean vector resultant length (*r*) are described by the arrows.

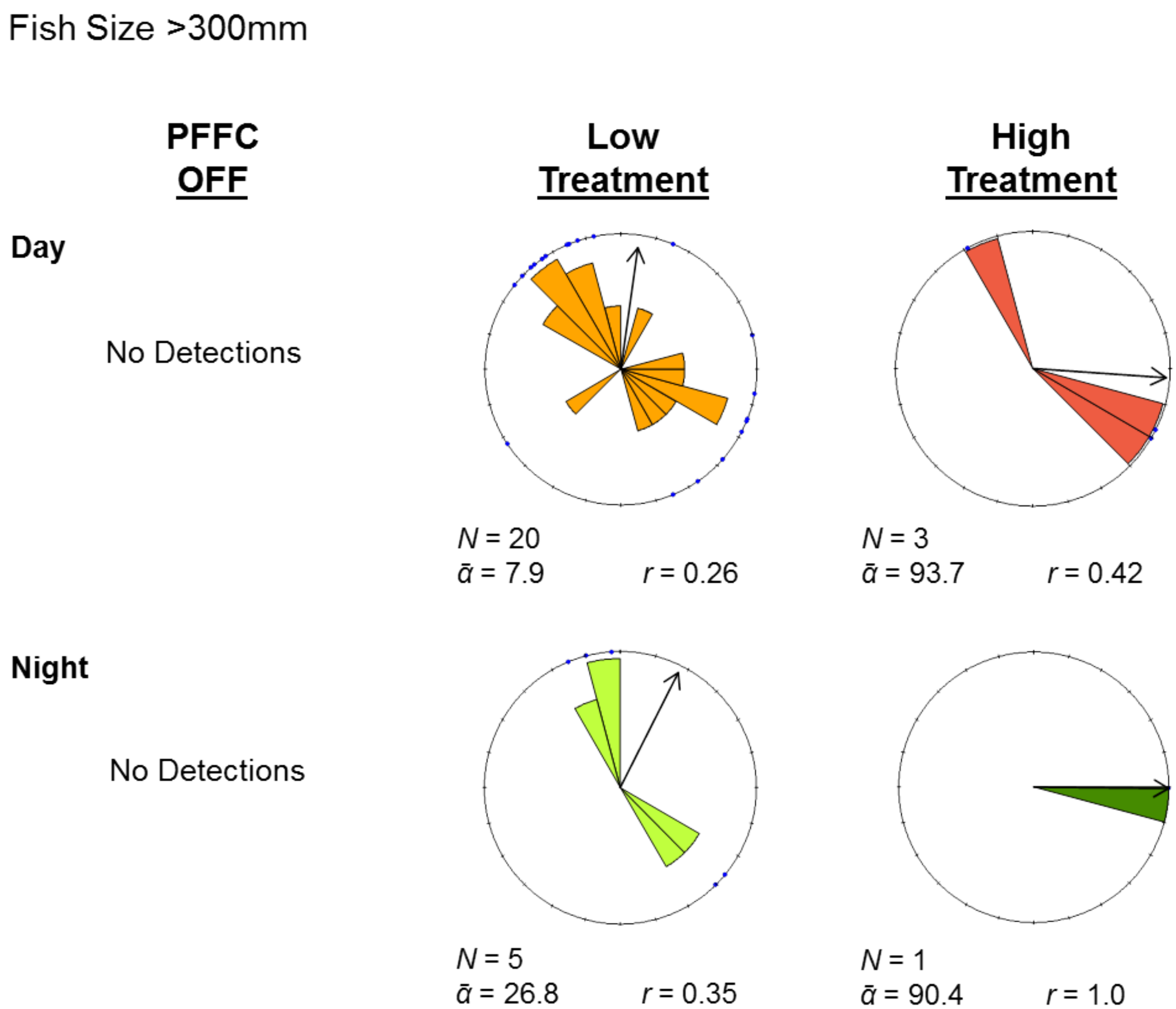

Figure G8. Rose diagrams of mean travel directions (in degrees) by diel period (Day or Night) and portable floating fish collector (PFFC) condition (PFFC Off, Low Treatment, or High Treatment) for the greater than (>) 300 millimeter (mm) size category of fish detected outside the entrance of the PFFC using an ARIS® acoustic camera inside the PFFC at Cougar Reservoir, Oregon, 2014. The heading to the entrance of the PFFC is normalized to 0° (top). Sample sizes represent the number of fish (*N*) observed during each period. The mean vector (ᾱ) and mean vector resultant length (*r*) are described by the arrows.

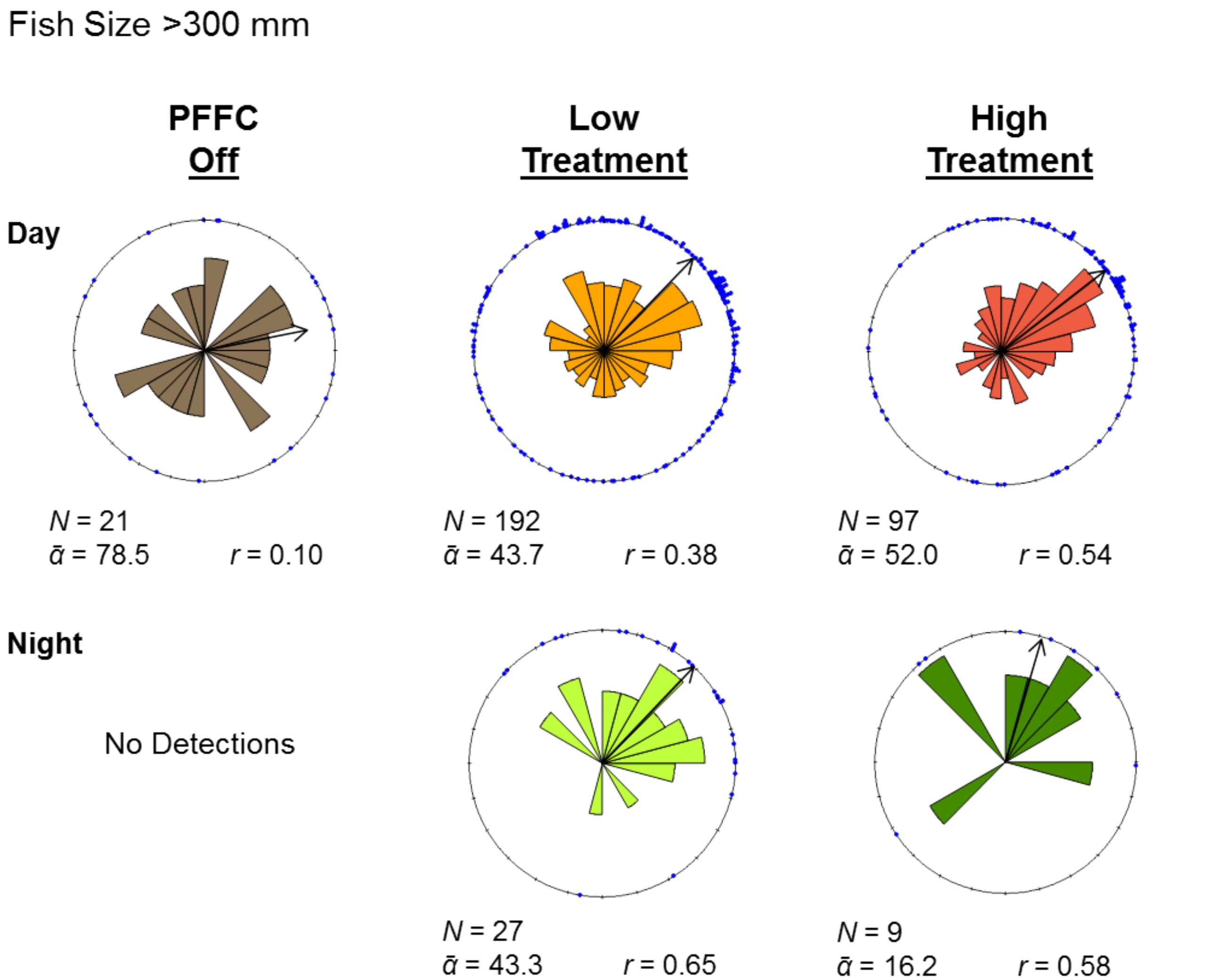

Figure G9. Rose diagrams of mean travel directions (in degrees) by diel period (Day or Night) and portable floating fish collector (PFFC) condition (PFFC Off, Low Treatment, or High Treatment) for the greater than (>) 300 millimeter (mm) size category of fish detected inside the entrance of the PFFC using a DIDSON® acoustic camera inside the PFFC at Cougar Reservoir, Oregon, 2014. The heading to the entrance of the PFFC is normalized to 0° (top). Sample sizes represent the number of fish (*N*) observed during each period. The mean vector ($\bar{\alpha}$) and mean vector resultant length (*r*) are described by the arrows.

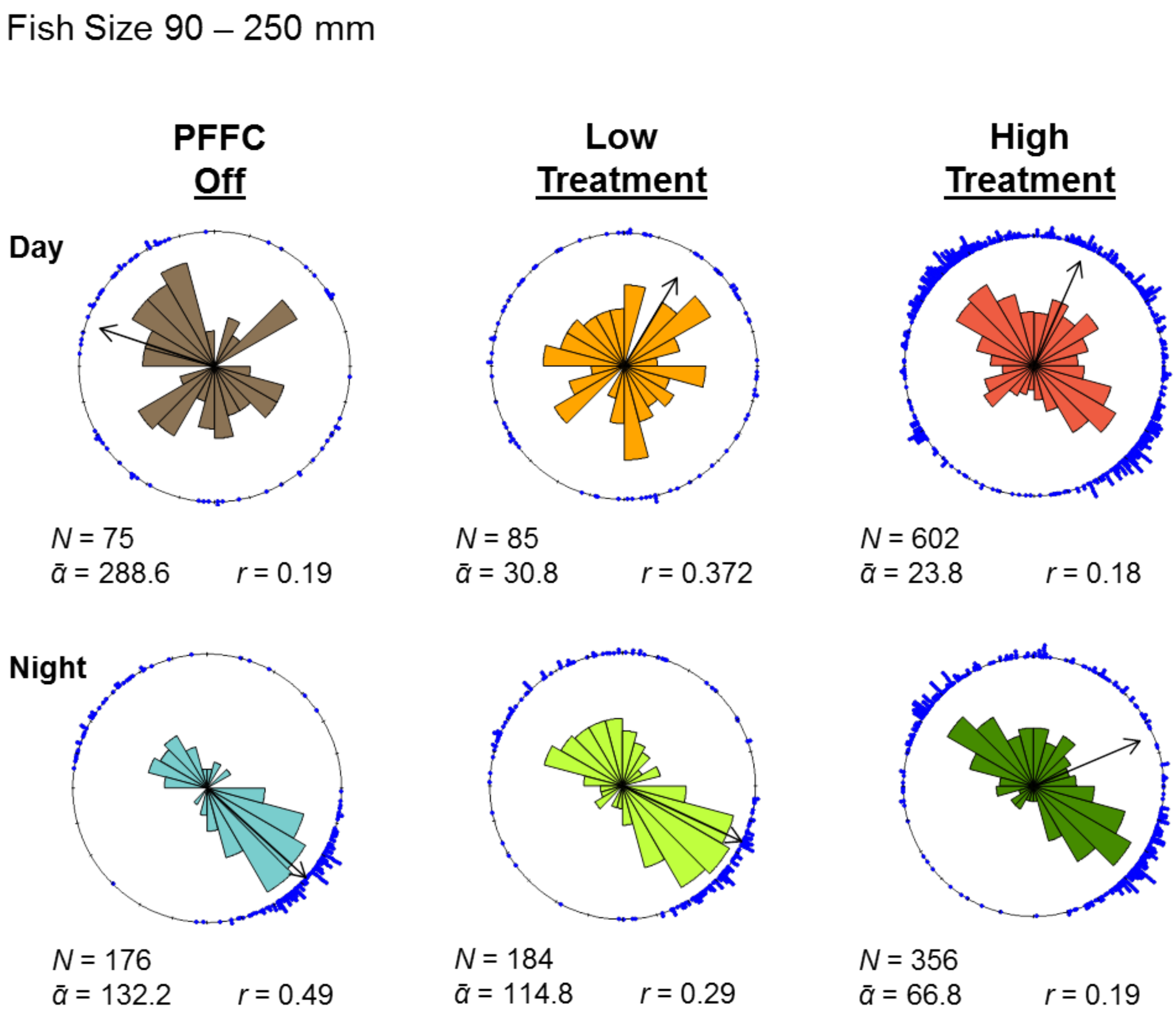

Figure G10. Rose diagrams of mean travel directions (in degrees) by diel period (Day or Night) and portable floating fish collector (PFFC) condition (PFFC Off, Low Treatment, or High Treatment) for the 90–250 millimeter (mm) size category of fish detected outside the entrance of the PFFC using a DIDSON® acoustic camera inside the PFFC at Cougar Reservoir, Oregon, 2014. The heading to the entrance of the PFFC is normalized to 0° (top). Sample sizes represent the number of fish (*N*) observed during each period. The mean vector ($\bar{\alpha}$) and mean vector resultant length (*r*) are described by the arrows.

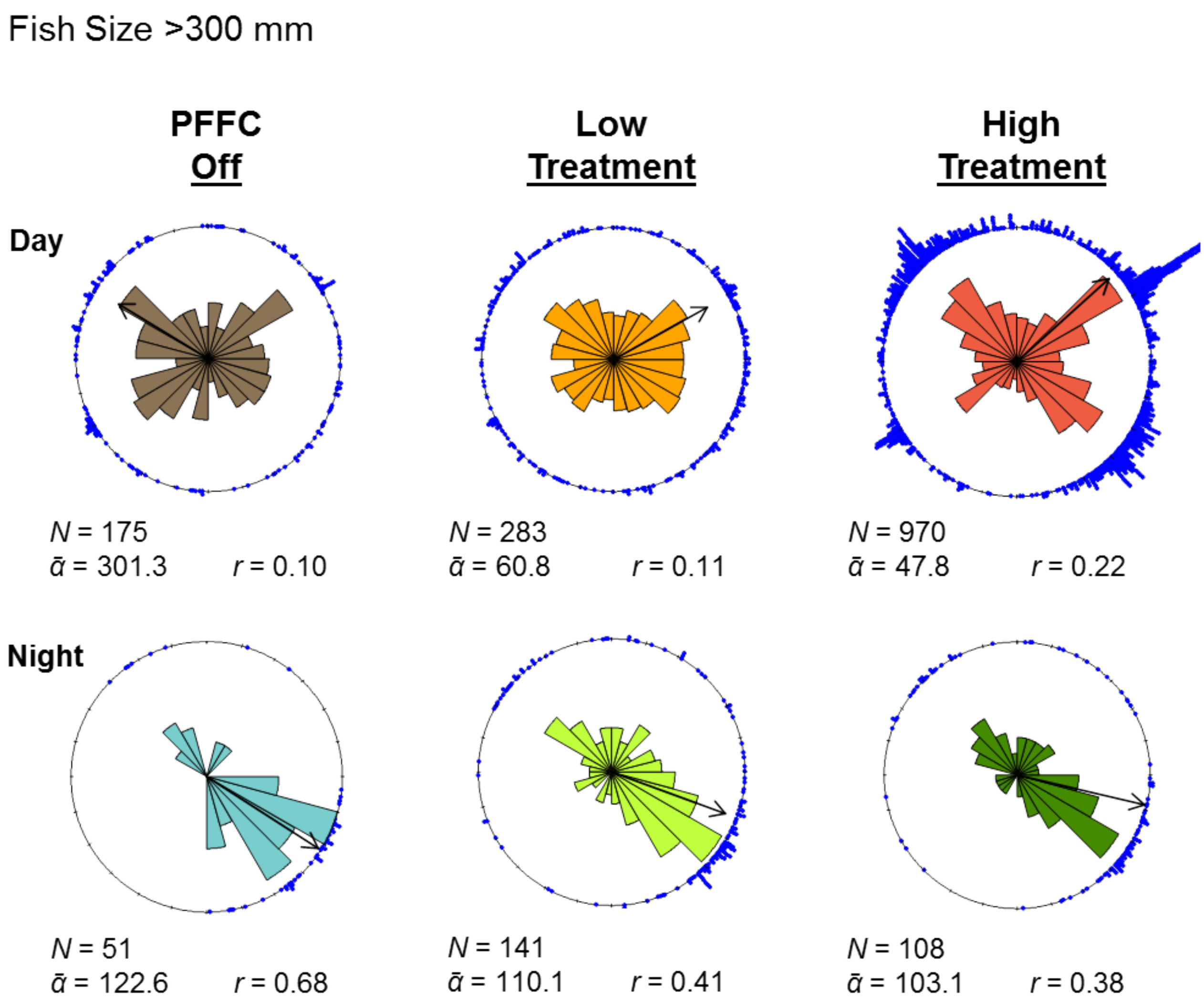

Figure G11. Rose diagrams of mean travel directions (in degrees) by diel period (Day or Night) and portable floating fish collector (PFFC) condition (PFFC Off, Low Treatment, or High Treatment) for the greater than (>) 300 millimeter (mm) size category of fish detected outside the entrance of the PFFC using a DIDSON® acoustic camera inside the PFFC at Cougar Reservoir, Oregon, 2014. The heading to the entrance of the PFFC is normalized to 0° (top). Sample sizes represent the number of fish (*N*) observed during each period. The mean vector ($\bar{\alpha}$) and mean vector resultant length (*r*) are described by the arrows.

Publishing support provided by the U.S. Geological Survey
Science Publishing Network, Tacoma Publishing Service Center

For more information concerning the research in this report, contact the
Director, Western Fisheries Research Center
U.S. Geological Survey
6505 NE 65th Street
Seattle, Washington 98115
http://wfrc.usgs.gov/

Beeman and others—**Evaluation of the Portable Floating Fish Collector at Cougar Reservoir and Dam, Oregon, 2014**—Open-File Report 2016–1003

ISSN 2331-1258 (online)
http://dx.doi.org/10.3133/ofr20161003